

MECHANISMS UNDERLYING THE DOWNREGULATION OF THE  
TRANSPORTER ASSOCIATED WITH ANTIGEN PROCESSING (TAP)-1 IN  
CARCINOMAS

by

ALVERNIA FRANCESCA SETIADI

B.Sc., University of British Columbia, 2001

A THESIS SUBMITTED IN PARTIAL FULFILLMENT OF  
THE REQUIREMENTS FOR THE DEGREE OF

DOCTOR OF PHILOSOPHY

in

THE FACULTY OF GRADUATE STUDIES

(Zoology)

THE UNIVERSITY OF BRITISH COLUMBIA

June 2007

© Alvernia Francesca Setiadi, 2007

## Abstract

Expression of Transporter associated with Antigen Processing (TAP)-1 is often lost in metastatic carcinomas, resulting in defective antigen processing and presentation, and escape of the cancer cell from immune surveillance. In this study, the nature of TAP-1 deficiencies in tumors was investigated. By chromatin immunoprecipitation assay, it was shown that the recruitment of RNA polymerase II to the *Tap-1* gene was impaired in TAP-deficient, metastatic cells derived from murine melanoma, prostate and lung carcinomas. Levels of TAP-1 promoter activity, as assessed by stable transfections with a reporter construct containing the TAP-1 promoter, were also relatively low in TAP-deficient cells. These suggest that the deficiency in TAP-1 expression resulted--at least partially--from a reduced level of transcriptional activity of the *Tap-1* gene.

In order to examine genetic heritability of regulators of TAP-1 promoter activity, TAP- and MHC class I-deficient cells of H-2<sup>b</sup> origin were fused with wild-type fibroblasts of H-2<sup>k</sup> origin. Fusion with TAP-expressing cells complemented the low levels of TAP-1 promoter activity in TAP-deficient cells. However, these fused cells exhibited lower levels of TAP-1 mRNA and H-2<sup>k</sup> than unfused fibroblasts. Further analysis showed that TAP-1 mRNA stability was lower in fused carcinoma-fibroblasts than in unfused fibroblasts. Taken together, TAP deficiency in many carcinomas appears to be caused by a decrease in activity/expression of *trans*-acting factors regulating TAP-1 promoter activity, as well as a decrease in TAP-1 mRNA stability.

The hypothesis that epigenetic regulation plays a fundamental role in controlling TAP-1 transcription was also tested. Chromatin immunoprecipitation analyses showed that the lack of TAP-1 transcription correlated with low levels of recruitment of a histone

acetyltransferase, CBP, and of histone H3 acetylation at the TAP-1 promoter, leading to a decrease in accessibility of the RNA polymerase II complex to the TAP-1 promoter. These findings lie at the heart of understanding immune escape mechanisms in tumors and suggest that the reversal of epigenetic codes may provide novel immunotherapeutic paradigms for intervention in cancer.

## Table of Contents

<i>Abstract</i>	<i>ii</i>
<i>Table of Contents</i>	<i>iv</i>
<i>List of Tables</i>	<i>vii</i>
<i>List of Figures</i>	<i>viii</i>
<i>List of Figures</i>	<i>viii</i>
<i>List of Abbreviations</i>	<i>xiv</i>
<i>List of Abbreviations</i>	<i>xiv</i>
<i>Acknowledgments</i>	<i>xviii</i>
<i>Dedication</i>	<i>xx</i>
<i>Co-Authorship Statement</i>	<i>xxi</i>
<b>Chapter 1 : General Introduction</b>	<b>1</b>
<b>1.1 Overview of the Immune System</b>	<b>2</b>
<b>1.2 Antigen Presentation</b>	<b>3</b>
1.2.1 Major Histocompatibility Complex (MHC) genetics	3
1.2.2 MHC molecules	5
1.2.3 MHC class I antigen presentation	6
1.2.4 Transporters associated with Antigen Processing (TAP) structure and function	7
1.2.5 MHC class II antigen presentation and CD4 <sup>+</sup> T cells in cancer immunity	8
<b>1.3 Disruption of the MHC Class I Antigen Processing Pathway and the Development of Tumors</b>	<b>11</b>
<b>1.4 TAP-based Immunotherapy</b>	<b>13</b>
<b>1.5 Regulation of TAP-1 Expression</b>	<b>15</b>
1.5.1 Organization of <i>Tap</i> and <i>Lmp</i> genes within the mouse MHC class II locus	15
1.5.2 Possible mechanisms of TAP-1 mRNA downregulation in carcinomas	16
1.5.2.1 Transcriptional mechanisms	16
1.5.2.2 Post-transcriptional mechanisms	16
1.5.2.3 Epigenetic mechanisms	17
<b>1.6 Synopsis of Thesis Objectives, Hypotheses and Results</b>	<b>19</b>
<b>1.7 References</b>	<b>21</b>
<b>Chapter 2 : Identification of Mechanisms Underlying TAP-1 Deficiency in Metastatic Murine Carcinomas</b>	<b>28</b>
<b>2.1 Introduction</b>	<b>28</b>
<b>2.2 Materials and Methods</b>	<b>30</b>
2.2.1 Cell lines	30
2.2.2 Reverse transcription-PCR analysis	30
2.2.3 Chromatin immunoprecipitation (ChIP) assays	33
2.2.4 Cloning of the TAP-1 promoter	33

2.2.5	Transfection and selection	34
2.2.6	Generation of pTAP-1-EGFP-transfected clones by FACS	34
2.2.7	Cell Fusion and FACS analysis	35
2.2.8	Endogenous levels and overexpression of IRF-1 and IRF-2 in cell lines	35
2.2.9	Luciferase and $\beta$ -Galactosidase Assays	36
2.2.10	Western Blot	36
2.2.11	Analysis of mRNA stability	37
2.2.12	Real time quantitative PCR analysis	37
<b>2.3</b>	<b>Results</b>	<b>38</b>
2.3.1	Levels of TAP-1 mRNA in CMT.64, LMD, B16, Ltk and RMA cells	38
2.3.2	The recruitment of RNA polymerase II to the <i>Tap-1</i> gene is lower in the CMT.64, LMD and B16, than in the Ltk and RMA cells	39
2.3.3	Cloning and analysis of the -557 to +1 region of the CMT.64-derived TAP-1 promoter	42
2.3.4	Activity of the -557 to +1 region of the TAP-1 promoter is impaired in TAP-deficient cells	43
2.3.5	Effects of fusions between carcinoma cells and wild type fibroblasts on TAP-1 promoter activity and MHC class I expression levels	47
2.3.6	Overexpression of IRF-1 and IRF-2 in CMT.64 cells did not result in significant changes in TAP-1 promoter activity	51
2.3.7	Analysis of TAP-1 expression in unfused and fused cells	54
2.3.8	TAP-1 mRNA stability decreases in carcinoma-fused fibroblasts	56
<b>2.4</b>	<b>Discussion</b>	<b>58</b>
<b>2.5</b>	<b>References</b>	<b>61</b>
<b>Chapter 3 : Epigenetic Control of TAP-1 expression and the Immune Escape Mechanisms in Malignant Carcinomas</b>		<b>65</b>
<b>3.1</b>	<b>Introduction</b>	<b>65</b>
<b>3.2</b>	<b>Materials and Methods</b>	<b>68</b>
3.2.1	Cell lines and reagents	68
3.2.2	Reverse transcription-PCR analysis	69
3.2.3	Real-time quantitative PCR analysis	70
3.2.4	Flow cytometry	71
3.2.5	Chromatin immunoprecipitation assays	71
3.2.6	Plasmid construction	71
3.2.7	Transfection and selection	72
3.2.8	Luciferase assays	73
3.2.9	Western Blots	73
3.2.10	Cytotoxicity assays	74
3.2.11	Establishment of HPV-positive cancer xenografts and treatment with Trichostatin A	75
<b>3.3</b>	<b>Results</b>	<b>76</b>
3.3.1	Chromatin remodeling regulates TAP-1 transcription	76
3.3.2	Histone H3 acetylation within the TAP-1 promoter is low in MHC class I-deficient carcinomas	80
3.3.3	Identification of a region in TAP-1 promoter responsible for the differential activity in TAP-expressing and TAP-deficient cells	82
3.3.4	CBP binding to TAP-1 promoter is impaired in metastatic carcinomas	85
3.3.5	IFN- $\gamma$ treatment increases the level of CBP, acetyl-histone H3 and RNA polymerase II recruitment to the TAP-1 promoter in TAP-deficient metastatic carcinomas	86
3.3.6	Trichostatin A (TSA), a histone deacetylase inhibitor, increases the expression of TAP-1 and other antigen-processing machinery (APM) components in metastatic (TAP-deficient) and pre-metastatic (TAP-expressing) carcinomas	88

3.3.7	TSA treatment increases the expression of TAP-1 and surface MHC class I, resulting in an increased susceptibility of TAP-deficient metastatic carcinomas to CTL killing	91
3.3.8	TSA treatment suppresses the growth of TAP-deficient, metastatic tumors <i>in vivo</i> .	95
<b>3.4</b>	<b>Discussion</b>	<b>98</b>
<b>3.5</b>	<b>References</b>	<b>103</b>
<b>Chapter 4 : Characterization of Novel TAP-1 Regulator Genes</b>		<b>109</b>
<b>4.1</b>	<b>Introduction</b>	<b>109</b>
<b>4.2</b>	<b>Materials and Methods</b>	<b>111</b>
4.2.1	Cell lines	111
4.2.2	Human cDNA library	111
4.2.3	Cell Fusion and FACS analysis	111
4.2.4	Determination of target cell transduction efficiency using the pFB-Luc control viral supernatant	112
4.2.5	Transduction of 1E10 cells with ViraPort cDNA library retroviral supernatants	112
4.2.6	Selection of positive transductants	112
4.2.7	Recovery of cDNA clones from positive transductants	113
4.2.8	Sub-cloning of TAP-regulator gene candidates	114
4.2.9	Transfection and selection	115
4.2.10	Reverse transcription-PCR analysis	115
4.2.11	Flow cytometry	116
<b>4.3</b>	<b>Results</b>	<b>117</b>
4.3.1	Mouse TAP-1 promoter activity is up-regulated in the fused 1E10-A549 cells	117
4.3.2	The transduction efficiency of 1E10 cells is three times lower than that of the NIH/3T3 cells	118
4.3.3	Identification of gene candidates from human lung cDNA library transductants	118
4.3.4	Identification of gene candidates from human spleen cDNA library transductants	121
4.3.5	Cancer-related information about the screened genes	124
4.3.6	Overexpression of several TAP-regulator gene candidates in CMT.64 and LMD cells up-regulates TAP-1 expression, but not H-2K <sup>b</sup> expression	126
<b>4.4</b>	<b>Discussion</b>	<b>129</b>
<b>4.5</b>	<b>References</b>	<b>133</b>
<b>Chapter 5 : General Discussion</b>		<b>137</b>
<b>5.1</b>	<b>Summary and Conclusions</b>	<b>137</b>
<b>5.2</b>	<b>Future Work</b>	<b>143</b>
<b>5.3</b>	<b>The Big Picture</b>	<b>147</b>
<b>5.4</b>	<b>References</b>	<b>148</b>
<b>Appendix A: Details of Methods</b>		<b>153</b>
<b>A.1</b>	<b>Chromatin Immunoprecipitation Assay</b>	<b>153</b>
<b>A.2</b>	<b>Calculation of copy numbers of pTAP-1-EGFP construct integrated in stable transfectants</b>	<b>154</b>
<b>Appendix B: List of Cloning Vectors</b>		<b>155</b>
<b>Appendix C: Comparison of TAP-1 Coding Sequence of CMT.64 and Ltk cells</b>		<b>156</b>

## List of Tables

Table 2.2.2.1: Primers used for RT-PCR analysis. ....	32
Table 2.2.5.1: G418 doses for selection of transfectants in various cell lines. ....	34
Table 2.3.4.1: Statistical Evaluation of the Transfected pTAP-1-EGFP Copy Numbers Per Cell. ....	44
Table 3.2.2.1: Primers used for RT-PCR and real time PCR analysis. ....	70
Table 3.2.6.1: Primers used for PCR amplifications of full TAP-1 promoter and its truncations. ....	72
Table 4.2.8.1: Primers used for PCR amplification. ....	114
Table 4.3.3.1: Identity of cDNAs recovered from bulk-sorted cells of human lung cDNA library transductants. ....	119
Table 4.3.3.2: Identity of cDNAs recovered from single-cell clones of human lung cDNA library transductants. ....	120
Table 4.3.4.1: Identity of cDNAs recovered from single-cell clones of human spleen cDNA library transductants. ....	123
Table 4.3.5.1: Cancer-related information about the proteins that match the hits obtained from the screenings of human lung and spleen cDNA libraries. ....	125

## List of Figures

- Figure 1.2.1.1: Genetic organization of human and mouse MHC genes (image reprinted from reference no. [10], by permission). ..... 4
- Figure 1.2.3.1: MHC class I antigen presentation pathway (image reprinted from reference no. [7], by permission). ..... 6
- Figure 1.2.4.1: A heterodimer of the TAP-1 and TAP-2 molecules (image reprinted from reference no. [7], by permission). ..... 8
- Figure 1.2.5.1: MHC class II antigen presentation pathway (image reprinted from reference no. [22], by permission). ..... 9
- Figure 1.2.5.2: The complex interaction between a tumor cell, professional antigen-presenting cells, CTLs, Th cells, B cells and other lymphocytes in the tumor microenvironment. A (+) sign indicates an activating signal on the antitumor response while a (-) sign indicates an inhibitory effect (image reprinted from reference no. [24], by permission). ..... 10
- Figure 1.5.1.1: Organization of *Tap* and *Lmp* genes in the mouse MHC class II locus. The sizes of the coding sequences (CDS) and intergenic regions are shown in the diagram. .... 15
- Figure 2.3.1.1: IFN- $\gamma$ -treatment restores TAP-1 expression in TAP-deficient murine lung, prostate and skin carcinoma cells (CMT.64, LMD and B16). Amplification of  $\beta$ -actin cDNA served as an internal control. RT-PCR analyses were performed at least three times and representative data are shown. .... 38
- Figure 2.3.2.1: The recruitment of RNA polymerase II to 3' coding region of the *Tap-1* gene in CMT.64, LMD and B16 is impaired in comparison to that in Ltk and RMA. Chromatin immunoprecipitation using anti-RNA polymerase II antibody was performed in each cell line, and the eluted DNA fragments were purified and used as templates for real time PCR analysis using primers specific for the 3' coding region of the *Tap-1* gene. Relative RNA polymerase II levels were determined as the ratio of copy numbers of the eluted 3' coding region of the *Tap-1* gene and copy numbers of the corresponding inputs. The smallest ratio in each group of experiments was arbitrarily determined as 1. *Columns*, average of three to six experiments; *bars*, SEM. \*  $P < .05$  compared with TAP-expressing cells (Student's t-test). .... 40
- Figure 2.3.2.2: The recruitment of RNA pol II to the TAP-1 promoter was low in TAP-deficient CMT.64, LMD and B16 cells. Chromatin immunoprecipitation using anti-RNA polymerase II antibody was performed, and the relative levels of RNA polymerase II recruitment to the TAP-1 promoter were assessed as described above using primers specific for the TAP-1 promoter. *Columns*, average of three to six experiments; *bars*, SEM. \*  $P < .05$  compared with TAP-expressing cells (Student's t-test). .... 41
- Figure 2.3.3.1: Nucleotide sequence of the CMT.64-derived TAP-1 promoter region is identical to the corresponding region in murine MHC class II locus. The ATG codon was arbitrarily determined as +1. Motifs located on the sense strand are indicated by a (+), and motifs located on the antisense strand are indicated by a (-). .... 43
- Figure 2.3.4.1: TAP-1 promoter activity is impaired in TAP-deficient CMT.64, LMD and B16 cells. Flow cytometry analysis was performed to measure TAP-1 promoter activity, based on the levels of EGFP expression in pTAP-1-EGFP stable

- transfectants after selection in G418 for 1 month. The IFN- $\gamma$ -treated cells were incubated with 50 ng/ml IFN- $\gamma$  for 48 hours prior to the FACS analysis. Levels of EGFP in the cells transfected the pTAP-1-EGFP were normalized against corresponding values obtained upon transfection with pEGFP-1 vector alone. Data shown are the mean fluorescence intensity  $\pm$  SEM of three independent experiments. \* P < .05 compared with TAP-expressing cells; \*\* P < .05 compared with untreated cells (Student's t-test). ..... 46
- Figure 2.3.5.1: TAP-1 promoter-driven EGFP expression increased in the fused CMT.64-Ltk and LMD-Ltk cells (thick line) in comparison to that in the unfused pTAP-1-EGFP-transfected CMT.64 and LMD cells (thin line). Wild type CMT.64 and LMD were used as negative controls for EGFP expression (shaded area). ..... 48
- Figure 2.3.5.2: Surface expression of K<sup>b</sup> was increased when CMT.64 or LMD (shaded areas) were fused to Ltk cells (broken line). Expression of K<sup>b</sup> on fused CMT.64-Ltk and fused LMD-Ltk cells are displayed by thick lines. As a positive control, expression of K<sup>b</sup> was assessed on IFN- $\gamma$ -treated CMT.64 and LMD cells (thin lines). ..... 48
- Figure 2.3.5.3: No induction of K<sup>b</sup> surface expression in the fused CMT.64(pTAP-1-EGFP)-CMT.64(pEYFP-N1) cells (thick line). CMT.64 cells untreated (shaded area) or treated with IFN- $\gamma$  (thin line) were used as negative or positive control, respectively, for K<sup>b</sup> expression. .... 49
- Figure 2.3.5.4: K<sup>k</sup> surface expression was reduced in the fused CMT.64-Ltk and LMD-Ltk (thick lines) in comparison to that in the wild type Ltk cells (thin lines). Wild type CMT.64 and LMD cells were used as negative controls for K<sup>k</sup> expression (shaded area). ..... 50
- Figure 2.3.6.1: Endogenous levels of IRF-1 and -2 mRNA did not correlate with TAP levels in the cell lines. .... 51
- Figure 2.3.6.2: Overexpression of IRF-1 or -2 in a clone of pTAP-1-EGFP construct-transfected CMT.64 cells did not result in significant changes of the TAP-1 promoter activity. Representative histograms show EGFP expressed by the IRF-1 or IRF-2-overexpressing cells. The shaded areas indicate background green fluorescence of the cells transfected with PBS as negative controls, the thin and thick lines represent EGFP expression in cells overexpressing the IRF that were treated with IFN- $\gamma$  or left untreated, respectively. .... 52
- Figure 2.3.6.3: Overexpression of IRF-1 and -2 modulated IFN- $\beta$  promoter activity linked to a *luciferase* gene. Luciferase activities were normalized against  $\beta$ -galactosidase activities, to correct for variations in transfection efficiencies. Data shown are the average  $\pm$  SEM of three independent experiments. .... 53
- Figure 2.3.7.1: No expression of TAP-1 mRNA from the CMT.64 genome was detectable by RT-PCR in the fused CMT.64-Ltk cells. Amplifications of reverse-transcribed CMT.64 TAP-1 mRNA from IFN- $\gamma$ -treated cells and  $\beta$ -actin mRNA were used as positive controls and loading controls, respectively. .... 55
- Figure 2.3.7.2: Total TAP-1 expression was reduced when CMT.64 and LMD cells were fused with wild type Ltk cells. Results from RT-PCR analysis and Western Blot were shown in top and bottom panel, respectively. Levels of  $\beta$ -actin were used as loading controls. .... 56
- Figure 2.3.8.1: TAP-1 mRNA is rapidly degraded in fused carcinoma-fibroblast cells. . 57

- Figure 2.3.8.2: The stability of S15 and prion mRNA is similar in unfused and fused cells. .... 57
- Figure 3.3.1.1: Differences in TAP-1 promoter activity in stable transfectants generally match the TAP-1 expression profiles better than in transient transfectants. Relative luciferase activity (RLA) in transient (12-72 hours post-transfection) and stable (3-4 weeks post-transfection) transfectants. In the transient transfectants, the luciferase unit in each cell line was determined as the ratio of firefly:renilla luciferase unit. In the stable transfectants, the luciferase unit in each cell line was determined as the ratio of firefly luciferase:copy number of pTAP1-Luc construct integrated into the genome. Relative luciferase activity (RLA) was determined as the luciferase unit in a particular cell line divided by the lowest value of luciferase unit obtained in that particular group of cells. *Columns*, average of three to six independent experiments; *bars*, SEM. \* P < .05 compared with cells that expressed higher TAP-1 and MHC class I in the same group of cells (Student's t-test)..... 77
- Figure 3.3.1.2: Analysis of TAP- 1 and surface MHC class I expression by RT-PCR and flow cytometry, respectively. Shaded area, thin and thick lines represent low (A9 or LMD), medium (D11) and high (TC-1 or PA) levels of MHC class I expression, respectively. Amplification of  $\beta$ -actin cDNA served as an internal control in the RT-PCR analysis. Data are representatives of three experiments..... 78
- Figure 3.3.1.3: RNA pol II binding to TAP-1 promoter is low in TAP-deficient carcinomas. The levels of RNA pol II in TAP-1 promoter of each cell line were assessed by chromatin immunoprecipitation using anti-RNA pol II Ab. The eluted DNA fragment were purified and used as templates for real-time PCR analysis using primers specific for the 3'-end of the TAP-1 promoter. Relative RNA pol II levels were determined as the ratio of copy numbers of the eluted TAP-1 promoter and copy numbers of the corresponding inputs. The smallest ratio in each group of experiments was arbitrarily determined as 1. *Columns*, average of three to six experiments; *bars*, SEM. \* P < .05 compared with cells that expressed higher TAP-1 and MHC class I in the same group of cells (Student's t-test)..... 80
- Figure 3.3.2.1: Acetyl-histone H3 binding to TAP-1 promoter is low in TAP-deficient carcinomas. The levels of acetyl-histone H3 in TAP-1 promoter of each cell line were assessed by chromatin immunoprecipitation using anti-acetyl-histone H3 Ab. The eluted DNA fragments were purified and used as templates for real-time PCR analysis using primers specific for the 3'-end of the TAP-1 promoter. Relative acetyl-histone H3 levels were determined as the ratio of copy numbers of the eluted TAP-1 promoter and copy numbers of the corresponding inputs. The smallest ratio in each group of experiments was arbitrarily determined as 1. *Columns*, average of three to six experiments; *bars*, SEM. \* P < .05 compared with cells that expressed higher TAP-1 and MHC class I in the same group of cells (Student's t-test)..... 82
- Figure 3.3.3.1: TAP-1 promoter sequence with transcription factor binding motifs and 5' truncation sites. The TAP-1 ATG codon was arbitrarily determined as +1. Truncation sites are indicated by numbered arrows. Motifs located on the sense strand are indicated by a (+) and motifs located on the antisense strand are indicated by a (-)..... 83
- Figure 3.3.3.2: A critical region that is responsible for differential activity of the TAP-1 promoter in TAP-expressing and TAP-deficient cells is found in-between -427 and -

- 401 region of the promoter. RLA was measured in stable transfectants. The largest value in each group of experiments was arbitrarily determined as 1. *Columns*, average of five experiments; *bars*, SEM. \* P < .05 compared with TAP-expressing cells in the same group (Student's t-test). ..... 84
- Figure 3.3.4.1: Expression of CBP proteins is similar in TAP-expressing and in TAP-deficient carcinoma cells..... 85
- Figure 3.3.4.2: CBP binding to TAP-1 promoter is impaired in TAP-deficient, metastatic carcinomas. Chromatin immunoprecipitation using anti-CBP antibody was performed as described earlier. *Columns*, average of four experiments; *bars*, SEM. \* P < .05 compared with cells that expressed the highest TAP-1 and MHC class I in the same group of cells (Student's t-test)..... 86
- Figure 3.3.5.1: IFN- $\gamma$  treatment improves the recruitment of CBP, acetyl-histone H3 and RNA pol II to TAP-1 promoter, most significantly in TAP-deficient cells. Chromatin immunoprecipitation using *A*, anti-CBP, *B*, anti-acetyl-histone H3 or *C*, anti-RNA pol II antibody was performed as described earlier. *Columns*, average of three to four experiments; *bars*, SEM. \* P < .05 compared with untreated cells (Student's t-test)..... 87
- Figure 3.3.6.1: TSA treatment enhances RNA pol II recruitment to TAP-1 promoter and TAP-1 promoter activity. *A*, The levels of RNA Pol II in TAP-1 promoter of each cell line were assessed by chromatin immunoprecipitation using anti-RNA pol II. *B*, TAP-1 promoter activity in stable transfectants was determined by luciferase assay. *Columns*, average of three to six experiments; *bars*, SEM. \* P < .05 compared with untreated cells (Student's t-test)..... 89
- Figure 3.3.6.2: TSA treatment does not significantly alter the levels of histone H3 acetylation in TAP-1 promoter. The levels of acetyl-histone H3 in TAP-1 promoter of each cell line were assessed by chromatin immunoprecipitation using anti-acetyl-histone H3 antibody. *Columns*, average of three to six experiments; *bars*, SEM. ... 90
- Figure 3.3.7.1: TAP-1 expression in all cell lines, particularly in the TAP-deficient carcinomas, was up-regulated with TSA treatment. Up-regulated TAP-1 expression from IFN- $\gamma$ -treated cells was used as a positive control.  $\beta$ -actin expression served as a loading control. Data are representatives of three experiments. .... 91
- Figure 3.3.7.2: Expression of LMP-2, TAP-2 and tapasin in all cell lines, particularly in the TAP-deficient carcinomas, was up-regulated with TSA treatment. Amplification of APM cDNA from IFN- $\gamma$ -treated cells was used as a positive control.  $\beta$ -actin expression served as a loading control. Data are representatives of three experiments. .... 92
- Figure 3.3.7.3: Surface H-2K<sup>b</sup> expression, particularly on MHC class I-deficient cells, was enhanced by TSA treatment. Cells untreated (shaded areas) or treated with 100 ng/ml TSA (thick lines) or 50 ng/ml IFN- $\gamma$  (thin lines) were stained with PE-conjugated anti-H-2K<sup>b</sup> mAb. Data are representatives of three experiments. .... 93
- Figure 3.3.7.4: TSA treatment improves HPV-positive tumor cell killing by CTLs. Target cells were uninfected or VSV-infected, untreated or treated with TSA or IFN- $\gamma$  for 24 hours before infection with the VSV. CTL assays were performed using effector:target ratio of 0.8:1 to 200:1. Representative data using 22:1 effector:target ratio are shown in this figure. All cells were infected with VSV at a MOI of 7.5 for

- 16hr. *Columns*, average of three experiments; *bars*, SEM. \*  $P \leq .05$  compared with untreated cells (Student's t-test)..... 94
- Figure 3.3.7.5: TSA treatment improves B16F10 tumor cell killing by CTLs. Target cells were uninfected or VSV-infected, untreated or treated with various concentrations of TSA for 24 hours before infection with the VSV. CTL assay was performed using effector:target ratio of 2.5:1 to 67:1. All cells were infected with VSV at a MOI of 7.5 for 16hr..... 95
- Figure 3.3.8.1: TSA treatment suppresses tumor growth *in vivo*. A9 (MHC class I-deficient cells) tumor growth was suppressed in mice treated with 500  $\mu\text{g}/\text{kg}$  of TSA daily compared to in those treated with DMSO vehicle control ( $n = 8$  per treatment group). TC-1 group represented tumor growth in mice injected with high MHC class I-expressing cells ( $n = 9$ ). Data represent the mean tumor volume  $\pm$  SEM..... 96
- Figure 3.3.8.2: TAP-1 promoter activity is enhanced in TAP-deficient tumor cells isolated from TSA-treated mice. TAP-1 promoter-driven Luciferase (pTAP1-Luc) expression is higher in A9 cells isolated from TSA-treated mice than in those isolated from DMSO-treated mice ( $n=4$  per treatment group). \*  $P < .05$  compared with cells from DMSO-treated mice (Student's t-test). ..... 97
- Figure 4.3.1.1: TAP-1 promoter-driven EGFP expression is enhanced in the fused 1E10-A549 cells. The levels of EGFP expression in untransfected CMT.64 cells, 1E10 (pTAP1-EGFP-transfected CMT.64) cells and fused 1E10-A549 cells are represented by a shaded area, a thin line and a thick line, respectively..... 117
- Figure 4.3.3.1: The ORF found in the homologous region of human chromosome 3 clone RP11-27016 map 3p (NCBI accession no. AC090885) and the 1.3 kb sequence obtained from human lung cDNA library screening..... 119
- Figure 4.3.6.1: RT-PCR analysis of the overexpression of the TAP-1 activator candidate genes in CMT.64 and LMD cells. G: cDNA template was derived from pIRES2-gene transfectants; V: cDNA template was derived from pIRES2-EGFP transfectants. Amplification of  $\beta$ -actin cDNA served as a loading control. .... 126
- Figure 4.3.6.2: TAP-1 expression was up-regulated in some of the CMT.64 and LMD cells transfected with individual pIRES2-gene constructs. Amplification of cDNA from IFN- $\gamma$ -treated cells was used as a positive control.  $\beta$ -actin expression served as a loading control. Data are representatives of one set of RT-PCR analysis per group of CMT.64 and LMD transfectants..... 127
- Figure 4.3.6.3: No upregulation of H-2K<sup>b</sup> expression was detected on the surface of LMD cells overexpressing HLA-Cw\*04 null allele and HC3 (thick lines). H-2K<sup>b</sup> expression in pIRES-2-EGFP-transfected LMD cells (shaded areas) was similar to the negative control, the unstained pIRES-2-gene-transfected cells (thin lines). As a positive control, H-2K<sup>b</sup> expression was assessed in IFN- $\gamma$ -treated LMD cells (broken lines)..... 128
- Figure 5.1.1: A proposed model of the mechanisms underlying TAP-1 deficiency in carcinomas and release of the transcriptional repression upon relaxation of chromatin structure around the *Tap-1* gene locus. The boxes on the DNA strand represent critical binding sites for various transcription factors that regulate TAP-1 transcription. CBP is a transcriptional co-activator that possesses intrinsic HAT activity. In this model, the recruitment of CBP to TAP-1 promoter facilitates histone acetylation that leads to relaxation of the chromatin structure around the region,

increasing the accessibility of the DNA template by transcription factors (TFs) and  
RNA pol II complex..... 140

## List of Abbreviations

<sup>51</sup> Cr	: chromium-51
ABC	: ATP-binding cassette
ACCRE	: autonomous chromatin condensation regulatory element
AMP	: adenosine monophosphate
APC	: antigen-presenting cell
APM	: antigen processing machinery
ARE	: adenosine-uracil-rich element
ATP	: adenosine triphosphate
β2m	: beta-2 microglobulin
bp	: base pair
CBP	: CREB-binding protein
cDNA	: complementary DNA
CDS	: coding sequence
ChIP	: chromatin immunoprecipitation
CREB	: cyclic AMP (cAMP) response element-binding
CTL	: cytotoxic T lymphocyte
DNA	: deoxyribonucleic acid
dsDNA	: double-stranded DNA
EDTA	: ethylenediaminetetraacetic acid
EGFP	: enhanced green fluorescent protein
EYFP	: enhanced yellow fluorescent protein
ER	: endoplasmic reticulum

FACS	: fluorescent-activated cell sorting
FBS	: fetal bovine serum
FCS	: fetal calf serum
FITC	: fluorescein isothiocyanate
GM-CSF	: granulocyte-macrophage colony-stimulating factor
HAT	: histone acetyltransferase
HDAC	: histone deacetylase
HDACi	: histone deacetylase inhibitor
HLA	: human leukocyte antigen
HPV	: human papillomavirus
IFN	: interferon
Ii	: invariant chain
IL-2	: interleukin-2
i.p.	: intraperitoneal
IRES	: internal ribosome entry site
IRF	: interferon regulatory factor
kb	: kilo base pair
LMP	: low-molecular-weight protein
MHC	: major histocompatibility complex
MIIC	: major histocompatibility complex class II compartment
MOI	: multiplicity of infection
MW	: molecular weight
mRNA	: messenger ribonucleic acid

NBD	: nucleotide-binding domain
NK cell	: natural killer cell
PAGE	: polyacrylamide gel electrophoresis
PBS	: phosphate-buffered saline
PCAF	: p300/CBP-associated factor
PCR	: polymerase chain reaction
PE	: phycoerythrin
Poly(A)	: poly-adenylated
RNA	: ribonucleic acid
RNA pol II	: RNA polymerase II
RT-PCR	: reverse transcriptase PCR
s.c.	: subcutaneous
SD	: standard deviation
SDS	: sodium dodecyl sulfate
SEM	: standard error of the mean
TAP	: transporter associated with antigen processing
TCR	: T-cell receptor
TF	: transcription factor
TGF- $\beta$	: transforming growth factor beta
TMD	: transmembrane domain
TNF- $\alpha$	: tumor necrosis factor alpha
TSA	: trichostatin A
TTP	: tristetraprolin

UTR : untranslated region

VSV : vesicular stomatitis virus

## Acknowledgments

This thesis could not have been written without the invaluable support I received from my thesis committee, family, friends and colleagues. I would like to acknowledge my thesis supervisor, Dr. Wilf Jefferies, for giving me the opportunity to do this graduate work in his laboratory, and for the support and guidance he has provided throughout my studies. I would also like to thank my committee members: Dr. Doug Waterfield, Dr. John Gosline, Dr. Linda Matsuuchi and Dr. Fumio Takei, and my external examiner, Dr. Soldano Ferrone, for discussions, guidance and encouragement throughout my studies, as well as for thorough reading of my thesis and excellent suggestions for improvements. I am deeply grateful to my mentor, Dr. Penny Le Couteur, who always believed in me and encouraged me to fly high. Penny has been an amazing role model as a great scientist, a good mother and a wonderful person.

Many thanks to Dr. Muriel David, Susan Chen and Robyn Seipp for their great collaborations, ideas and input. This project would not have been a success without help from hardworking undergraduate project students, Alonso Garduno and Jennifer Hartikainen, as well as excellent technical assistance from Andy Johnson in flow cytometry, Kyung-Bok Choi, Linda Li and Bing Cai in molecular biology and immunology, and Ray Gopaul in *in vivo* experimentation. I would like to acknowledge the National Cancer Institute of Canada, Canadian Institutes of Health Research, Canadian Network for Vaccines and Immunotherapeutics, Prostate Cancer Research Foundation of Canada and Genemax, Inc. for providing grant support. I am grateful to all my wonderful labmates, especially Cheryl, Robyn, Anna, Kyla, Meimei and Kaan, for discussions and input, for being with me in good and in bad times at the lab, and of

course for all the good times we had together. I would also like to thank past and present members of the Biomedical Research Centre and Michael Smith Laboratories for their help, friendship and for a wonderful work environment.

Finally, I would like to thank my parents, sister and grandparents for their unconditional love and support all these years. Very special thanks to Simon for his love and encouragement all along, especially over the miles in the past 3.5 years. This separation has been very difficult, but will hopefully only make us stronger. At the same time, this gave me an interesting thesis-writing experience up in the sky above every continent in-between Vancouver and Boston.

## **Dedication**

This thesis is dedicated to my mother, Christiana Budiono, for her unconditional love, support and tireless encouragement from 12,783 km away.

## Co-Authorship Statement

Dr. Muriel D. David (Biomedical Research Centre, Vancouver, BC) provided guidance and technical help with promoter analysis, chromatin immunoprecipitation and luciferase assays reported in this thesis. She also performed the  $\beta$ -galactosidase assays and their data analysis reported in Chapter 2.

Susan S. Chen (Department of Zoology, University of British Columbia, Vancouver, BC) trained and helped me to master new laboratory techniques during the early stage of my doctoral research.

Dr. John Hiscott (Lady Davis Institute of Medical Research, McGill University, Montreal, QC) provided the interferon regulatory factor (IRF) expression vectors and the interferon beta (IFN- $\beta$ ) promoter construct reported in Chapter 2.

Robyn P. Seipp (Department of Zoology, University of British Columbia, Vancouver, BC) performed the cytotoxicity (CTL) assays and CTL data analysis reported in Chapter 3.

Jennifer A. Hartikainen (Department of Microbiology and Immunology, University of British Columbia, Vancouver, BC) provided help with the construction of truncated TAP-1 promoter constructs and the luciferase assays reported in Chapter 3.

Rayshad Gopaul (Michael Smith Laboratories, Vancouver, BC) shared the duties with me in injecting mice, recording data and monitoring the animals during the *in vivo* experiment reported in Chapter 3.

I performed all the other experiments and data analyses reported in this thesis.

## Chapter 1 : General Introduction

Recognition of pre-cancerous and virus-infected cells by our immune system is critical for protecting us against malignant cells and viral infections. The host's immune system has the potential to kill abnormal cells before they become malignant cancers; however, many cancer cells have defects in components of the antigen processing and presentation pathways that allow them to avoid detection by the immune system [1-4]. One of the key components that is often missing in tumors is a heterodimer of the Transporters associated with Antigen Processing (TAP)-1 and TAP-2 molecules that normally functions in transporting self-, virus-, or tumor-derived peptides into the endoplasmic reticulum, in which the peptides can be loaded into Major Histocompatibility Complex (MHC) class I molecules. In a functional pathway, the MHC class I - peptide complexes are then transported via the Golgi and further displayed on the cell surface, where they can be recognized by the circulating cytotoxic T lymphocytes (CTLs). The CTLs function to bind to and eventually kill the cancer or virus-infected cells. The importance of TAP-1 function in immunosurveillance has been highlighted in previous studies that demonstrated that by restoring TAP-1 expression in TAP-deficient cancer cells, the entire MHC class I antigen presentation pathway can be reconstituted, leading to the elimination of the cancer cells by CTLs [1, 5-8]. However, the mechanisms underlying TAP-1 downregulation in cancer cells remain poorly understood [7]. The goal of this research is to contribute to a better understanding of the mechanisms that lead to TAP downregulation in malignant cells, as well as to further characterize novel transcriptional regulators of TAP-1.

## **1.1 Overview of the Immune System**

The immune system that protects organisms from infections is divided into 2 components: the innate and the adaptive immune system. Innate immune systems, which are found in nearly all living organisms, provide an immediate, non-specific response against all invading pathogens [9, 10]. Jawed vertebrates possess another layer of protection provided by the adaptive immune system that elicits delayed, but specific and long-lasting immune responses against pathogens, as well as pre-cancerous cells that express tumor-specific antigens [10].

Tumor specific antigens can be classified either as self- or non-self antigens, depending on their origin. Tumor-specific antigens in cells transformed by viral infection, such as human papillomaviruses (HPV), the Epstein-Barr virus (EBV) and the human herpesvirus-8 (HHV-8), are mainly derived from viral proteins and can potentially be recognized by the host's immune system as non-self antigens [11]. Alternatively, tumors may develop from spontaneous transformation of normal cells, for example, due to mutations of self molecules [12]. Although T-cell receptors (TCRs) can often discriminate even single amino acid changes in peptides, thus allowing activated T cells to recognize cancer cells that express mutated self peptides bound to MHC class I molecules [12], immunotherapy approaches for these types of tumors are facing great challenges due to low immunogenicity against cells that express self antigens. Additional special strategies, such as vaccination and breaking of tolerance [11, 12], are required to be implemented in parallel with the treatments in order to enhance immune responses against the abnormal cells.

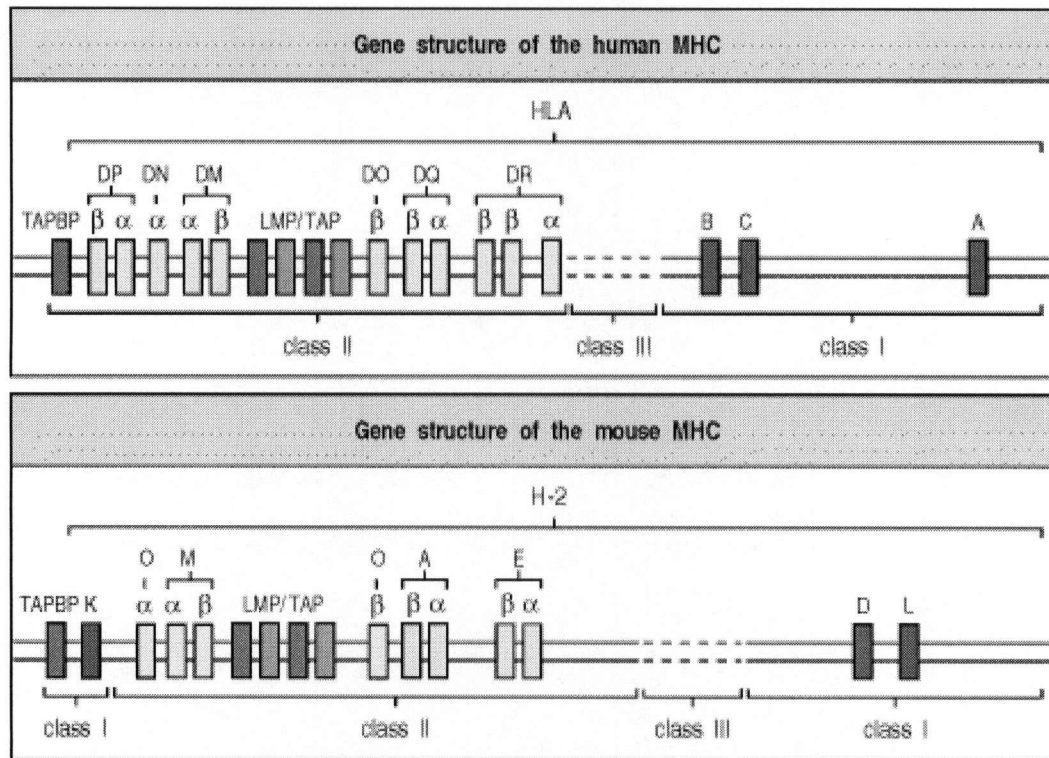
## 1.2 Antigen Presentation

Adaptive immunity relies on the ability of the T-cell receptors (TCRs) to distinguish between self and non-self molecules, bound by MHC molecules and presented on the cell surface. Presentation of peptides derived from self proteins on a cell surface does not normally trigger immune response, since T cells with the ability to recognize self-derived peptides are deleted during T-cell development in the thymus, in a process known as negative selection [10]. In contrast, recognition of cells that express foreign antigens or mutated self antigens by the T cells generally triggers a cascade of activation of components of the immune system, such as B cells, macrophages and other T cells, that leads to the elimination of the invading pathogens and the abnormal cells [10, 12].

### 1.2.1 Major Histocompatibility Complex (MHC) genetics

The MHC locus that is located on chromosome 6 in humans and chromosome 17 in the mouse, contains the most polymorphic genes known in the living organisms [10]. MHC polymorphism is highly advantageous for the presentation of a wide range of diversity of peptides to T-cell receptors. In humans, the MHC is called the Human Leukocyte Antigen (HLA). In the mouse, the MHC genes are known as the *H-2* genes. The cluster of MHC genes is divided into *MHC class I*, *MHC class II* and *MHC class III* genes. The organization of the MHC locus is similar in both species, although the *H-2k* gene in the mouse is translocated to the edge of the MHC gene cluster, near the *Tapbp* gene and the centromere (Figure 1.2.1.1). There are three main MHC class I genes in both species: *HLA-A*, *-B* and *-C* in humans, or *H-2k*, *-d* and *-l* in the mouse. The MHC class II region includes the genes for *HLA-DP*, *-DQ* and *-DR* in humans, or *H-2A* and *-E*

in the mouse. MHC class III region includes the genes encoding various other immune function proteins, including the complement proteins C4, C2 and factor B, as well as the tumor necrosis factor (TNF)- $\alpha$  and lymphotoxin.



© Janeway C., et al., 2001. Copied under license from Access Copyright. Further reproduction prohibited.

**Figure 1.2.1.1: Genetic organization of human and mouse MHC genes** (image reprinted from reference no. [10], by permission).

### 1.2.2 MHC molecules

An MHC molecule functions by binding peptide fragments and presenting the complex on the cell surface. Activation of immune responses only occurs upon TCR recognition of a complex of a foreign peptide or a mutated self peptide bound to an MHC molecule on the cell surface. The MHC molecules are divided into 2 classes: MHC class I and MHC class II molecules, which differ in their structure, their expression pattern on tissues, and the types and sizes of antigen presented [10]. MHC class I molecules are expressed on the surface of all nucleated cells, whereas MHC class II molecules are normally present only on B cells and on special antigen-presenting cells (APCs): dendritic cells and macrophages. MHC class I molecules generally present short (8-10 amino acids) intracellularly-derived peptides, such as viral antigens and tumor-specific antigens. Recognition of MHC class I - peptide complexes by specific TCRs on CD8<sup>+</sup> cytotoxic T lymphocytes (CTLs) triggers the activation of CTL responses that ultimately result in killing of the virus-infected or cancerous cells. MHC class II molecules are capable of presenting longer (i.e., more than 13 amino acids) extracellularly-derived peptides, such as peptides generated from bacterial proteins. Peptides bound by MHC class II molecules can be recognized by CD4<sup>+</sup> T cells, also known as T helper (Th) cells, which mainly function to activate other effector cells of the immune system. MHC class II antigen presentation and the importance of Th cells in cancer immunity will be further discussed in section 1.2.5.

### 1.2.3 MHC class I antigen presentation

The work in this thesis focuses on the presentation of tumor-specific antigens by MHC class I molecules, since the recognition of neoplastic cells by CD8<sup>+</sup> CTLs has been shown to be one of the most important events required for an effective anti-tumor response [13]. MHC class I molecules generally present peptides that are generated intracellularly, hence the name endogenous antigens. Viral antigens and tumor-specific antigens are examples of intracellularly-derived proteins. In some cases, MHC class I molecules can present peptides derived from extracellular proteins, or exogenous antigens, in a process called cross presentation [14, 15]. This thesis focuses on the study of tumor antigen presentation via the classical MHC class I antigen presentation pathway (Figure 1.2.3.1).

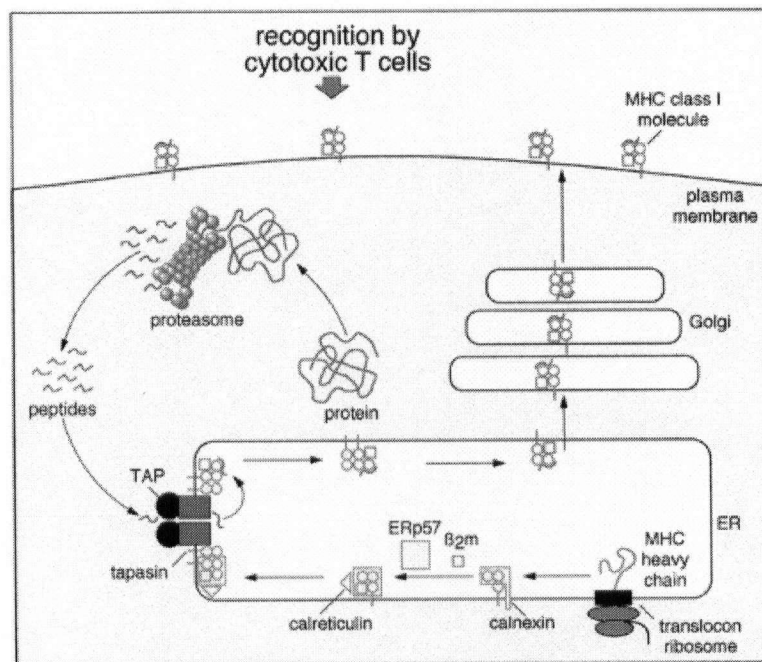


**Figure 1.2.3.1: MHC class I antigen presentation pathway** (image reprinted from reference no. [7], by permission).

In this pathway, endogenous proteins are degraded into smaller peptides by the action of multicatalytic enzyme subunits of the proteasome. The peptides are then transported by a heterodimer transporter that consists of TAP-1 and TAP-2 subunits into the lumen of endoplasmic reticulum (ER), in which MHC class I heavy chains are synthesized *de novo*, folded and coupled with beta-2 microglobulin ( $\beta 2m$ ) molecules in a process assisted by chaperone proteins (BiP, calnexin, calreticulin, ERp57 and tapasin) [16, 17]. In the lumen of ER, the peptides are loaded into an MHC class I heavy chain/ $\beta 2m$  molecule, forming a stable ternary complex that can be transported onto the cell surface via the *trans*-Golgi network. The host's cytotoxic T lymphocytes (CTLs) have the potential to recognize neoplastic cells that express tumor-specific antigens on their surface, and furthermore, to kill the abnormal cells through the release of cytolytic granules: perforin and granzymes [10].

#### **1.2.4 Transporters associated with Antigen Processing (TAP) structure and function**

TAP-1 and TAP-2 molecules belong to the superfamily of ATP-binding cassette (ABC) transporters, one of the largest protein families that span bacteria to humans. They are characterized by the presence of two cytoplasmic ATP-binding domains and two hydrophobic transmembrane domains (TMDs) [7, 18] (Figure 1.2.4.1). Most ABC transporters function by transporting a broad range of substrates, including amino acids, lipids, sugars, ions and drugs, across membranes by using the energy obtained from ATP hydrolysis [18, 19]. The TAP transporter, which consists of a heterodimer of TAP-1 and TAP-2 molecules embedded in the membranes of the endoplasmic reticulum (ER) and *cis*-Golgi, specializes in transporting endogenous peptides from the cytosol into the

lumen of ER [7, 20, 21]. The energy resulted from ATP hydrolysis triggers conformational changes in the nucleotide-binding domain (NBD) and the TMDs, causing the binding and movement of peptides across the ER membrane [21].

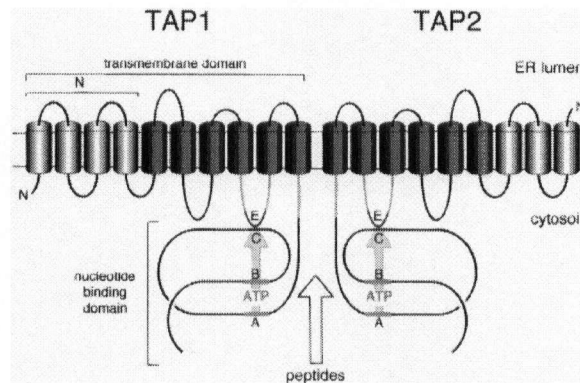


**Figure 1.2.4.1: A heterodimer of the TAP-1 and TAP-2 molecules** (image reprinted from reference no. [7], by permission).

## 1.2.5 MHC class II antigen presentation and CD4<sup>+</sup> T cells in cancer immunity

In the MHC class II antigen presentation pathway (Figure 1.2.5.1), extracellular proteins are endocytosed into intracellular vesicles and degraded into peptides by the action of cathepsins in the vesicles. Similarly to the MHC class I molecules, the MHC class II molecules are synthesized *de novo* inside the endoplasmic reticulum (ER). An invariant chain (Ii) molecule binds in the groove of a newly synthesized MHC class II molecule to prevent the binding of peptides in the ER. The MHC class II - Ii complex is then transported from the ER into a vesicle, called the MHC class II compartment (MIIC), where Ii is trimmed into a short fragment—called the CLIP peptide—that is still bound to the MHC class II groove. A peptide-loaded vesicle then fuses with the MIIC,

where CLIP is removed by HLA-DM and antigenic peptides are loaded onto MHC class II molecules. The MHC class II - peptide complexes are then transported to the cell surface for surveillance by CD4<sup>+</sup> T-helper (Th) cells.

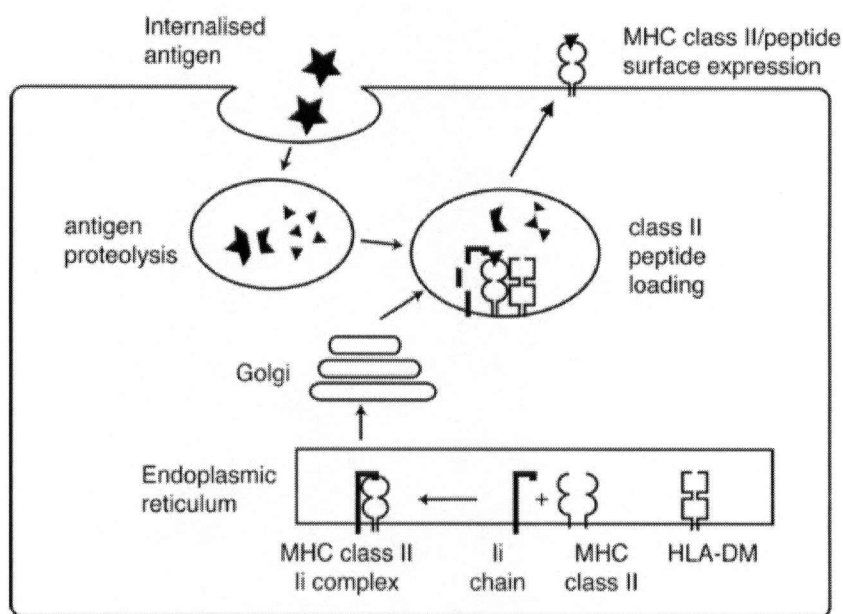


**Figure 1.2.5.1: MHC class II antigen presentation pathway** (image reprinted from reference no. [22], by permission).

The two main subsets of CD4<sup>+</sup> Th cells are the Th1 and Th2 cells. They are classified based on their distinct cytokine production patterns [23]. The Th1 cells are particularly important for antitumor immunity due to their ability to produce interferon gamma (IFN- $\gamma$ ), tumor necrosis factor alpha (TNF- $\alpha$ ) and interleukin-2 (IL-2), which are important for the development and sustained proliferation of CD8<sup>+</sup> CTLs [24, 25]. The Th2 cells are predominantly involved in humoral immune response, producing IL-4 and IL-5 that stimulate antibody production by activated B cells [24]. The presence of a large number of Th2 cells in a tumor microenvironment generally impairs tumor immunity due

to their production of IL-10 and TGF- $\beta$  that act as immunosuppressive cytokines [26, 27]. However, in rare cases, Th2 cells can produce natural antibodies against tumors [28]. A simplified diagram outlining complex interactions between tumor cells, professional antigen-presenting cells and various lymphocytes is shown in Figure 1.2.5.2 below.

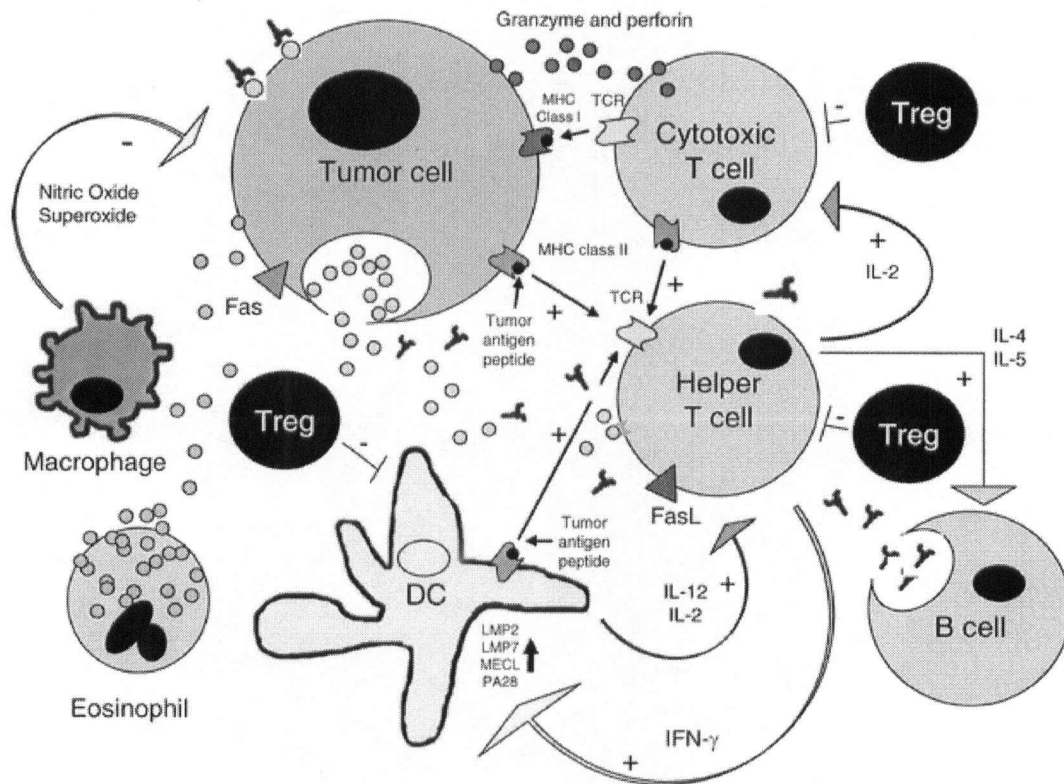


**Figure 1.2.5.2: The complex interaction between a tumor cell, professional antigen-presenting cells, CTLs, Th cells, B cells and other lymphocytes in the tumor microenvironment.** A (+) sign indicates an activating signal on the antitumor response while a (-) sign indicates an inhibitory effect (image reprinted from reference no. [24], by permission).

### **1.3 Disruption of the MHC Class I Antigen Processing Pathway and the Development of Tumors**

Forty to ninety percent of HLA (or MHC in the mouse) class I-positive precursors of human tumors are found to develop into HLA class I-negative tumors [29]. TAP deficiency is one of the common phenotypes that distinguish malignant transformed cells from their normal precursors [20]. TAP downregulation leads to the disruption of the process by which tumor-specific peptides are transported into the lumen of ER and loaded onto MHC class I –  $\beta$ 2m complex [1]. As a consequence, no stable complex of tumor peptide - MHC class I can be presented on the cell surface, rendering the abnormal cell to stay undetected by the immune surveillance. Downregulated or total loss of expression of TAP-1 and TAP-2 has been observed in many tumor cell lines and surgically-removed tumor specimens, such as Hodgkin's lymphoma, myeloma, melanoma and many types of carcinomas, such as, colorectal, cervical, breast, lung, prostate, renal cell and hepatocellular carcinomas [1, 2, 4]. Interestingly, the level of TAP-1 downregulation in carcinomas was found to significantly correlate with tumor progression and reduced survival [1, 7, 8, 20]. The downregulation is more often caused by regulatory defects rather than by structural defects due to mutations within the *TAP-1* gene itself [2, 4]. Other mechanisms that lead to an impaired MHC class I antigen presentation in tumor cells include the loss of one copy of the chromosome in which MHC class I genes are located, structural alterations, methylation, or deregulation of genes coding for the MHC class I heavy chain and  $\beta$ 2m, as well as of those coding for antigen processing machinery (APM) components, such as Tapasin, and the proteasome subunits: LMP-2 and LMP-7 [4, 30].

Based on surface MHC class I expression levels, a major anti-tumor mechanism other than that exerted by the CD8<sup>+</sup> CTLs is provided by natural killer (NK) cells [31]. CD8<sup>+</sup> CTLs recognize and destroy target cells that express the surface MHC class I-tumor antigen complex, whereas NK cell activity is triggered upon recognition of cells that do not express surface MHC class I, since MHC class I molecules generally serve as ligands for NK cell inhibitory receptors [31]. NK cell-mediated cytotoxicity is regulated by a balance of signals transmitted by activating and inhibitory receptors. Unfortunately, NK cell infiltration is generally low in neoplastic tissues [29] and the NK activating signal is often hampered by immunosuppressive cytokines, such as TGF- $\beta$ , within the tumor microenvironment [13, 32]. Therefore, NK cell-mediated cytotoxicity is generally not sufficient to provide complete protection against a large proportion of cancer cells with down-regulated expression of MHC class I. Further research is needed in order to create ways to attract more NK cells into neoplastic tissues and to make the NK cell activating signal more favorable within the tumor microenvironment.

## 1.4 TAP-based Immunotherapy

The importance of TAP-1 function in immunosurveillance against cancers has been highlighted in several studies that demonstrated the reconstitution of MHC class I antigen presentation upon restoration of TAP-1 expression in cancer cell lines exhibiting down-regulated expression of several APM components [27, 33]. This finding is encouraging for the development of a general immunotherapy method for different types of cancers that possess multiple deficiencies of APM components. Moreover, reconstitution of TAP-1 function in highly metastatic, MHC class I-deficient murine lung carcinoma and melanoma cell lines, CMT.64 and B16, respectively, has been shown to improve immune recognition of the cancer cells *in vivo*, resulting in a decrease of tumor growth and metastatic ability [5, 20, 34]. Restoration of TAP-1 alone resulted in an improved ability of cancer cells to present viral and/or tumor-specific peptides, yielding similar anti-viral and anti-tumor effects as those resulted from the induction of both TAP-1 and TAP-2, whereas expression of TAP-2 alone did not show the effects [6, 35, 36]. This may be caused by instability of TAP-2 molecule in the absence of pre-existing TAP-1, whereas TAP-1 molecule and assembled TAP heterodimer are highly stable *in vivo* [5, 6]. Heterodimerization of TAP subunits is required to protect TAP-2 from rapid degradation by a proteasome-dependent pathway [21]. These observations indicate that induction of TAP-1 expression is an important aspect that shall be considered in the development of immunotherapy for various types of cancers.

The TAP-based immunotherapy approach possesses several advantages over many other immunotherapy methods. One of the advantages is that TAP is a component of normal cells, and to-date, no toxicity or autoimmunity reaction has been observed in

animal tumor models that were given TAP-based therapy [21]. Therefore, based on the low risk of toxicity, it may not be necessary to target TAP exclusively into the cancer cells. This would make TAP an attractive candidate for cancer gene therapy since the development of methods to deliver an efficient dose of therapeutic gene remains the primary challenge in cancer gene therapy [6].

Another advantage of TAP-based therapy is that it is not restricted by the haplotype of MHC molecules and the type of tumor antigens, since TAP molecules act independently of the two factors [37]. MHC polymorphism and various types of tumor-associated antigens—many of them not yet characterized—remain as challenges in the development of immunotherapy approaches [6, 36].

Finally, recent studies have demonstrated that recombinant TAP could be used as a novel, non-toxic adjuvant that increases vaccine efficiency [38-41]. Adverse responses to standard doses of inocula are common problems encountered in vaccination, due to toxicity of vaccine components [42]. With the use of an adjuvant, immune responses could potentially be triggered by administering lower doses of inocula, thus decreasing the risk of adverse side effects. This finding denotes the importance of TAP, which is to be considered in the development of vaccines against cancers and widespread infectious diseases.

## 1.5 Regulation of TAP-1 Expression

The goal of this thesis is to gain an understanding of how *Tap-1* gene expression is impaired in metastatic carcinomas. Initially, this work was focused on transcriptional regulation of TAP-1, since the TAP-1 downregulation observed in many carcinomas occurred at the mRNA level [5, 6, 43]. This work was then expanded to study epigenetic mechanisms that often also play significant roles in the regulation of gene expression [44]. Defects in translational mechanisms can also contribute to the impairment of a gene expression; however, translational regulation of TAP-1 is beyond the scope of this thesis.

### 1.5.1 Organization of *Tap* and *Lmp* genes within the mouse MHC class II locus

The genes encoding TAP-1 and TAP-2 molecules are located within the MHC class II region, in close association with the genes encoding two proteasomal subunits: low-molecular-mass polypeptides (LMP)-2 and LMP-7 [7, 10]. Multicatalytic enzyme subunits of the proteasome are capable of degrading intracellular proteins into smaller peptides that can be loaded into the lumen of the endoplasmic reticulum by a heterodimer of TAP-1 and TAP-2 molecules. A diagram outlining the organization of these genes within the mouse MHC class II locus is shown in Figure 1.5.1.1 below.

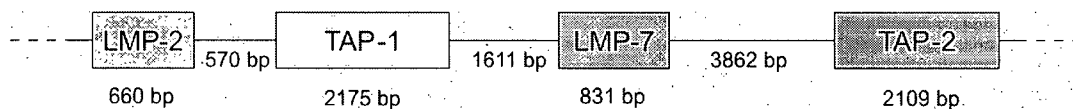


**Figure 1.5.1.1: Organization of *Tap* and *Lmp* genes in the mouse MHC class II locus.** The sizes of the coding sequences (CDS) and intergenic regions are shown in the diagram.

In humans, it was found that a bi-directional promoter of *LMP-2* and *TAP-1* genes is located in the 593 bp region in-between the two genes [45]. This promoter contains GC-rich regions characterizing putative Sp-1 binding sites, but does not contain a TATA box. At least 18 transcriptional start sites of *TAP-1* gene were found within the promoter. This finding of multiple transcriptional start sites is consistent with observations in other TATA-less, GC-rich promoters [46]. Prior to the work in this thesis, mouse TAP-1 promoter had never been cloned and analysed. This work is described for the first time in Chapter 2.

### **1.5.2 Possible mechanisms of TAP-1 mRNA downregulation in carcinomas**

Several mechanisms tested in this thesis include:

#### **1.5.2.1 Transcriptional mechanisms**

Reduced transcription of *Tap-1* gene could be caused by mutations in *cis*-acting consensus sequences within its promoter. This might lead to the inability of important transcription factors to recognize and to bind to the mutated DNA template in the promoter. Other possible mechanisms include overexpression of transcriptional repressors and/or the lack of *trans*-activators binding to the TAP-1 promoter.

#### **1.5.2.2 Post-transcriptional mechanisms**

Degradation of mRNA transcripts is a normal turnover process of coordinated gene expression [44, 47, 48]. Stability of an mRNA depends on its structure and sequence, such as the presence of a cap in its 5' end that protects against 5'-3' exonucleases, the presence of de-stabilizing sequences, for example AU-rich elements

(ARE) in the 3'-untranslated region (3'UTR), and the length of poly-adenylated (poly(A)) sequence in its 3' end that protects against 3'-5' exonucleases [44]. Gene mutation and/or aberrant expression of RNA-binding proteins with the ability to either promote or inhibit mRNA degradation might lead to accelerated rate of mRNA degradation, thus reduced expression of the gene.

### 1.5.2.3 Epigenetic mechanisms

Epigenetic mechanism is described as a heritable change in gene expression that occurs without a change in DNA sequence [49]. Epigenetic modifications affect gene expression through modulation of chromatin structures and/or DNA methylation [44]. Epigenetic mechanisms could provide an extra layer of transcriptional control that regulates how genes are expressed, by modulating the interaction between histone and DNA complexes [49]. This would in turn affect the accessibility of DNA templates by transcriptional machinery.

The key event that leads to the modulation of chromatin structures is the modification of N-terminal tails of the histone proteins, particularly of histone H3 and H4 [44]. Known modifications of histone proteins include: acetylation, methylation, phosphorylation, ubiquitination and sumoylation [44, 50-54]. To-date, histone acetylation is the most widely studied mechanism. A high level of acetylated core histones in a chromatin template, particularly in the proximal region of an acetylation-sensitive promoter [55, 56], has been associated with transcriptionally active sites [50, 51, 53, 56, 57]. The acetylation of N-terminal lysines of histones neutralizes positive charges in the proteins, thus loosening histone-DNA contacts and increasing the accessibility of transcription factors to the DNA template [56].

Epigenetic abnormalities have been found to be responsible for development of several cancers, genetic disorders and autoimmune diseases [49]. In parallel with the investigation of genetic-related mechanisms, epigenetic modifications are clearly important to be considered in the study of gene regulation.

## **1.6 Synopsis of Thesis Objectives, Hypotheses and Results**

- Chapter 2 focuses on elucidating the mechanisms underlying the transcriptional deficiency of TAP-1 in several metastatic murine carcinoma cell lines. The hypothesis tested was whether the deficiency is caused by mutations in *cis*-acting elements of the TAP-1 promoter, the lack of transcription factors binding to TAP-1 promoter, overexpression of transcriptional repressors, and/or post-transcriptional defects. Experimental outcomes showed no mutation in *cis*-acting elements of the TAP-1 promoter, and that TAP-1 downregulation is caused by the lack of *trans*-acting factors binding to TAP-1 promoter and accelerated degradation of TAP-1 mRNA.
- The work in Chapter 3 aims to study the epigenetic regulation of TAP-1 expression and antigen processing in malignant cells. The hypothesis is that TAP-1 transcription is controlled by epigenetic mechanisms that regulate the permissive/repressive state of nucleosomal structure around the TAP-1 locus, thus controlling the accessibility of the DNA template by RNA pol II complex and general transcription factors. Experimental results revealed the lack of histone H3 acetylation in TAP-1 promoter as an epigenetic mechanism that is likely to contribute to a condensed nucleosomal structure around the TAP-1 promoter in TAP-deficient cells, thus preventing the binding of transcriptional activators to the promoter.
- Chapter 4 describes the characterization of several novel TAP-1 activator gene candidates obtained by cDNA library screenings. With the assumption that TAP-1 regulator genes are present in the highly complex cDNA library used, the hypothesis tested was that expression of genes (cDNAs) that have the ability to up-regulate TAP-

I promoter activity would enhance the expression of TAP-1 and surface MHC class I in TAP- and MHC class I-deficient carcinoma cells. Several TAP-activator gene candidates were recovered from cells that showed up-regulated TAP-1 promoter activity upon infection with cDNA library retroviral supernatants.

- The overall objective of this research is to contribute to a better understanding of tumor antigen presentation deficiency and furthermore, to the development of effective immunotherapeutic strategies for the treatment of cancer.

## 1.7 References

1. Seliger, B., M.J. Maeurer, and S. Ferrone. TAP off--tumors on. *Immunol Today*, 1997. 18:292-9.
2. Seliger, B., M.J. Maeurer, and S. Ferrone. Antigen-processing machinery breakdown and tumor growth. *Immunol Today*, 2000. 21:455-64.
3. Ritz, U. and B. Seliger. The transporter associated with antigen processing (TAP): structural integrity, expression, function, and its clinical relevance. *Mol Med*, 2001. 7:149-58.
4. Seliger, B., T. Cabrera, F. Garrido, and S. Ferrone. HLA class I antigen abnormalities and immune escape by malignant cells. *Semin Cancer Biol*, 2002. 12:3-13.
5. Gabathuler, R., G. Reid, G. Kolaitis, J. Driscoll, and W.A. Jefferies. Comparison of cell lines deficient in antigen presentation reveals a functional role for TAP-1 alone in antigen processing. *J Exp Med*, 1994. 180:1415-25.
6. Alimonti, J., Q.J. Zhang, R. Gabathuler, G. Reid, S.S. Chen, and W.A. Jefferies. TAP expression provides a general method for improving the recognition of malignant cells in vivo. *Nat Biotechnol*, 2000. 18:515-20.
7. Lankat-Buttgereit, B. and R. Tampe. The transporter associated with antigen processing: function and implications in human diseases. *Physiol Rev*, 2002. 82:187-204.
8. Kageshita, T., S. Hirai, T. Ono, D.J. Hicklin, and S. Ferrone. Down-regulation of HLA class I antigen-processing molecules in malignant melanoma: association with disease progression. *Am J Pathol*, 1999. 154:745-54.

9. Litman, G.W., J.P. Cannon, and L.J. Dishaw. Reconstructing immune phylogeny: new perspectives. *Nat Rev Immunol*, 2005. 5:866-79.
10. Janeway, C., P. Travers, M. Walport, and M. Shlomchik. *Immunobiology: the immune system in health and disease*. 5th ed. 2001, New York, NY Garland Publishing.
11. Klein, G. and E. Klein. Surveillance against tumors--is it mainly immunological? *Immunol Lett*, 2005. 100:29-33.
12. Houghton, A.N. and J.A. Guevara-Patino. Immune recognition of self in immunity against cancer. *J Clin Invest*, 2004. 114:468-71.
13. Tomasi, T.B., W.J. Magner, and A.N. Khan. Epigenetic regulation of immune escape genes in cancer. *Cancer Immunol Immunother*, 2006. 55:1159-84.
14. Rock, K.L. and L. Shen. Cross-presentation: underlying mechanisms and role in immune surveillance. *Immunol Rev*, 2005. 207:166-83.
15. Cresswell, P., A.L. Ackerman, A. Giodini, D.R. Peaper, and P.A. Wearsch. Mechanisms of MHC class I-restricted antigen processing and cross-presentation. *Immunol Rev*, 2005. 207:145-57.
16. Germain, R.N. and D.H. Margulies. The biochemistry and cell biology of antigen processing and presentation. *Annu Rev Immunol*, 1993. 11:403-50.
17. Cresswell, P. and J. Howard. Antigen recognition. *Curr Opin Immunol*, 1999. 11:61-3.
18. Altenberg, G.A. The engine of ABC proteins. *News Physiol Sci*, 2003. 18:191-5.
19. Chang, G. Multidrug resistance ABC transporters. *FEBS Lett*, 2003. 555:102-5.

20. Abele, R. and R. Tampe. Modulation of the antigen transport machinery TAP by friends and enemies. *FEBS Lett*, 2006. 580:1156-63.
21. Keusekotten, K., R.M. Leonhardt, S. Ehses, and M.R. Knittler. Biogenesis of functional antigenic peptide transporter TAP requires assembly of pre-existing TAP1 with newly synthesized TAP2. *J Biol Chem*, 2006. 281:17545-51.
22. Kelly, A. *MHC class II antigen presentation*. [website] 2006 [cited; Available from: <http://www.path.cam.ac.uk/pages/kelly/image/>].
23. Murakami, H., H. Ogawara, and H. Hiroshi. Th1/Th2 cells in patients with multiple myeloma. *Hematology*, 2004. 9:41-5.
24. Knutson, K.L. and M.L. Disis. Tumor antigen-specific T helper cells in cancer immunity and immunotherapy. *Cancer Immunol Immunother*, 2005. 54:721-8.
25. Wang, J.C. and A.M. Livingstone. Cutting edge: CD4+ T cell help can be essential for primary CD8+ T cell responses in vivo. *J Immunol*, 2003. 171:6339-43.
26. Kidd, P. Th1/Th2 balance: the hypothesis, its limitations, and implications for health and disease. *Altern Med Rev*, 2003. 8:223-46.
27. Wahl, S.M., J. Wen, and N. Moutsopoulos. TGF-beta: a mobile purveyor of immune privilege. *Immunol Rev*, 2006. 213:213-27.
28. Chamuleau, M.E., G.J. Ossenkoppele, and A.A. van de Loosdrecht. MHC class II molecules in tumour immunology: prognostic marker and target for immune modulation. *Immunobiology*, 2006. 211:619-25.
29. Bubenik, J. MHC class I down-regulation: tumour escape from immune surveillance? *Int J Oncol*, 2004. 25:487-91.

30. Meissner, M., T.E. Reichert, M. Kunkel, W. Gooding, T.L. Whiteside, S. Ferrone, and B. Seliger. Defects in the human leukocyte antigen class I antigen processing machinery in head and neck squamous cell carcinoma: association with clinical outcome. *Clin Cancer Res*, 2005. 11:2552-60.
31. Garrido, F., F. Ruiz-Cabello, T. Cabrera, J.J. Perez-Villar, M. Lopez-Botet, M. Duggan-Keen, and P.L. Stern. Implications for immunosurveillance of altered HLA class I phenotypes in human tumours. *Immunol Today*, 1997. 18:89-95.
32. Albertsson, P.A., P.H. Basse, M. Hokland, R.H. Goldfarb, J.F. Nagelkerke, U. Nannmark, and P.J. Kuppen. NK cells and the tumour microenvironment: implications for NK-cell function and anti-tumour activity. *Trends Immunol*, 2003. 24:603-9.
33. Rook, A.H., J.H. Kehrl, L.M. Wakefield, A.B. Roberts, M.B. Sporn, D.B. Burlington, H.C. Lane, and A.S. Fauci. Effects of transforming growth factor beta on the functions of natural killer cells: depressed cytolytic activity and blunting of interferon responsiveness. *J Immunol*, 1986. 136:3916-20.
34. Seliger, B., U. Ritz, R. Abele, M. Bock, R. Tampe, G. Sutter, I. Drexler, C. Huber, and S. Ferrone. Immune escape of melanoma: first evidence of structural alterations in two distinct components of the MHC class I antigen processing pathway. *Cancer Res*, 2001. 61:8647-50.
35. Agrawal, S., K. Reemtsma, E. Bagiella, S.F. Oluwole, and N.S. Braunstein. Role of TAP-1 and/or TAP-2 antigen presentation defects in tumorigenicity of mouse melanoma. *Cell Immunol*, 2004. 228:130-7.

36. Lou, Y., T.Z. Vitalis, G. Basha, B. Cai, S.S. Chen, K.B. Choi, A.P. Jeffries, W.M. Elliott, D. Atkins, B. Seliger, and W.A. Jefferies. Restoration of the expression of transporters associated with antigen processing in lung carcinoma increases tumor-specific immune responses and survival. *Cancer Res*, 2005. 65:7926-33.
37. Scanlon, K.J. Cancer gene therapy: challenges and opportunities. *Anticancer Res*, 2004. 24:501-4.
38. Lazoura, E. and V. Apostolopoulos. Insights into peptide-based vaccine design for cancer immunotherapy. *Curr Med Chem*, 2005. 12:1481-94.
39. Mocellin, S. Cancer vaccines: the challenge of developing an ideal tumor killing system. *Front Biosci*, 2005. 10:2285-305.
40. Morris, E., D. Hart, L. Gao, A. Tsallios, S.A. Xue, and H. Stauss. Generation of tumor-specific T-cell therapies. *Blood Rev*, 2006. 20:61-9.
41. Ruttinger, D., H. Winter, N.K. van den Engel, R.A. Hatz, M. Schlemmer, H. Pohla, S. Grutzner, D.J. Schendel, B.A. Fox, and K.W. Jauch. Immunotherapy of lung cancer: an update. *Onkologie*, 2006. 29:33-8.
42. Vitalis, T.Z., Q.J. Zhang, J. Alimonti, S.S. Chen, G. Basha, A. Moise, J. Tiong, M.M. Tian, K.B. Choi, D. Waterfield, A. Jeffries, and W.A. Jefferies. Using the TAP component of the antigen-processing machinery as a molecular adjuvant. *PLoS Pathog*, 2005. 1:e36.
43. Seliger, B., D. Atkins, M. Bock, U. Ritz, S. Ferrone, C. Huber, and S. Storkel. Characterization of human lymphocyte antigen class I antigen-processing machinery defects in renal cell carcinoma lesions with special emphasis on

- transporter-associated with antigen-processing down-regulation. *Clin Cancer Res*, 2003. 9:1721-7.
44. Lewin, B. *Genes IX*, ed. J. Louis C. Bruno. 2008, Sudbury, MA: Jones and Bartlett Publishers.
  45. Wright, K.L., L.C. White, A. Kelly, S. Beck, J. Trowsdale, and J.P. Ting. Coordinate regulation of the human TAP1 and LMP2 genes from a shared bidirectional promoter. *J Exp Med*, 1995. 181:1459-71.
  46. Azizkhan, J.C., D.E. Jensen, A.J. Pierce, and M. Wade. Transcription from TATA-less promoters: dihydrofolate reductase as a model. *Crit Rev Eukaryot Gene Expr*, 1993. 3:229-54.
  47. Benjamin, D., M. Colombi, G. Stoecklin, and C. Moroni. A GFP-based assay for monitoring post-transcriptional regulation of ARE-mRNA turnover. *Mol Biosyst*, 2006. 2:561-7.
  48. Hau, H.H., R.J. Walsh, R.L. Ogilvie, D.A. Williams, C.S. Reilly, and P.R. Bohjanen. Tristetraprolin recruits functional mRNA decay complexes to ARE sequences. *J Cell Biochem*, 2006.
  49. Rodenhiser, D. and M. Mann. Epigenetics and human disease: translating basic biology into clinical applications. *Cmaj*, 2006. 174:341-8.
  50. Berger, S.L. Histone modifications in transcriptional regulation. *Curr Opin Genet Dev*, 2002. 12:142-8.
  51. Legube, G. and D. Trouche. Regulating histone acetyltransferases and deacetylases. *EMBO Rep*, 2003. 4:944-7.

52. Mahadevan, L.C., A.L. Clayton, C.A. Hazzalin, and S. Thomson. Phosphorylation and acetylation of histone H3 at inducible genes: two controversies revisited. *Novartis Found Symp*, 2004. 259:102-11; discussion 111-4, 163-9.
53. Eberharter, A., R. Ferreira, and P. Becker. Dynamic chromatin: concerted nucleosome remodelling and acetylation. *Biol Chem*, 2005. 386:745-51.
54. Iniguez-Lluhi, J.A. For a healthy histone code, a little SUMO in the tail keeps the acetyl away. *ACS Chem Biol*, 2006. 1:204-6.
55. Gregory, P.D., K. Wagner, and W. Horz. Histone acetylation and chromatin remodeling. *Exp Cell Res*, 2001. 265:195-202.
56. Struhl, K. Histone acetylation and transcriptional regulatory mechanisms. *Genes Dev*, 1998. 12:599-606.
57. Eberharter, A. and P.B. Becker. Histone acetylation: a switch between repressive and permissive chromatin. Second in review series on chromatin dynamics. *EMBO Rep*, 2002. 3:224-9.

## Chapter 2 : Identification of Mechanisms Underlying TAP-1 Deficiency in Metastatic Murine Carcinomas

### 2.1 Introduction

Antigen processing and presentation play a crucial role in immune surveillance. Peptides derived from self, viral, or tumor-related proteins are generated in the cytoplasm by the action of proteasome. Transporter associated with antigen processing (TAP), a member of the ATP-binding cassette (ABC) transporter family, functions by transporting these peptides from the cytoplasm to the lumen of the endoplasmic reticulum (ER), where each peptide forms a ternary complex with beta-2 microglobulin ( $\beta$ 2m) and major histocompatibility complex (MHC) class I heavy chain, a process promoted by chaperone proteins (BiP, calnexin, calreticulin, ERp57 and tapasin) [1, 2]. These complexes are then transported to the cell surface and recognized by cytotoxic T lymphocytes (CTLs), which eventually kill cells that present non-self antigens.

Studies have shown that components of the antigen presentation pathway are impaired in the majority of human tumor cells [3, 4], allowing them to evade immune surveillance. In particular, low expression or absence of TAP (TAP-1 and -2) molecules, a feature common to many tumors [5-7], impairs the formation of the ternary complex in the lumen of ER. This results in a lack of MHC class I expression on the cell surface. As

A version of this chapter has been published.

Setiadi, A.F., David, M.D., Chen, S.S., Hiscott, J., and Jefferies, W.A. (2005) Identification of Mechanisms Underlying TAP Deficiency in Metastatic Murine Carcinomas. *Cancer Research*. 65: 7485-92.

© Cancer Research, 2005, 65: (16), adapted by permission.

a consequence, specific CTLs are unable to recognize and destroy many malignant cells [6].

The importance of TAP-1 function in immunosurveillance has been highlighted in studies using a mouse lung carcinoma cell line, CMT.64 [8]. It was demonstrated that the restoration of TAP-1 expression by introducing exogenous TAP-1 or by up-regulating endogenous TAP-1 expression upon interferon gamma (IFN- $\gamma$ ) treatment, could correct the MHC class I deficiency, resulting in recognition of these antigen-presenting cells by CTLs in vitro, as well as in a decrease of tumor growth and incidence in vivo [3, 7, 9]. This finding is encouraging for the development of therapeutic approaches that could restore TAP deficiencies in cancer cells, therefore resurrecting immune recognition of neoplastic cells. However, the mechanisms underlying TAP-1 deficiency in tumor cells remain poorly understood. Previous studies reported that downregulation of TAP-1 expression in many cancer cells likely occurs at the mRNA level [3, 7, 10]; however, these studies did not distinguish between defects in transcription or stability of the RNA. Therefore, in this study, the properties and activities of the TAP-1/LMP-2 bi-directional promoter in TAP-expressing and TAP-deficient cells were investigated in order to provide a better understanding of the transcriptional regulation of TAP-1 mRNA in tumor cells.

## **2.2 Materials and Methods**

### **2.2.1 Cell lines**

The CMT.64 cell line established from a spontaneous lung carcinoma of a C57BL/6 (H-2<sup>b</sup>) mouse [8] and the Ltk fibroblast cell line derived from a C3H/An (H-2<sup>k</sup>) mouse were grown in DMEM media. The LMD cell line derived from a metastatic prostate carcinoma of a 129/Sv mouse (a kind gift of Dr. T. C. Thompson) [11], as well as the B16F10 (B16) melanoma [12] and RMA lymphoma cell lines, both derived from C57BL/6 mice, were maintained in RPMI 1640 media. RPMI 1640 and DMEM media were supplemented with 10% heat-inactivated FBS, 2 mM L-glutamine, 100 U/ml penicillin, 100 µg/ml streptomycin, and 10 mM HEPES.

### **2.2.2 Reverse transcription-PCR analysis**

All primers used for PCR amplifications were purchased from Sigma-Genosys, Oakville, ON, and are listed in Table 2.2.2.1. Total cellular RNA were extracted using RNeasy Mini Kit (Qiagen, Mississauga, ON), and contaminating DNA was removed by treating the RNA samples with DNase 1 (Ambion Inc., Austin, TX). Reverse transcription of 1 µg of total cellular RNA was performed using the reverse transcription kit from Invitrogen (Carlsbad, CA), in a total volume of 20 µl. Two microliters aliquots of cDNA were used as a template for PCR in a total of 50 µl reaction mixture containing 1x PCR buffer, 250 µM deoxynucleotide triphosphate, 1.5 mM MgCl<sub>2</sub>, 0.2 µM of each primer and 2.5 units Platinum Taq DNA Polymerase. All PCR reagents were obtained from Invitrogen. cDNA amplifications were carried out with specific primer sets in a *T*-

*gradient* thermocycler (Biometra, Goettingen, Germany) with 25-35 cycles of denaturation (1 min, 95°C), annealing (1 min, 54-64°C), and elongation (2 min, 72°C). The cycling was concluded with a final extension at 72°C for 10 min. Twenty microliters of amplified products were analysed on agarose gels, stained with ethidium bromide and photographed under UV light.

**Table 2.2.2.1: Primers used for RT-PCR analysis.**

Oligonucleotide	Primer sequence (5'-3') <sup>a</sup>	T <sub>m</sub> (°C)	bp <sup>b</sup>
Mouse $\beta$ -actin	F: ATGGATGACGATATCGCTGC R: TTCTCCAGGGAGGAAGAGGAT	54.0	713
TAP-1 5'-end	F: ATGGCTGCGCACGTCTGG R: ACTCAGGCCACCACCCA	63.0	138
TAP-1 3'-end	F: TGGCTCGTTGGCACCCCTCAA R: TCAGTCTGCAGGAGCCGCAAGA	64.0	775
TAP-1 3'-end (last 155 bp)	F: TTATCACCCAGCAGCTCAGCCT R: TCAGTCTGCAGGAGCCGCAA	61.0	155
TAP-1 promoter <sup>c</sup>	F: <u>cggaattc</u> GGCTCGGCTTTCCAATCA R: <u>gaggatcc</u> GAGCGTGAGCTGTCCAGAGTCT	60.0	557
pTAP-1-EGFP	F (TAP-1 promoter): TTCTTCCTCTAAACGCCAGCA R (EGFP): CTCGCCCTTGCTCACCAT	61.0	190
CMT.64 TAP-1	F: CTCACTCTGGTCACCCTGATCAAC R: TGGTCCAGACTTCAGCCACG	62.0	225
IRF1	F: CAACTTCCAGGTGTCACCCAT R: CACAGGGAATGGCCTGGAT	54.9	363
IRF2	F: TGATGAAGAGAACGCAGAGGG R: TTAACAGCTCTTGACACGGGC	54.0	328
S15	F: TTCCGCAAGTTCACCTACC R: CGGGCCGGCCATGCTTTACG	60.0	357
Prion protein	F: ATGGCGAACCTTGGCTACT R: CCAACTACCACCATGAGGTTG	58.0	239

<sup>a</sup> F: forward primer; R: reverse primer.

<sup>b</sup> Length of the PCR amplification product.

<sup>c</sup> Restriction enzyme sites are underlined.

### 2.2.3 Chromatin immunoprecipitation (ChIP) assays

Chromatin immunoprecipitation experiments using  $2 \times 10^7$  cells of CMT.64, LMD, B16, Ltk or RMA cell lines were performed as described in Appendix A.1. Five micrograms of anti-RNA polymerase II antibody (N-20, sc-899, Santa Cruz) was used for the immunoprecipitation. Levels of murine TAP-1 promoter or TAP-1 coding region co-immunoprecipitating with RNA polymerase II from each sample were quantified by real time PCR, using primers specific for the TAP-1 promoter or the last 155 bp of TAP-1 coding region (3'end) as listed in Table 2.2.2.1. Serial dilutions of genomic DNA or plasmid containing the murine TAP-1 promoter were used to generate standard curves for real time PCR using the corresponding primer sets.

### 2.2.4 Cloning of the TAP-1 promoter

Sequence of the murine *Tap-1* gene region was obtained from the National Center for Biotechnology Information database (GenBank Accession No. AF027865). In order to predict putative transcription factor binding sites, the region in-between *Lmp-2* and *Tap-1* genes was analysed using the MatInspector software from Genomatix website. The predicted murine TAP-1 promoter region was then amplified by PCR, using genomic DNA from CMT.64 cells as a template and the following primers (Sigma): 5'cggaattcGGCTCGGCTTTCCAATCA3' (forward), 5'gaggatccGAGCGTGAGCTGTCCAGAGTCT3' (reverse). A TAP-1 promoter construct (pTAP-1-EGFP) was then created by inserting the PCR product in-between the EcoRI and BamHI sites of promoterless pEGFP-1 vector (Clontech, Palo Alto, CA) (Appendix B).

## 2.2.5 Transfection and selection

The CMT.64, LMD, B16, Ltk and RMA cells were transfected with the pTAP-1-EGFP construct or the promoterless pEGFP-1 vector using LIPOFECTAMINE PLUS Reagent (Invitrogen). Transfected cells were then selected in the presence of geneticin (G418) (Sigma) for 1 month (Table 2.2.5.1). Levels of EGFP expression in transfectants, treated or untreated with 50 ng/ml IFN- $\gamma$  for 48 hours, were assessed by flow cytometry (FACScan, Becton Dickinson, Mountain View, CA).

**Table 2.2.5.1: G418 doses for selection of transfectants in various cell lines.**

Cell line	Description	G418 dose (mg/ml)
CMT.64	TAP-deficient, mouse lung carcinoma	1
LMD	TAP-deficient, mouse prostate carcinoma	1
B16	TAP-deficient, mouse melanoma	1
Ltk	TAP-expressing, mouse fibroblast	0.8
RMA	TAP-expressing, mouse lymphoma	0.5

## 2.2.6 Generation of pTAP-1-EGFP-transfected clones by FACS

The pTAP-1-EGFP-transfected CMT.64, LMD and B16 cells that displayed a small level of EGFP were selected by flow cytometry using a FACSVantage DiVa cytometer (Becton Dickinson), grown in bulk culture, and treated with 50 ng/ml

recombinant murine IFN- $\gamma$  (R&D Systems, Minneapolis, MN) for 2 days. Cells that express high fluorescence in response to IFN- $\gamma$  were then sorted twice and cloned.

### 2.2.7 Cell Fusion and FACS analysis

Twenty million cells from clones of the TAP- and MHC class I-deficient CMT.64, LMD and B16 cells stably transfected with pTAP-1-EGFP were fused with TAP- and MHC class I-expressing Ltk fibroblasts in a 1:1 ratio, following a polyethylene glycol cell fusion protocol [13]. Cells were then incubated with PE-conjugated anti-K<sup>k</sup> mouse monoclonal antibody at 4°C for 30 minutes. The fused cells, which displayed both red (PE-anti-K<sup>k</sup>) and green (EGFP) fluorescence, were selected by FACS. Flow cytometry analyses of EGFP, K<sup>b</sup> and K<sup>k</sup> expression were performed 1 week after the fusions. PE-conjugated anti-K<sup>b</sup> and anti-K<sup>k</sup> mouse monoclonal antibodies were purchased from BD Pharmingen (San Diego, CA).

Fusion experiments between a clone of pTAP-1-EGFP-transfected CMT.64 cells and a clone of pEYFP-N1-transfected CMT.64 cells were also performed. The fused cells were then selected based on both yellow (EYFP) and green (EGFP) fluorescence. One week after the fusion, levels of EGFP and K<sup>b</sup> in the fused cells were analysed by FACS.

### 2.2.8 Endogenous levels and overexpression of IRF-1 and IRF-2 in cell lines

Levels of endogenous IRF-1 and -2 in CMT.64, LMD, B16, Ltk and RMA cells were assessed by RT-PCR using primers specific for IRF-1 and IRF-2, following the conditions described above. In order to investigate the effects of IRF-1 and -2 overexpression on TAP-1 promoter activity in TAP-deficient carcinoma cells, a pTAP-1-

EGFP-transfected CMT.64 clone was co-transfected with 0.1  $\mu$ g of pEYFP-N1 (enhanced yellow fluorescent protein) vector (Clontech) and 1  $\mu$ g of pCMV/IRF-1 or pCMV/IRF-2 [14] expression vector. Since the pCMV/IRF vectors contained no selection gene, the EYFP served as a marker to select for successfully transfected cells by FACS. 48 hours after transfection, levels of EGFP in the CMT.64 transfectants were analysed by flow cytometry.

### 2.2.9 Luciferase and $\beta$ -Galactosidase Assays

In order to demonstrate whether the overexpressed IRF-1 and -2 were functional, cells were co-transfected with the IRF-coding constructs, an IFN- $\beta$  promoter-luciferase construct [14], and a pCMV/ $\beta$ -galactosidase vector (Promega, Madison, WI) used to monitor transfection efficiency. A promoterless pGL3-luciferase vector (Promega) was also used as a background control. 48 hours after transfection, the cells were washed twice with PBS and lysed with Reporter Lysis Buffer (Promega). The luciferase and the  $\beta$ -galactosidase activity were measured using the Luciferase Assay System (Promega), and the  $\beta$ -galactosidase Enzyme Assay System (Promega), respectively.

### 2.2.10 Western Blot

Fifty micrograms proteins per sample were separated through 8% SDS-PAGE. Proteins were transferred to a nitrocellulose membrane (Bio-rad, Hercules, CA). Blots were blocked with 5% skim milk in PBS, probed with rabbit anti-mouse TAP-1 polyclonal Ab (made by Linda Li in Jefferies Lab), followed by HRP-conjugated goat anti-rabbit secondary Ab (Jackson Immunoresearch Lab., West Grove, PA). The rabbit anti-mouse TAP-1 polyclonal antibody was made by immunizing rabbits with a common

TAP1 peptide sequence, RGGCYRAMVEALAAPAD-C with a cysteine at the C-terminal, linked to keyhole limpet hemocyanin (Pierce Biotechnology, Rockford, IL) [15]. For the loading controls, anti- $\beta$ -actin mouse monoclonal Ab (Sigma) was used, followed by HRP-conjugated goat anti-mouse secondary Ab (Pierce Biotechnology). Blots were developed using Lumi-light reagents (Pierce).

### **2.2.11 Analysis of mRNA stability**

Unfused Ltk fibroblasts, and fused CMT.64-Ltk, LMD-Ltk and Ltk-Ltk cells were treated with 5  $\mu$ g/ml actinomycin D (Sigma) for 2, 4 or 8 hours, or left untreated. 4  $\mu$ g of total cellular RNA were used as templates for reverse transcription and amplification by real time PCR, using TAP-1 (5'-end) or S15 or prion protein-specific primer sets listed in Table 1. Serial dilutions of RT products were used as templates for PCR to generate the corresponding standard curves.

### **2.2.12 Real time quantitative PCR analysis**

In this study, this method was employed for quantification of levels of endogenous TAP-1 promoter or TAP-1 coding region co-precipitating with RNA polymerase II in ChIP assays, quantification of copy number of the pTAP-1-EGFP construct integrated in stably transfected cells, and measurement of TAP-1 mRNA levels in cells upon actinomycin D treatment. cDNAs reverse-transcribed from 1-4  $\mu$ g RNA and genomic DNA were used as templates for amplifications using 200-500 nM of each primer and 10  $\mu$ l SYBR Green Taq ReadyMix (Sigma). Thirty five cycles of denaturation (5 seconds, 95oC), annealing (5 seconds, 61-63oC), and elongation (20 seconds, 72oC) were performed using a Roche LightCycler.

## 2.3 Results

### 2.3.1 Levels of TAP-1 mRNA in CMT.64, LMD, B16, Ltk and RMA cells

To investigate the mechanism underlying the lack of TAP-1 expression in carcinoma cells, CMT.64 (lung), LMD (prostate) and B16 (melanoma) cell lines were used as models for TAP-deficient cells [3, 7, 11, 16], and Ltk and RMA cell lines [7] as models for TAP-expressing cells. RT-PCR analysis confirmed that the levels of TAP-1 mRNA were higher in Ltk and RMA cells than in CMT.64, LMD and B16 cells (Figure 2.3.1.1). Treatment of the TAP-deficient cells with IFN- $\gamma$  increased the TAP-1 mRNA expression to similar levels as in TAP-expressing cells (Figure 2.3.1.1).

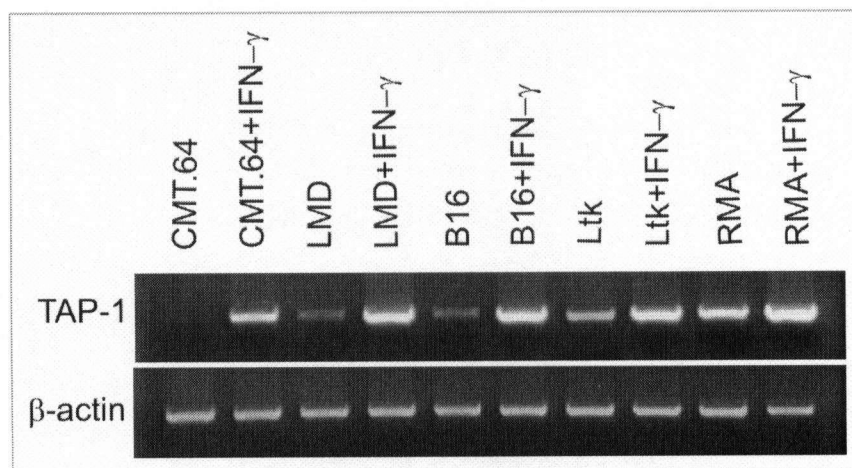


**Figure 2.3.1.1: IFN- $\gamma$ -treatment restores TAP-1 expression in TAP-deficient murine lung, prostate and skin carcinoma cells (CMT.64, LMD and B16).**

Amplification of  $\beta$ -actin cDNA served as an internal control. RT-PCR analyses were performed at least three times and representative data are shown.

### **2.3.2 The recruitment of RNA polymerase II to the *Tap-1* gene is lower in the CMT.64, LMD and B16, than in the Ltk and RMA cells**

In order to investigate whether the lack of TAP-1 mRNA expression in CMT.64, LMD and B16 cells is due to an impairment of TAP-1 transcription, the levels of RNA pol II within the 3' end of the TAP-1 coding region in TAP-deficient and TAP-expressing cells were compared, by means of chromatin immunoprecipitation assay. The results showed that the levels of RNA pol II within the 3' end of the TAP-1 coding region were lower in CMT.64, LMD and B16 than in Ltk and RMA cells (Figure 2.3.2.1), indicating that deficiency in transcription is, at least partially, underlying TAP deficiency in the carcinoma cells.

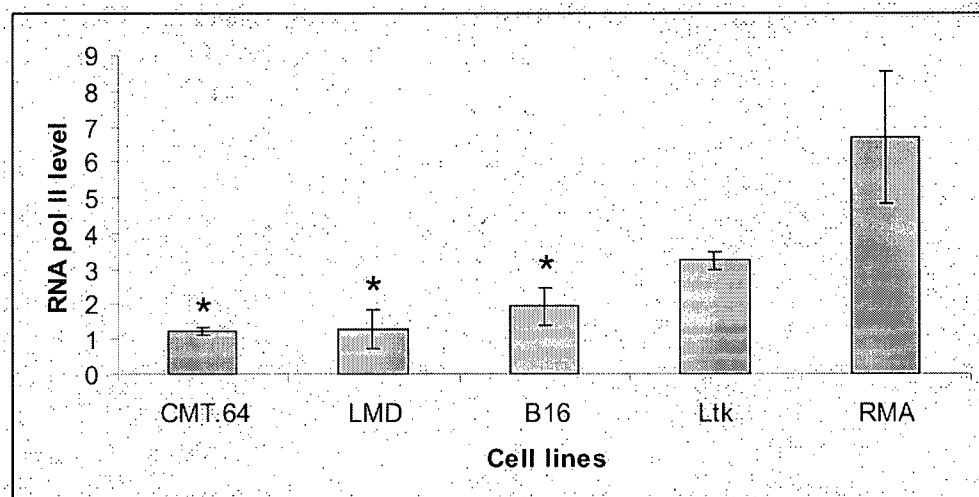


**Figure 2.3.2.1: The recruitment of RNA polymerase II to 3' coding region of the *Tap-1* gene in CMT.64, LMD and B16 is impaired in comparison to that in Ltk and RMA.** Chromatin immunoprecipitation using anti-RNA polymerase II antibody was performed in each cell line, and the eluted DNA fragments were purified and used as templates for real time PCR analysis using primers specific for the 3' coding region of the *Tap-1* gene. Relative RNA polymerase II levels were determined as the ratio of copy numbers of the eluted 3' coding region of the *Tap-1* gene and copy numbers of the corresponding inputs. The smallest ratio in each group of experiments was arbitrarily determined as 1. *Columns*, average of three to six experiments; *bars*, SEM. \*  $P < .05$  compared with TAP-expressing cells (Student's t-test).

Using the same approach, but with primers specific for the TAP-1 promoter region, it was found that the recruitment of RNA pol II to the TAP-1 promoter was also relatively lower in TAP-deficient cells (Figure 2.3.2.2). Recruitment of RNA pol II complex to genes' promoters is an important event that supports transcription initiation [17]. Therefore, this result directly supported the notion that initiation of TAP-1 transcription was impaired in TAP-deficient cells.

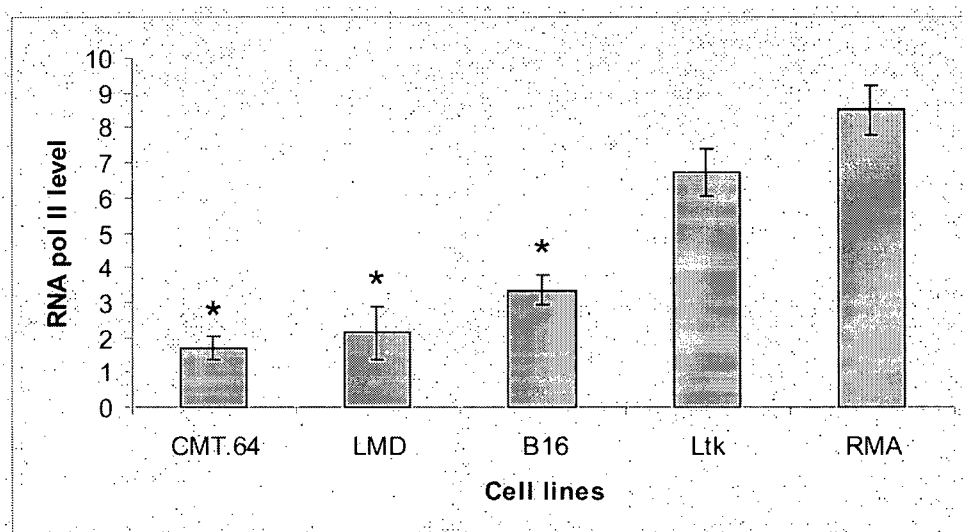


**Figure 2.3.2.2: The recruitment of RNA pol II to the TAP-1 promoter was low in TAP-deficient CMT.64, LMD and B16 cells.** Chromatin immunoprecipitation using anti-RNA polymerase II antibody was performed, and the relative levels of RNA polymerase II recruitment to the TAP-1 promoter were assessed as described above using primers specific for the TAP-1 promoter. Columns, average of three to six experiments; bars, SEM. \*  $P < .05$  compared with TAP-expressing cells (Student's t-test).

### 2.3.3 Cloning and analysis of the -557 to +1 region of the CMT.64-derived TAP-1 promoter

One possible explanation for the impairment of transcription of the *Tap-1* gene in TAP-deficient cells was the presence of mutation(s) in *cis*-acting elements involved in the regulation of TAP-1 promoter activity. Previous studies have demonstrated that the 593-bp-long region located in-between *TAP-1* and *LMP-2* genes in humans acts as a bi-directional promoter that drives the transcription of both genes [18]. Analysis of the murine TAP-1 promoter had not been reported in prior work; however, the organization of the murine *Lmp-2/Tap-1* genes within the MHC class II locus is reminiscent of its human ortholog [19]. Therefore, primers flanking the LMP-2/TAP-1 intergenic region were used to amplify the murine TAP-1 promoter region, using genomic DNA from CMT.64 cells as a template. The resulting PCR product was then cloned and sequenced. Analysis of the CMT.64-derived TAP-1 promoter region revealed the presence of putative binding sites for various transcription factors, including SP1, CREB, AP-1, PU.1, NF- $\kappa$ B and IRF (Figure 2.3.3.1). By alignment, the nucleotide sequence of the CMT.64-derived TAP-1 promoter region was found to be identical to the corresponding region in the murine MHC class II locus (NCBI accession no. AF027865). This result demonstrated that there was no mutation present in the -557 to +1 region of the CMT.64-derived TAP-1 promoter. Additional analysis of TAP-1 promoter sequence amplified from genomic DNA of TAP-deficient LMD cells and TAP-expressing RMA cells also showed that the LMD-derived TAP-1 promoter sequence was identical to the published sequence in NCBI and to that of RMA cells.

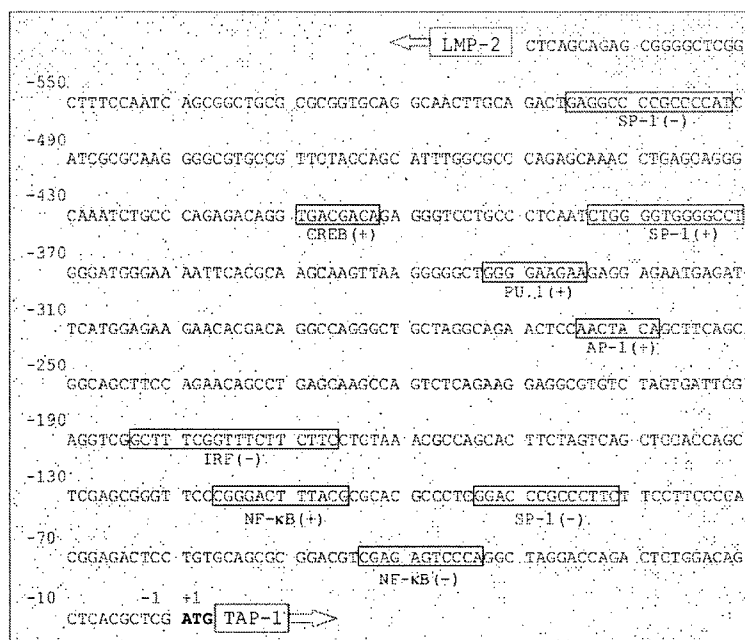


**Figure 2.3.3.1: Nucleotide sequence of the CMT.64-derived TAP-1 promoter region is identical to the corresponding region in murine MHC class II locus.**

The ATG codon was arbitrarily determined as +1. Motifs located on the sense strand are indicated by a (+), and motifs located on the antisense strand are indicated by a (-).

### 2.3.4 Activity of the -557 to +1 region of the TAP-1 promoter is impaired in TAP-deficient cells

To demonstrate that this murine LMP-2/TAP-1 intergenic region indeed displays promoter activity, and to assess whether it contains *cis*-acting elements conferring a differential activity of the TAP-1 promoter between TAP-expressing and TAP-deficient cells, a reporter plasmid (pTAP-1-EGFP) was generated, containing the -557 to +1 region of the murine TAP-1 promoter upstream of the *egfp* gene in the pEGFP-1 vector.

CMT.64, LMD, B16, Ltk and RMA cells were then transfected with the pTAP-1-EGFP construct, or the pEGFP-1 vector as a control, and cultured for one month under selective pressure to generate stable transfectants. Real time PCR analysis was performed using TAP-1 promoter-specific forward and EGFP-specific reverse primers (Table 2.2.2.1), and 100 ng of genomic DNA from the stable pTAP-1-EGFP transfectants as templates. The results showed that, on average, one copy of the pTAP-1-EGFP construct was integrated per cell in all the cell lines used (Table 2.3.4.1). An example of detailed calculations used to determine the copy numbers is outlined in Appendix A.2.

**Table 2.3.4.1: Statistical Evaluation of the Transfected pTAP-1-EGFP Copy Numbers Per Cell.**

Transfected cells	pTAP-1-EGFP-1 average copy number	SD
CMT.64	1.59	0.06
LMD	1.49	0.03
B16	1.42	0.01
Ltk	1.51	0.02
RMA	1.41	0.02

Furthermore, EGFP levels in these stable transfectants were assessed by flow cytometry. In all the cell lines, the promoterless pEGFP-1 vector transfectants displayed low levels of background EGFP expression; however, the levels of fluorescence were higher in cells transfected with the pTAP-1-EGFP construct than in cells transfected with the vector alone. In addition, the TAP-expressing Ltk and RMA cells expressed higher levels of EGFP than the TAP-deficient CMT.64, LMD and B16 cells (Figure 2.3.4.1). This indicated that the -557 to +1 region indeed displayed promoter activity. Finally, treatment

with IFN- $\gamma$  resulted in 3- to 6-fold increases in EGFP expression in CMT.64, B16 and LMD cells (Figure 2.3.4.1). This treatment elevated EGFP expression of the TAP-deficient cells to similar or even higher levels than those in untreated TAP-expressing cells, suggesting that treatment with IFN- $\gamma$  was able to overcome the deficiencies responsible for the low activity of the TAP-1 promoter in TAP-deficient cells. Taken together, these results indicated that the cloned TAP-1 promoter region possesses faithful promoter activity and contains *cis*-acting elements conferring the relatively low promoter activity in TAP-deficient cells. Furthermore, based on the observation that the levels of EGFP triggered by the cloned TAP-1 promoter correlated with the levels of recruitment of RNA Pol II to the endogenous TAP-1 promoter observed by CHIP, these transfected cells were proven to be suitable as tools to further investigate the mechanisms underlying the differential activation of TAP-1 promoter in TAP-deficient and TAP-expressing cells.

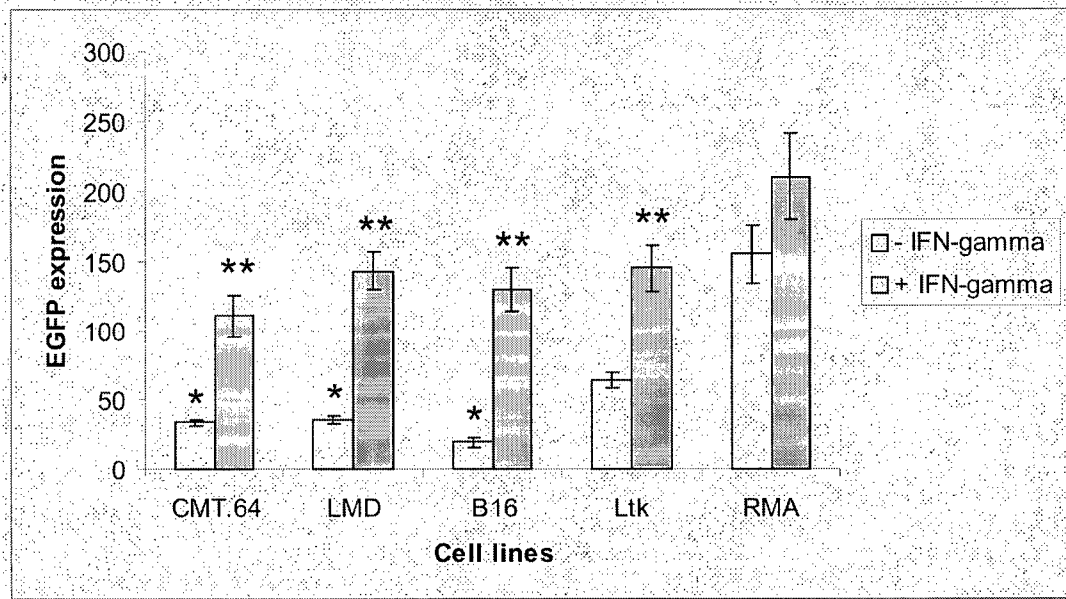


**Figure 2.3.4.1: TAP-1 promoter activity is impaired in TAP-deficient CMT.64, LMD and B16 cells.** Flow cytometry analysis was performed to measure TAP-1 promoter activity, based on the levels of EGFP expression in pTAP-1-EGFP stable transfectants after selection in G418 for 1 month. The IFN- $\gamma$ -treated cells were incubated with 50 ng/ml IFN- $\gamma$  for 48 hours prior to the FACS analysis. Levels of EGFP in the cells transfected the pTAP-1-EGFP were normalized against corresponding values obtained upon transfection with pEGFP-1 vector alone. Data shown are the mean fluorescence intensity  $\pm$  SEM of three independent experiments. \*  $P < .05$  compared with TAP-expressing cells; \*\*  $P < .05$  compared with untreated cells (Student's t-test).

### **2.3.5 Effects of fusions between carcinoma cells and wild type fibroblasts on TAP-1 promoter activity and MHC class I expression levels**

The relatively low activity of the -557 to +1 region of the TAP-1 promoter in TAP-deficient cells suggested that these cells might be deficient in positive *trans*-acting factors that regulate TAP-1 promoter activity, or that they might display an abnormally high level of activity of *trans*-acting factors that negatively regulate TAP-1 promoter activity. To test these hypotheses, the effects of fusing the TAP- and MHC class I-expressing Ltk cells with TAP- and MHC class I-deficient carcinoma cells (CMT.64, LMD and B16) were investigated.

Before fusion, stable pTAP-1-EGFP transfectants of carcinoma cells were sorted into single-cell clones by FACS, and a clone that displayed high induction of TAP-1 promoter activity and MHC class I expression in response to IFN- $\gamma$  treatment was chosen. By flow cytometry, it was found that levels of EGFP were higher in the fused CMT.64-Ltk and LMD-Ltk cells than in the unfused CMT.64 and LMD cells (Figure 2.3.5.1).

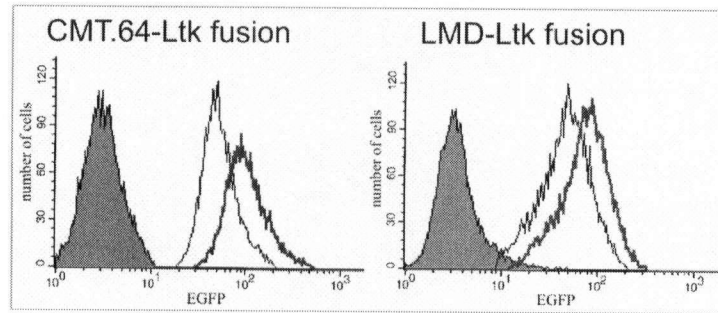


**Figure 2.3.5.1: TAP-1 promoter-driven EGFP expression increased in the fused CMT.64-Ltk and LMD-Ltk cells (thick line) in comparison to that in the unfused pTAP-1-EGFP-transfected CMT.64 and LMD cells (thin line). Wild type CMT.64 and LMD were used as negative controls for EGFP expression (shaded area).**

Further flow cytometric analysis indicated that  $K^b$  was expressed on the surface of the fused CMT.64-Ltk and LMD-Ltk cells, while the unfused cells did not express  $K^b$  (Figure 2.3.5.2).

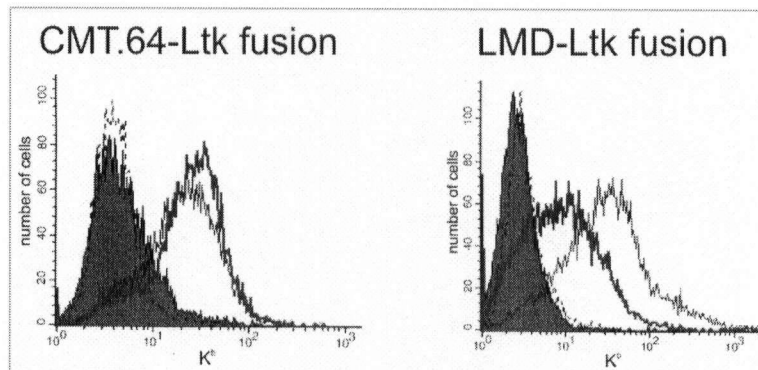


**Figure 2.3.5.2: Surface expression of  $K^b$  was increased when CMT.64 or LMD (shaded areas) were fused to Ltk cells (broken line). Expression of  $K^b$  on fused CMT.64-Ltk and fused LMD-Ltk cells are displayed by thick lines. As a positive control, expression of  $K^b$  was assessed on IFN- $\gamma$ -treated CMT.64 and LMD cells (thin lines).**

As a control, two groups of TAP-deficient cells were fused: the CMT.64 cells stably transfected with the pTAP-1-EGFP construct with another group of CMT.64 cells expressing EYFP. The results showed no induction of K<sup>b</sup> surface expression in the fused CMT.64(pTAP-1-EGFP)-CMT.64(pEYFP-N1) cells (Figure 2.3.5.3).

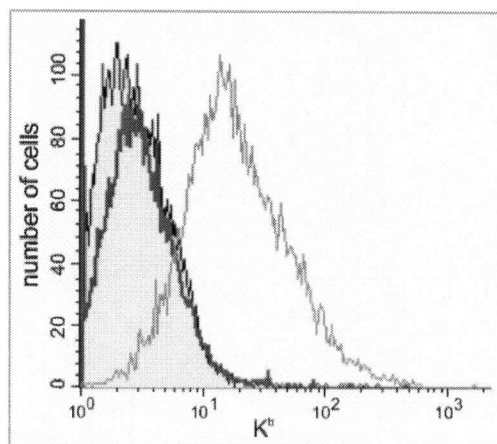


**Figure 2.3.5.3: No induction of K<sup>b</sup> surface expression in the fused CMT.64(pTAP-1-EGFP)-CMT.64(pEYFP-N1) cells (thick line).** CMT.64 cells untreated (shaded area) or treated with IFN-γ (thin line) were used as negative or positive control, respectively, for K<sup>b</sup> expression.

The increase in EGFP expression of the pTAP-1-EGFP-transfected TAP-deficient carcinoma cells that were fused with TAP-expressing fibroblasts suggests that the TAP-deficient cell lines studied display a relatively low level of activity of *trans*-acting factor(s) positively regulating the TAP-1 promoter activity. This deficiency could, at least partially, be corrected by a fusion with TAP-expressing cells. Furthermore, the expression of MHC class I allotype of the fibroblasts (K<sup>k</sup>) in the fused CMT.64-Ltk and

LMD-Ltk cells were also assessed. The results showed a slight but consistent decrease in the level of  $K^k$  expressed (Figure 2.3.5.4).

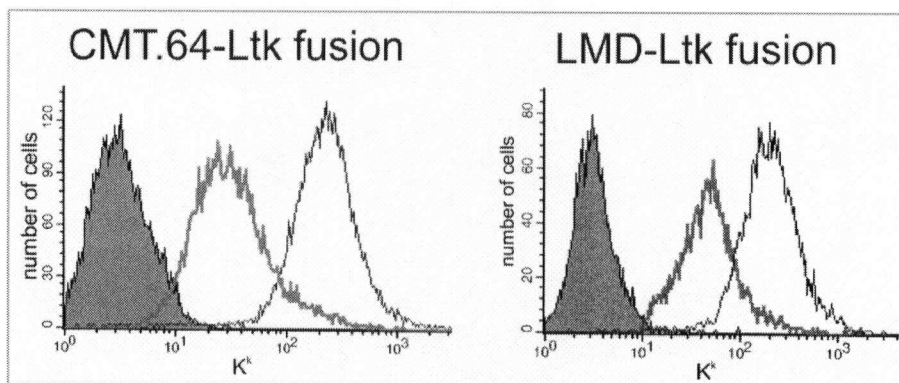


**Figure 2.3.5.4:  $K^k$  surface expression was reduced in the fused CMT.64-Ltk and LMD-Ltk (thick lines) in comparison to that in the wild type Ltk cells (thin lines). Wild type CMT.64 and LMD cells were used as negative controls for  $K^k$  expression (shaded area).**

### 2.3.6 Overexpression of IRF-1 and IRF-2 in CMT.64 cells did not result in significant changes in TAP-1 promoter activity

IFN- $\gamma$  treatment resulted in high induction of TAP-1 promoter activity and could subsequently overcome TAP and MHC class I deficiencies in carcinoma cells [11, 20, 21]. Therefore, factors that are known to be activated in response to IFN- $\gamma$  are attractive candidates for the future discovery of positive *trans*-acting factors that are either absent or functionally defective in TAP-deficient cells, thus accounting for the impairment of TAP-1 promoter activity in carcinoma cells. The interferon regulatory factors (IRFs), that binding motif was found in the TAP-1 promoter (Figure 2.3.3.1), were examples of proteins that expression could be regulated by IFN- $\gamma$  [22]. In order to investigate whether TAP downregulation might be caused by abnormally low or high levels of IRF-1 and IRF-2, respectively, endogenous levels of IRF-1 and -2 mRNAs in TAP-expressing and TAP-deficient cells were observed by RT-PCR. The results indicated that both IRF-1 and -2 mRNA levels did not correlate with TAP levels in the cell lines (Figure 2.3.6.1).

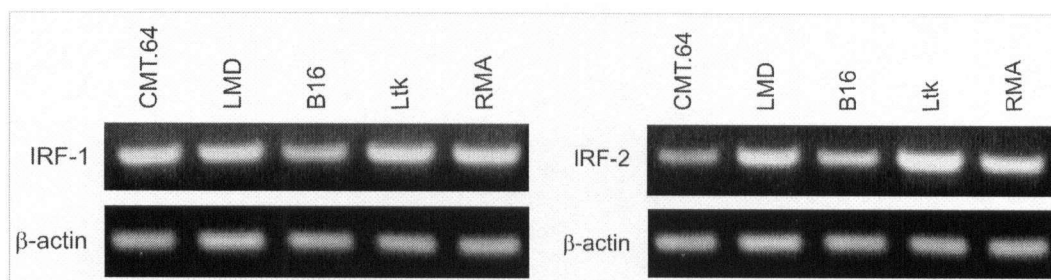


**Figure 2.3.6.1: Endogenous levels of IRF-1 and -2 mRNA did not correlate with TAP levels in the cell lines.**

In order to further investigate the putative role of IRF-1 and -2 in modulating TAP-1 promoter activity in TAP-deficient cells, human IRF-1 and -2 [14] were overexpressed in a clone of CMT.64 cells containing the pTAP-1-EGFP construct. Flow cytometry analysis showed that the overexpression of the IRFs had no significant effect on EGFP levels in the transfectants (Figure 2.3.6.2).

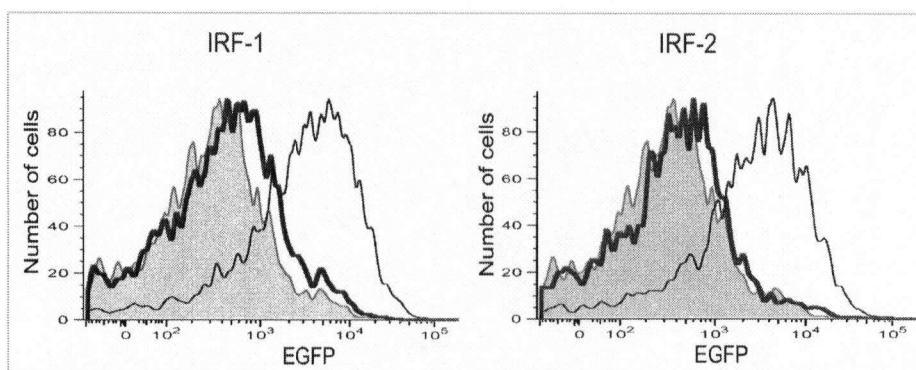


**Figure 2.3.6.2: Overexpression of IRF-1 or -2 in a clone of pTAP-1-EGFP construct-transfected CMT.64 cells did not result in significant changes of the TAP-1 promoter activity.** Representative histograms show EGFP expressed by the IRF-1 or IRF-2-overexpressing cells. The shaded areas indicate background green fluorescence of the cells transfected with PBS as negative controls, the thin and thick lines represent EGFP expression in cells overexpressing the IRF that were treated with IFN- $\gamma$  or left untreated, respectively.

In order to test whether the transfected IRFs were functional, the cells were co-transfected with either an IFN- $\beta$  promoter-luciferase construct or a promoterless pGL3-luciferase vector. As expected [14], the overexpression of exogenous IRF-1 was found to increase the basal level of IFN- $\beta$  promoter activity, whereas the IRF-2 decreased it (Figure 2.3.6.3). This indicated that overexpression of IRF-1 and IRF-2 alone was not sufficient for modulating the TAP-1 promoter activity in CMT.64 cells.

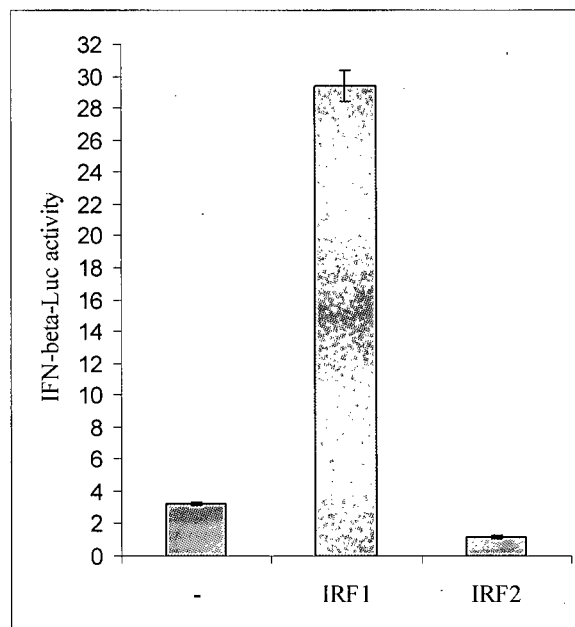


**Figure 2.3.6.3: Overexpression of IRF-1 and -2 modulated IFN- $\beta$  promoter activity linked to a *luciferase* gene.** Luciferase activities were normalized against  $\beta$ -galactosidase activities, to correct for variations in transfection efficiencies. Data shown are the average  $\pm$  SEM of three independent experiments.

### 2.3.7 Analysis of TAP-1 expression in unfused and fused cells

During the course of these studies, it was noted that the TAP-1 promoter displayed a low but detectable activity in TAP-deficient cells, while TAP-1 mRNA was barely detectable in these cells. To investigate whether the low levels of TAP-1 mRNA in TAP-deficient cells resulted solely from the deficiency in TAP-1 promoter activity demonstrated above, the levels of TAP-1 mRNA transcribed from the CMT.64 genome and from the Ltk genome in fused CMT.64-Ltk cells were compared. To distinguish between TAP-1 expressed from the two genomes, analysis of the TAP-1 mRNA polymorphism in both cells was carried out by PCR amplifications of TAP-1 mRNA transcribed in each cell line. A total of 12 bp differences was found between the nucleotide sequence of CMT.64-derived and Ltk-derived TAP-1 mRNAs (Appendix C). These polymorphisms are most likely strain-specific and are not responsible for TAP-deficiency in CMT.64 cells, since another analysis showed that the CMT.64 TAP-1 sequence was identical to that of TAP-expressing RMA cells. Both CMT.64 and RMA cells originated from C57/BL6 mice, whereas Ltk cells were derived from a C3H/An mouse. Primers specific to CMT.64-derived TAP-1 mRNA were then designed in order to investigate its levels in the fused CMT.64-Ltk cells. Non-polymorphic primers were used for further analysis of total TAP-1 expression in the fused cells.

Despite the increase in TAP-1 promoter activity driving the *egfp* gene in the fused CMT.64-Ltk cells (Figure 2.3.5.1), no TAP-1 mRNA from the CMT.64 genome could be detected in cells that were not treated with IFN- $\gamma$  (Figure 2.3.7.1).

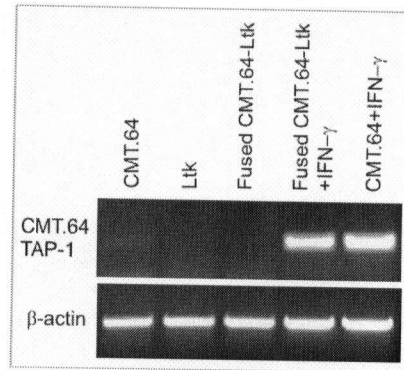


**Figure 2.3.7.1: No expression of TAP-1 mRNA from the CMT.64 genome was detectable by RT-PCR in the fused CMT.64-Ltk cells.** Amplifications of reverse-transcribed CMT.64 TAP-1 mRNA from IFN- $\gamma$ -treated cells and  $\beta$ -actin mRNA were used as positive controls and loading controls, respectively.

In fact, analysis of total TAP-1 expression showed that the fused CMT.64-Ltk and LMD-Ltk cells displayed drastically lower levels of TAP-1 mRNA and protein than the unfused Ltk fibroblasts did (Figure 2.3.7.2). This suggested the existence of post-transcriptional mechanisms that further down-regulate levels of TAP-1 mRNA in TAP-deficient cells. Therefore, the possibility of a difference in TAP-1 mRNA stability between TAP-expressing and TAP-deficient cells was further investigated.

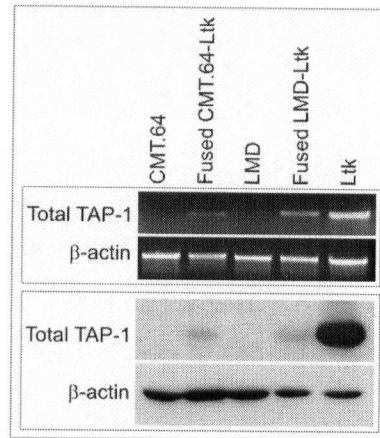


**Figure 2.3.7.2: Total TAP-1 expression was reduced when CMT.64 and LMD cells were fused with wild type Ltk cells.** Results from RT-PCR analysis and Western Blot were shown in top and bottom panel, respectively. Levels of  $\beta$ -actin were used as loading controls.

### 2.3.8 TAP-1 mRNA stability decreases in carcinoma-fused fibroblasts

To assess the regulation of TAP-1 at the level of mRNA stability, unfused Ltk fibroblasts, as well as fused CMT.64-Ltk, LMD-Ltk and Ltk-Ltk cells were treated with actinomycin D (Act. D) for 2 to 8 hours, in order to block neo-synthesis of mRNA. Residual levels of TAP-1 mRNA after treatment of cells with Act. D were then assessed by real time PCR, using constant amounts of total RNA as templates. Levels of TAP-1, S15 and prion mRNA in actinomycin D-treated cells are expressed as percentages of the levels of the corresponding mRNA in untreated cells. The results showed that TAP-1 mRNA stability decreased when fibroblasts were fused to carcinoma cells (Figure 2.3.8.1).

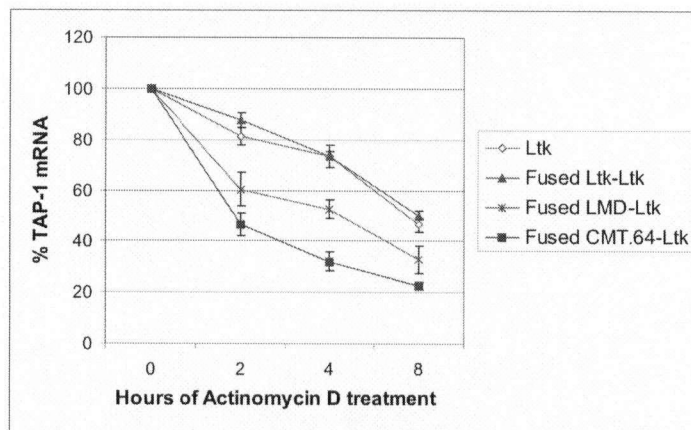


**Figure 2.3.8.1: TAP-1 mRNA is rapidly degraded in fused carcinoma-fibroblast cells.**

As a control, the stability of unrelated mRNA, such as the mRNA coding for S15 and prion protein (Figure 2.3.8.2) was assessed. The results demonstrated that the S15 and prion mRNA stability was unaffected by the cell fusion events, and that the decrease in mRNA stability is fairly specific to TAP-1 in carcinoma-fused cells. These results suggest the existence of factors, which remain to be identified, that enhanced TAP-1 mRNA degradation in carcinoma cells.

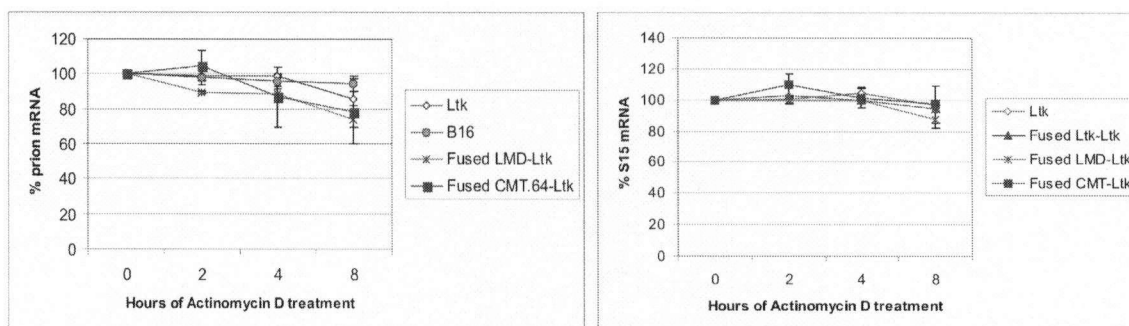


**Figure 2.3.8.2: The stability of S15 and prion mRNA is similar in unfused and fused cells.**

## 2.4 Discussion

TAP-1 downregulation in tumors has been reported in many studies [6, 10, 23-25]; however, the molecular mechanisms underlying this defect remain poorly understood. One of the recently proposed mechanisms of APM downregulation is the overexpression of oncogenes, for example HER-2/neu, that gives rise to the emergence of immune escape phenotype of tumors [26]. Related mechanisms of TAP downregulation may include an impairment of TAP-1 promoter activity (due to mutation in *cis*-acting elements in the promoter or in distal enhancer/silencer regions, chromatin remodeling at the TAP-1 locus, and/or difference in expression or functionality of *trans*-acting factors), as well as a relatively low stability of TAP-1 mRNA in these cells.

In this study, murine lung, prostate and skin carcinoma cells (CMT.64, LMD and B16) were used as models for TAP- and MHC class I-deficient cancer cells. The results in this study suggested that TAP deficiency in these cells is caused by the lack of activation or expression of TAP-1 transcriptional activators, as well as a decrease in TAP-1 mRNA stability. These results demonstrated that: a) treatment of the TAP-deficient cells with IFN- $\gamma$  increased the TAP-1 mRNA expression to similar levels as in TAP-expressing cells; b) the initiation of TAP-1 transcription was impaired in TAP-deficient cells; c) the relatively low activity of TAP-1 promoter in the carcinoma cells is due to regulatory defects rather than mutations in the TAP-1 promoter; d) low TAP-1 promoter activity and MHC class I deficiency in carcinoma cells could be corrected, at least partially, by fusions with wild type fibroblasts; and e) a decrease in TAP-1 mRNA stability also contributed to TAP-1 deficiency in murine lung carcinoma cells.

Based on the structural and functional analysis of TAP-1 promoter of TAP-deficient cells, as well as results obtained from chromatin immunoprecipitation assays of endogenous TAP-1 promoter in various TAP-expressing and TAP-deficient cells, it was proposed that one mechanism underlying TAP deficiency in these cells is the impairment of the ability of TAP-1 promoter to drive transcription. As no mutation was observed in the CMT.64- and LMD-derived TAP-1 promoter, this deficiency was likely to be caused by the lack of transcriptional activators necessary for optimal binding of the RNA polymerase II complex to the TAP-1 promoter, or conversely, by the presence of transcriptional inhibitors that prevent the binding.

FACS analysis of the fusions between TAP- and MHC class I-deficient carcinoma cells (CMT.64, LMD and B16) of H-2<sup>b</sup> origin and TAP- and MHC class I-expressing fibroblasts (Ltk) of H-2<sup>k</sup> origin showed an increase of TAP-1 promoter activity and some increase in K<sup>b</sup> expression. However, despite the increase of the promoter activity in the fused CMT.64-Ltk, no TAP-1 mRNA from the CMT.64 genome could be detected by RT-PCR (Figure 2.3.7.1); instead, total levels of TAP-1 mRNA and protein in the fused CMT.64-Ltk and LMD-Ltk cells were lower than in the unfused Ltk cells (Figure 2.3.7.2). This might have accounted for the decrease in surface expression of K<sup>k</sup> that was observed in the fused cells (Figure 2.3.5.4). These unexpectedly low levels of TAP-1 mRNA and protein in the fused fibroblasts-carcinoma cells had prompted the investigation whether other mechanisms contribute to the TAP-1 deficiency in carcinoma cells, in addition to the impairment of TAP-1 promoter activity that would also account for the disappearance of TAP-1 in the fused cells. It was then found that the stability of TAP-1 mRNA was decreased when fibroblasts were fused with carcinoma cells. This

result suggests that the stability of TAP-1 mRNA is lower in CMT.64 and LMD cells than in the Ltk cells. Unfortunately, the extremely low levels of TAP-1 mRNA in the carcinoma cells, even in absence of actinomycin D, preclude direct confirmation of this hypothesis. Further studies will be required in order to precisely characterize the positive regulatory factors that are lacking or defective in carcinoma cells, as well as the mechanism that leads to a reduction of TAP-1 mRNA stability in carcinoma cells.

These studies are of fundamental importance, as they will significantly contribute to a better understanding of the underlying cause of antigen processing deficiency in many tumor types. This will in turn lead to new approaches to modify the immunogenicity and antigenicity of tumor cells, thereby allowing recognition of tumors by immune surveillance mechanisms.

## 2.5 References

1. Germain, R.N. and D.H. Margulies. The biochemistry and cell biology of antigen processing and presentation. *Annu Rev Immunol*, 1993. 11:403-50.
2. Cresswell, P. and J. Howard. Antigen recognition. *Curr Opin Immunol*, 1999. 11:61-3.
3. Alimonti, J., Q.J. Zhang, R. Gabathuler, G. Reid, S.S. Chen, and W.A. Jefferies. TAP expression provides a general method for improving the recognition of malignant cells in vivo. *Nat Biotechnol*, 2000. 18:515-20.
4. Seliger, B., M.J. Maeurer, and S. Ferrone. Antigen-processing machinery breakdown and tumor growth. *Immunol Today*, 2000. 21:455-64.
5. Ritz, U. and B. Seliger. The transporter associated with antigen processing (TAP): structural integrity, expression, function, and its clinical relevance. *Mol Med*, 2001. 7:149-58.
6. Seliger, B., M.J. Maeurer, and S. Ferrone. TAP off--tumors on. *Immunol Today*, 1997. 18:292-9.
7. Gabathuler, R., G. Reid, G. Kolaitis, J. Driscoll, and W.A. Jefferies. Comparison of cell lines deficient in antigen presentation reveals a functional role for TAP-1 alone in antigen processing. *J Exp Med*, 1994. 180:1415-25.
8. Franks, L.M., A.W. Carbonell, V.J. Hemmings, and P.N. Riddle. Metastasizing tumors from serum-supplemented and serum-free cell lines from a C57BL mouse lung tumor. *Cancer Res*, 1976. 36:1049-55.
9. Jefferies, W.A., G. Kolaitis, and R. Gabathuler. IFN-gamma-induced recognition of the antigen-processing variant CMT.64 by cytolytic T cells can be replaced by

- sequential addition of beta 2 microglobulin and antigenic peptides. *J Immunol*, 1993. 151:2974-85.
10. Seliger, B., D. Atkins, M. Bock, U. Ritz, S. Ferrone, C. Huber, and S. Storkel. Characterization of human lymphocyte antigen class I antigen-processing machinery defects in renal cell carcinoma lesions with special emphasis on transporter-associated with antigen-processing down-regulation. *Clin Cancer Res*, 2003. 9:1721-7.
  11. Lee, H.M., T.L. Timme, and T.C. Thompson. Resistance to lysis by cytotoxic T cells: a dominant effect in metastatic mouse prostate cancer cells. *Cancer Res*, 2000. 60:1927-33.
  12. Poste, G., J. Doll, I.R. Hart, and I.J. Fidler. In vitro selection of murine B16 melanoma variants with enhanced tissue-invasive properties. *Cancer Res*, 1980. 40:1636-44.
  13. Ausubel, F.M., R. Brent, R.E. Kingston, D.D. Moore, J.G. Seidman, J.A. Smith, and K. Struhl, *Production of antibodies*, in *Current Protocols in Molecular Biology*. 2001, John Wiley & Sons, Inc. p. 11.7.1-11.7.3.
  14. Lin, R., A. Mustafa, H. Nguyen, D. Gewert, and J. Hiscott. Mutational analysis of interferon (IFN) regulatory factors 1 and 2. Effects on the induction of IFN-beta gene expression. *J Biol Chem*, 1994. 269:17542-9.
  15. Zhang, Q.J., R.P. Seipp, S.S. Chen, T.Z. Vitalis, X.L. Li, K.B. Choi, A. Jeffries, and W.A. Jefferies. TAP expression reduces IL-10 expressing tumor infiltrating lymphocytes and restores immunosurveillance against melanoma. *Int J Cancer*, 2007.

16. Seliger, B., U. Wollscheid, F. Momburg, T. Blankenstein, and C. Huber. Characterization of the major histocompatibility complex class I deficiencies in B16 melanoma cells. *Cancer Res*, 2001. 61:1095-9.
17. Burley, S.K. and R.G. Roeder. Biochemistry and structural biology of transcription factor IID (TFIID). *Annu Rev Biochem*, 1996. 65:769-99.
18. Wright, K.L., L.C. White, A. Kelly, S. Beck, J. Trowsdale, and J.P. Ting. Coordinate regulation of the human TAP1 and LMP2 genes from a shared bidirectional promoter. *J Exp Med*, 1995. 181:1459-71.
19. Janeway, C., P. Travers, M. Walport, and M. Shlomchik. *Immunobiology: the immune system in health and disease*. 5th ed. 2001, New York, NY Garland Publishing.
20. Matsui, M., S. Machida, T. Itani-Yohda, and T. Akatsuka. Downregulation of the proteasome subunits, transporter, and antigen presentation in hepatocellular carcinoma, and their restoration by interferon-gamma. *J Gastroenterol Hepatol*, 2002. 17:897-907.
21. Mikyskova, R., J. Bubenik, V. Vonka, M. Smahel, M. Indrova, J. Bieblova, J. Simova, and T. Jandlova. Immune escape phenotype of HPV16-associated tumours: MHC class I expression changes during progression and therapy. *Int J Oncol*, 2005. 26:521-7.
22. Brucet, M., L. Marques, C. Sebastian, J. Lloberas, and A. Celada. Regulation of murine Tap1 and Lmp2 genes in macrophages by interferon gamma is mediated by STAT1 and IRF-1. *Genes Immun*, 2004. 5:26-35.

23. Vitale, M., R. Rezzani, L. Rodella, G. Zauli, P. Grigolato, M. Cadei, D.J. Hicklin, and S. Ferrone. HLA class I antigen and transporter associated with antigen processing (TAP1 and TAP2) down-regulation in high-grade primary breast carcinoma lesions. *Cancer Res*, 1998. 58:737-42.
24. Restifo, N.P., F. Esquivel, Y. Kawakami, J.W. Yewdell, J.J. Mule, S.A. Rosenberg, and J.R. Bennink. Identification of human cancers deficient in antigen processing. *J Exp Med*, 1993. 177:265-72.
25. Murray, P.G., C.M. Constandinou, J. Crocker, L.S. Young, and R.F. Ambinder. Analysis of major histocompatibility complex class I, TAP expression, and LMP2 epitope sequence in Epstein-Barr virus-positive Hodgkin's disease. *Blood*, 1998. 92:2477-83.
26. Herrmann, F., H.A. Lehr, I. Drexler, G. Sutter, J. Hengstler, U. Wollscheid, and B. Seliger. HER-2/neu-mediated regulation of components of the MHC class I antigen-processing pathway. *Cancer Res*, 2004. 64:215-20.

## **Chapter 3 : Epigenetic Control of TAP-1 expression and the Immune Escape Mechanisms in Malignant Carcinomas**

### **3.1 Introduction**

The current paradigm is that emergence of tumors is limited by a robust adaptive immune response that recognizes aberrant expression of tumor associated antigens. This mechanism of immune-surveillance is thought to work efficiently until tumor cells undergo chromosomal alterations that result in phenotypic conversion to a form that is no longer recognizable by the immune system. This conversion closely parallels the emergence of metastatic forms of the tumor cells that, in turn, gain a growth advantage over non-metastatic forms that remain hampered by the fidelity of the immune system.

Several immune escape mechanisms that allow the metastatic tumor to go undetected have been observed; however, most tumors down-regulate a cassette of genes involved in antigen processing and presentation [1-3]. These include the genes encoding beta-2 microglobulin ( $\beta 2m$ ), the transporters associated with antigen processing (TAP) -1 and -2, tapasin, the low molecular weight proteins (LMP)-2 and -7, as well as the proteasome activator PA28 [1, 4, 5]. TAP-1 down-regulation has specifically been attributed to tumor growth and metastatic ability, and is used as a predictor of rapid tumor

A version of this chapter has been submitted for publication.

Setiadi, A.F., David, M.D., Seipp, R.P., Hartikainen, J.A., Gopaul, R., and Jefferies, W.A. (2007) Epigenetic Control of the Immune Escape Mechanisms in Malignant Carcinomas.

progression and poor survival rates in humans [1-3, 5-8]. Furthermore, this antigen presentation deficiency can be temporarily reversed *in vitro* by treatment of the tumor cells with interferon gamma (IFN- $\gamma$ ), and can also be genetically complemented *in vivo* by the sole restoration of TAP-1 expression [1, 8]. Therefore, the presence of TAP-1 improves the ability of the host to mount a therapeutic and protective tumor antigen-specific immune response. This finding is encouraging for the development of therapeutic approaches that can restore TAP deficiency in cancer cells, and thus result in restoration of immune recognition of tumors. However, the actual defect that leads to TAP downregulation and immune escape mechanisms remains undescribed.

Previous studies in this thesis concluded that TAP-deficiency in metastatic carcinomas is not caused by mutations within the TAP-1 promoter. Instead, it was found that the metastatic carcinomas lack positive *trans*-acting factors that regulate TAP-1 transcription [9]. An intriguing observation at the initiation of the present study was that transient expression of episomal copies of a reporter gene driven by TAP-1 promoter led to high levels of expression even in TAP-deficient carcinomas, while stable transfection and genomic integration of the same plasmid led to transcriptional silencing. This led to the investigation whether epigenetic mechanisms play a role in the regulation of antigen processing in tumors, and whether the transcriptional activators that are deficient or non-functional in malignant cells are those with intrinsic histone acetyltransferase (HAT) activity. Deregulation of genes involved in the modulation of chromatin structure has been closely linked to immune evasion, uncontrolled cell growth, and development of tumors [10-12]. The study in this chapter will provide fundamental insights into the

epigenetic mechanisms of tumor immune escape and metastatic diseases, which may help in revising immunotherapeutic methodologies for eradicating cancers.

## 3.2 Materials and Methods

### 3.2.1 Cell lines and reagents

The TC-1 cell line was developed by transformation of murine primary lung cells with HPV16 E6 and E7 oncogenes and activated *H-ras* [13]. TC-1 cells display high levels of TAP-1 and MHC class I. TC1-/D11 (= D11) and TC1-/A9 (= A9) were tumor cell clones that exhibited spontaneous downregulation of MHC class I expression, and were derived from TC-1-inoculated mice [14]. These cell lines were cultured in the presence of 0.4 mg/ml G418. Another model used in this study consists of a murine primary prostate cancer cell line, PA, and its metastatic, TAP- and MHC class I-deficient derivative, LMD, both derived from a 129/Sv mouse [15]. The TAP-deficient CMT.64 cell line was established from a spontaneous lung carcinoma in a C57BL/6 mouse [16]. The TAP-expressing Ltk (=L-M(TK-)) fibroblast cell line was derived from a C3H/An mouse (ATCC, Manassas, VA). All cell lines above were grown in DMEM. The C57BL/6-derived B16F10 melanoma [17] and RMA lymphoma [1] cell lines were cultured in RPMI 1640 media. RPMI 1640 and DMEM media were supplemented with 10% heat-inactivated fetal bovine serum (FBS), 2 mM L-glutamine, 100 U/ml penicillin, 100 µg/ml streptomycin, and 10 mM HEPES. When indicated, cells were treated with 100 ng/ml Trichostatin A (TSA) (Sigma, St. Louis, MO) for 24 hours (CMT.64, B16F10, PA and LMD) or 48 hours (TC-1, D11 and A9), or with 50 ng/ml IFN-γ for 48 hours.

### 3.2.2 Reverse transcription-PCR analysis

Total cellular RNA was extracted using Trizol Reagent (Invitrogen, Burlington, ON); contaminating DNA was removed by treatment with DNase-1 (Ambion Inc., Austin, TX). Reverse transcription of 1  $\mu\text{g}$  of total cellular RNA was performed using the reverse transcription kit (SSII RT) from Invitrogen, in a total volume of 20  $\mu\text{l}$ . Two microliters aliquots of cDNA were used as a template for PCR in a total of 50  $\mu\text{l}$  reaction mixture containing 1x PCR buffer, 250  $\mu\text{M}$  deoxynucleotide triphosphate, 1.5 mM  $\text{MgCl}_2$ , 200 nM of each primer and 2.5 units Taq or Platinum Taq DNA Polymerase. cDNA amplifications were carried out in a *T-gradient* thermocycler (Biometra, Goettingen, Germany) with 25-35 cycles of denaturation (1 min, 95°C), annealing (1 min, 54-64°C), and elongation (2 min, 72°C). The cycling was concluded with a final extension at 72°C for 10 min. Twenty microliters of amplified products were analyzed on agarose gels, stained with ethidium bromide and photographed under UV light. Primers used for PCR amplifications (Sigma-Genosys, Oakville, ON and Integrated DNA Technologies (IDT), Coralville, IA) are listed in Table 3.2.2.1 below. All PCR reagents were obtained from Invitrogen and Fermentas (Burlington, ON).

**Table 3.2.2.1: Primers used for RT-PCR and real time PCR analysis.**

Oligonucleotide	Primer sequence (5'-3') <sup>a</sup>	Tm(°C)	bp <sup>b</sup>
TAP-1	F: TGGCTCGTTGGCACCCCTCAAA R: TCAGTCTGCAGGAGCCGCAAGA	64.0	775
TAP-2	F: GCTGTGGGGACTGCTAAAAG R: TATTGGCATTGAAAGGGAGC	60.0	665
LMP-2	F: CGACAGCCCTTTACCATCG R: TCACTCATCGTAGAATTTTGGCAG	56.0	240
Tapasin	F: ACGTCACCCTGGAGGTGGCA R: ACTGGAGTCATCTGGGCCAG	60.0	166
B2M	F: ATGGCTCGCTCGGTGACC R: TCACATGTCTCGATCCCAGTAGA	56.0	360
$\beta$ -actin	F: ATGGATGACGATATCGCTGC R: TTCTCCAGGGAGGAAGAGGAT	54.0	713
TAP-1 promoter (5'-end)	F: GGCTCGGCTTTCCAATCA R: GGATGGGAAAATTCACGCAA	60.0	207
TAP-1 promoter (3'-end)	F: TTCTTCCTCTAAACGCCAGCA R: CGAGCGTGAGCTGTCCAGAGTCT	61.0	172
pTAP1-Luc copy number	F (TAP-1 promoter): TTCTTCCTCTAAACGCCAGCA R ( <i>luc2</i> ): AGTGGGTAGAAATGGCGCTG	61.0	190

<sup>a</sup> F: forward primer; R: reverse primer.

<sup>b</sup> Length of the PCR amplification product.

<sup>c</sup> Restriction enzyme sites are underlined.

### 3.2.3 Real-time quantitative PCR analysis

Purified genomic DNA was used as template for amplifications using 200-500 nM of each primer and 1  $\mu$ l SYBR Green Taq ReadyMix (Roche, Mannheim, Germany) in a total of 10  $\mu$ l reaction mixture. 35-40 cycles of denaturation (5 seconds, 95°C),

annealing (5 seconds, 61-63°C), and elongation (20 seconds, 72°C) were performed using a Roche LightCycler.

### 3.2.4 Flow cytometry

Flow cytometric analysis of H-2K<sup>b</sup> expression was performed using PE-conjugated anti-K<sup>b</sup> mouse monoclonal antibody (mAb) (BD Pharmingen, San Diego, CA) and a FACScan cytometer (Becton Dickinson, Mountain View, CA).

### 3.2.5 Chromatin immunoprecipitation assays

Chromatin immunoprecipitation experiments using  $7 \times 10^6$  cells per sample were done as previously described [18]. Five micrograms of anti-RNA pol II (N-20, sc-899, Santa Cruz Biotechnology Inc., Santa Cruz, CA), anti-acetyl-histone H3 (Upstate Biotechnology Inc., Lake Placid, NY) or anti-CBP (A-22, sc-369, Santa Cruz Biotechnology) polyclonal antibody (Ab) were used for the immunoprecipitation. Levels of murine TAP-1 promoter co-immunoprecipitating with the antibody from each sample were quantified by real-time PCR using primers specific for the TAP-1 promoter. Primers specific to the 3'-end of the TAP-1 promoter region were used for PCR when the templates were immunoprecipitated using anti-RNA pol II or anti-acetyl-histone H3 antibody, while 5'-end-specific primers were used for templates immunoprecipitated using anti-CBP antibody. Serial dilutions of plasmid containing the murine TAP-1 promoter were amplified following the same protocol to generate a standard curve.

### 3.2.6 Plasmid construction

The plasmid containing an EGFP coding region driven by the TAP-1 promoter (pTAP1-EGFP) was described previously [9]. A similar construct containing a *luciferase*

gene driven by the TAP-1 promoter region (pTAP1-Luc) was created by inserting the TAP-1 promoter between the Sac I and Bgl II sites of the pGL4.14[luc2/Hygro] vector (Promega, Madison, WI) (Appendix B). 5'-end truncations of the TAP-1 promoter region were also cloned into pGL4.14[luc2/Hygro] vector. The ATG codon of the *Tap-1* gene was arbitrarily numbered as +1, and the truncated promoters were named according to the starting base position of forward primers with respect to the ATG codon (-427, -401 and -150). Primers used for PCR amplifications of the full TAP-1 promoter and its truncations are listed in Table 3.2.6.1.

**Table 3.2.6.1: Primers used for PCR amplifications of full TAP-1 promoter and its truncations.**

Oligonucleotide	Primer sequence (5'-3') <sup>a</sup>	Tm(°C)	bp <sup>b</sup>
Full TAP-1 promoter <sup>c</sup>	F: <u>cgagagctc</u> GGCTCGGCTTTCCAATCA R: <u>gaagatct</u> GAGCGTGAGCTGTCCAGAGTCT	60.0	557
-427 truncated TAP-1 promoter <sup>c</sup>	F: <u>cgagagctc</u> ATCTGCCAGAGACAGGTGA R: <u>gaagatct</u> GAGCGTGAGCTGTCCAGAGTCT	55.0	427
-401 truncated TAP-1 promoter <sup>c</sup>	F: <u>cgagagctc</u> AGGGTCCTGCCCTCAATC R: <u>gaagatct</u> GAGCGTGAGCTGTCCAGAGTCT	55.0	401
-150 truncated TAP-1 promoter <sup>c</sup>	F: <u>cgagagctc</u> TTCTAGTCAGCTCCACCAGCTC R: <u>gaagatct</u> GAGCGTGAGCTGTCCAGAGTCT	60.0	150

<sup>a</sup> F: forward primer; R: reverse primer.

<sup>b</sup> Length of the PCR amplification product.

<sup>c</sup> Restriction enzyme sites are underlined.

### 3.2.7 Transfection and selection

TC-1, D11, A9, PA and LMD cells were transfected with the pTAP1-Luc constructs or the promoterless pGL4.14[luc2/Hygro] vector using ExGen 500 *in vitro*

Transfection Reagent (Fermentas). Transient transfectants were analysed between 12-72 hours after co-transfection of the pTAP1-Luc construct or the promoterless vector with pRL-TK plasmid (Promega) in 10:1 ratio. To obtain stable transfectants, the transfected cells were selected for three weeks in the presence of 200-550 ng/ml Hygromycin B (Sigma).

### 3.2.8 Luciferase assays

Relative luciferase activity (RLA) in transient transfectants was assessed by dual luciferase assay (Promega) 12-72 hours after transfection. Copy numbers of the pTAP1-Luc construct integrated into the genome of the stable transfectants were quantified by real time PCR using a forward primer specific for the TAP-1 promoter and a reverse primer specific for the *luc2* gene. RLA in stable transfectants (3-4 weeks post-transfection) was assessed by Bright-Glo luciferase assay (Promega) using 10,000 cells per sample and was determined by normalizing the luciferase values with copy number of plasmids integrated into the genome of each stable transfectant.

### 3.2.9 Western Blots

Fifty micrograms of protein per sample were separated with 6% (CBP and TAP-1) or 15% ( $\beta$ -actin and acetyl-histone H3) SDS-PAGE. Proteins were transferred to nitrocellulose membranes (Bio-rad, Hercules, CA). Blots were blocked with 5% skim milk in PBS and incubated with the following rabbit polyclonal antibodies: anti-mouse TAP-1 [19]; anti-acetyl-histone H3 (Upstate Biotechnology Inc.); anti-p300 (C-20, sc-585, Santa Cruz); anti-CBP (A-22, sc-369, Santa Cruz). Secondary antibody was an HRP-conjugated goat anti-rabbit polyclonal antibody (Jackson Immunoresearch Lab.,

West Grove, PA). For the loading controls, anti- $\beta$ -actin mouse monoclonal antibody (Sigma) was used, followed by HRP-conjugated goat anti-mouse secondary antibody (Pierce, Rockford, IL). Blots were visualized using Lumi-light ECL reagents (Pierce).

### 3.2.10 Cytotoxicity assays

CTL effector cells were generated by injecting a C57BL/6 mouse (Charles River, St. Constant, QC) with  $10^7$  tissue culture infectious particles (TCIP) of Vesicular Stomatitis Virus (VSV). The spleen was harvested seven days later, homogenized, and cells were incubated for five days in RPMI-1640 containing 10% FBS (Hyclone), 20 mM HEPES, 1% NEAA, 1% sodium pyruvate, 1% L-glutamine, 1% penicillin/streptomycin and 0.1% 2-ME, in the presence of 1  $\mu$ M VSV-NP peptide (RGYVYQGL). TC-1, D11 and A9 cells were treated with IFN- $\gamma$  (50 ng/ml) or TSA (100 ng/ml) for 24 hours, or left untreated; VSV at an MOI of 7.5 was then added and the experiment was performed 16 hours later. Cells were washed with PBS and loaded with  $^{51}\text{Cr}$  by incubating  $10^6$  cells with 100  $\mu\text{Ci}$  of  $^{51}\text{Cr}$  sodium chromate (Amersham, Arlington Heights, IL) in 250  $\mu\text{l}$  of culture media for one hour. Following three washes with PBS, the target cells were incubated with the effector cells at the indicated ratios for four hours. One hundred microliters of supernatant from each well were collected and the  $^{51}\text{Cr}$  release was measured by a  $\gamma$ -counter (LKB Instruments, Gaithersburg, MD). The specific  $^{51}\text{Cr}$  release was calculated as follows:  $((\text{experimental} - \text{media control}) / (\text{total} - \text{media control})) \times 100\%$ . The total release was obtained by lysis of the cells with a 5% Triton X-100 solution.

### **3.2.11 Establishment of HPV-positive cancer xenografts and treatment with Trichostatin A**

Four hundred thousand pTAP1-Luc stable transfectants of TC-1 or A9 cells were resuspended in PBS, then injected subcutaneously (s.c.) into seven-week-old female C57BL/6 syngeneic mice. TSA was dissolved in DMSO to a concentration of 0.2 mg/ml. Daily treatment with 50  $\mu$ l TSA (500  $\mu$ g/kg) or DMSO (vehicle control) was administered via intraperitoneal (i.p.) injection for 20 days, starting on day seven after injection with tumor cells. The dose of 500  $\mu$ g/kg TSA per animal per day was chosen as it had been successfully used by others to suppress other types of tumor growth in murine tumor models [20-22]. Mice were assigned to three groups (TC-1 treated with DMSO, A9 treated with DMSO and A9 treated with TSA) of four animals per group. Mice were weighed weekly, and their behavior and food intake were monitored throughout the course of the experiment. Tumors were measured three times a week and tumor volume was calculated using the formula: tumor volume = length x width x height x  $\pi/6$  [20]. The study period was determined by the size of the tumors in the A9 group treated with DMSO vehicle control. All procedures were performed in compliance with the Canadian Council on Animal Care (CCAC) guidelines.

### **3.3 Results**

#### **3.3.1 Chromatin remodeling regulates TAP-1 transcription**

In order to investigate transcriptional regulation of TAP-1, a luciferase reporter construct was generated by cloning the mouse TAP-1 promoter region upstream of the *luc* gene in the pGL4.14[luc2/Hygro] vector (pTAP1-Luc) and was transfected into the TAP-expressing (Ltk, RMA) and TAP-deficient (LMD, CMT.64, B16F10) cells. Consistent with previous results obtained with the TAP-1-promoter-EGFP reporter construct [9], the pattern of expression of luciferase (Luc) in these stable transfectants was found to correlate with the pattern of endogenous TAP-1 expression ([9] and Figure 3.3.1.1). However, when the TAP-expressing and TAP-deficient cells were transiently transfected with the same construct, the pattern of differential expression no longer correlate with endogenous TAP-1 expression. It was conceivable that this lack of correlation may have resulted, at least in part, from the fact that the cell lines used were derived from distinct types of carcinomas, and therefore were unrelated to each other. To avoid this problem, two other models of TAP-expressing (TC-1 and PA) and TAP-deficient (TC-1/A9 and LMD) cells that were derived from primary tumors and their metastases, respectively, were used in subsequent experiments.

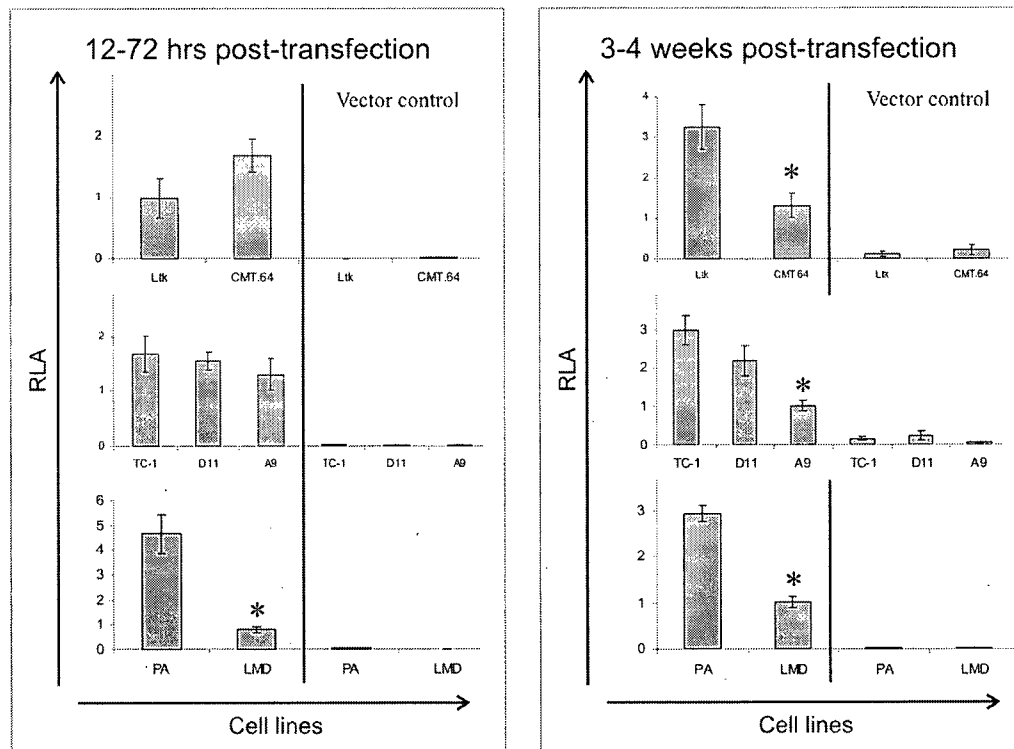


**Figure 3.3.1.1: Differences in TAP-1 promoter activity in stable transfectants generally match the TAP-1 expression profiles better than in transient transfectants.** Relative luciferase activity (RLA) in transient (12-72 hours post-transfection) and stable (3-4 weeks post-transfection) transfectants. In the transient transfectants, the luciferase unit in each cell line was determined as the ratio of firefly:renilla luciferase unit. In the stable transfectants, the luciferase unit in each cell line was determined as the ratio of firefly luciferase:copy number of pTAP1-Luc construct integrated into the genome. Relative luciferase activity (RLA) was determined as the luciferase unit in a particular cell line divided by the lowest value of luciferase unit obtained in that particular group of cells. *Columns*, average of three to six independent experiments; *bars*, SEM. \*  $P < .05$  compared with cells that expressed higher TAP-1 and MHC class I in the same group of cells (Student's t-test).

It was confirmed that TAP-1 expression levels in these new models of TAP-expressing and TAP-deficient cells correlated with MHC class I surface expression levels (Figure 3.3.1.2). In the prostate carcinoma model, PA cells that expressed a higher level of TAP-1 than LMD cells also expressed a higher level of surface MHC class I. Similarly, in the HPV-positive carcinoma model, TC-1, D11 and A9 cells that express high, moderate and low levels of TAP-1, respectively, also expressed the same pattern of surface MHC class I.

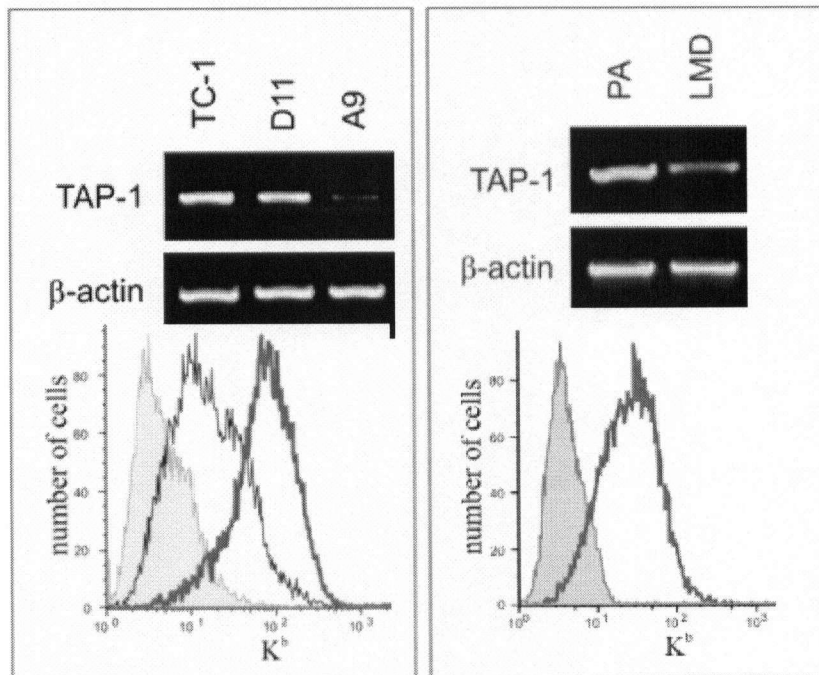


**Figure 3.3.1.2: Analysis of TAP- 1 and surface MHC class I expression by RT-PCR and flow cytometry, respectively.** Shaded area, thin and thick lines represent low (A9 or LMD), medium (D11) and high (TC-1 or PA) levels of MHC class I expression, respectively. Amplification of  $\beta$ -actin cDNA served as an internal control in the RT-PCR analysis. Data are representatives of three experiments.

These TAP-expressing and TAP-deficient cells were then transfected with the pTAP1-Luc construct. With the TC-1/D11/A9 model, it was found that, again, the relative levels of luciferase expression in stable population of transfectants matched the profiles of endogenous TAP-1 expression better than those in transient transfectants. Taken together with the results obtained with Ltk, RMA, CMT.64 and B16F10 cells, this observation suggests that integration of the reporter construct into the chromatin correlates with the differential activity of the TAP-1-promoter between TAP-expressing and TAP-deficient cells. The prostate carcinoma model was an exception to this trend, since the luciferase expression patterns obtained from stable and transient transfection both correlated with the endogenous TAP-1 expression (Figure 3.3.1.1). As a control, it was verified that luciferase expression in all cell lines transfected with pGL4.14[luc2/Hygro] vector alone was negligible compared to that in cells transfected with the pTAP1-Luc construct.

Furthermore, it was found that RNA polymerase II (pol II) binding to the endogenous TAP-1 promoter was lower in cells with low TAP-1 expression levels than that in cells with high TAP-1 expression levels (Figure 3.3.1.3). One possible explanation to account for this phenomenon was that the chromatin structure was forming a physical barrier, reducing the access of RNA pol II complex to the TAP-1 promoter. The LMD cells, the only cells that did not follow the TAP-1 expression trend in stable versus transient transfection, are likely to have additional defects that impair the activity of the TAP-1 promoter in addition to those related to chromatin remodeling.

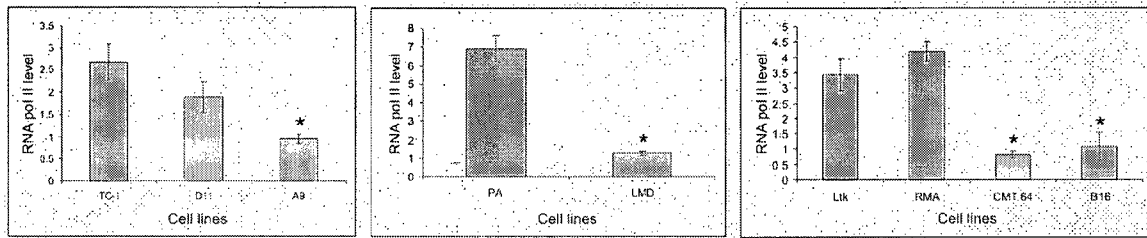


**Figure 3.3.1.3: RNA pol II binding to TAP-1 promoter is low in TAP-deficient carcinomas.** The levels of RNA pol II in TAP-1 promoter of each cell line were assessed by chromatin immunoprecipitation using anti-RNA pol II Ab. The eluted DNA fragment were purified and used as templates for real-time PCR analysis using primers specific for the 3'-end of the TAP-1 promoter. Relative RNA pol II levels were determined as the ratio of copy numbers of the eluted TAP-1 promoter and copy numbers of the corresponding inputs. The smallest ratio in each group of experiments was arbitrarily determined as 1. *Columns*, average of three to six experiments; *bars*, SEM. \*  $P < .05$  compared with cells that expressed higher TAP-1 and MHC class I in the same group of cells (Student's t-test).

### 3.3.2 Histone H3 acetylation within the TAP-1 promoter is low in MHC class I-deficient carcinomas

A well-known epigenetic mechanism that regulates gene expression is the acetylation of histone H3 within a gene locus [23-25], which promotes relaxation of the nucleosome structure and allows the transcriptional machinery to access the promoter [24, 26]. Therefore, the hypothesis tested was that the differential TAP-1 promoter

activity between TAP-expressing and TAP-deficient cells results from distinct levels of histone H3 acetylation within the TAP-1 promoter.

In the HPV-positive carcinoma model, it was found that histone H3 acetylation within TAP-1 promoter was impaired in A9 cells, which express the lowest level of TAP-1. D11 cells that express intermediate levels of TAP-1 compared to TC-1 and A9 also had intermediate levels of acetyl-histone H3 within the TAP-1 promoter (Figure 3.3.2.1). In the prostate carcinoma model, the metastatic, TAP-deficient LMD cells also had less acetyl-histone H3 within the TAP-1 promoter than in the non-metastatic, TAP-positive PA cells. In addition, the level of acetyl-histone H3 within the TAP-1 promoter in several other TAP-expressing (Ltk and RMA) and TAP-deficient (CMT.64 and B16F10) cell lines was also assessed. Acetyl-histone H3 was again found in low levels in the TAP-deficient carcinomas; in fact, it was absent in the highly metastatic CMT.64 cells. Taken together, these results demonstrate a clear correlation between the levels of TAP-1 expression and histone H3 acetylation within the TAP-1 promoter.

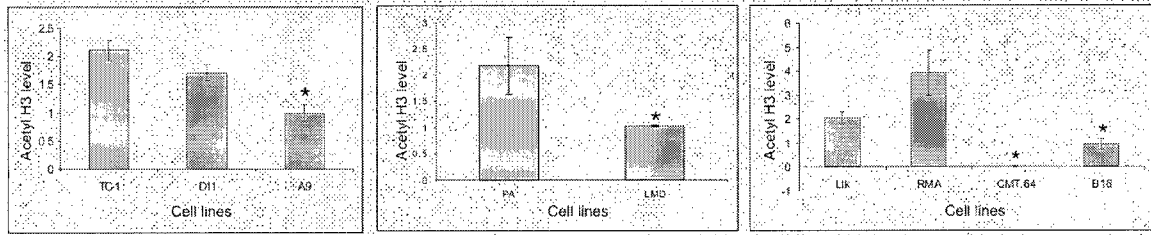


**Figure 3.3.2.1: Acetyl-histone H3 binding to TAP-1 promoter is low in TAP-deficient carcinomas.** The levels of acetyl-histone H3 in TAP-1 promoter of each cell line were assessed by chromatin immunoprecipitation using anti-acetyl-histone H3 Ab. The eluted DNA fragments were purified and used as templates for real-time PCR analysis using primers specific for the 3'-end of the TAP-1 promoter. Relative acetyl-histone H3 levels were determined as the ratio of copy numbers of the eluted TAP-1 promoter and copy numbers of the corresponding inputs. The smallest ratio in each group of experiments was arbitrarily determined as 1. *Columns*, average of three to six experiments; *bars*, SEM. \*  $P < .05$  compared with cells that expressed higher TAP-1 and MHC class I in the same group of cells (Student's t-test).

### 3.3.3 Identification of a region in TAP-1 promoter responsible for the differential activity in TAP-expressing and TAP-deficient cells

In order to determine the critical region of the TAP-1 promoter that is responsible for the differential promoter activity in TAP-expressing and TAP-deficient cells, several constructs were made by cloning 5'-end truncations of the TAP-1 promoter into the pGL4.14[luc2/Hygro] vector (constructs -427, -401 and -150 in Figure 3.3.3.1).

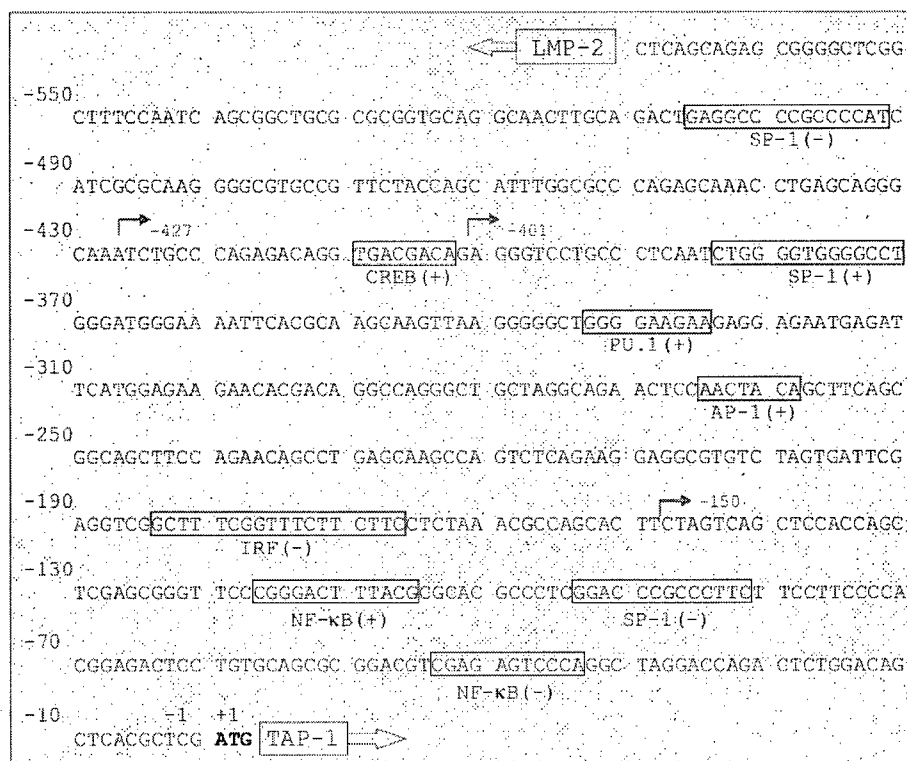


**Figure 3.3.3.1: TAP-1 promoter sequence with transcription factor binding motifs and 5' truncation sites.** The TAP-1 ATG codon was arbitrarily determined as +1. Truncation sites are indicated by numbered arrows. Motifs located on the sense strand are indicated by a (+) and motifs located on the antisense strand are indicated by a (-).

It was found that progressive truncations of 5'-end of the TAP-1 promoter resulted in a gradual decrease in the promoter's activity (as measured by Luc expression) in the TAP-expressing cells (Figure 3.3.3.2). This decrease in promoter activity indicates that the deleted regions normally participate in TAP-1 promoter activity. Interestingly, the truncations up to -401 did not affect the activity of the TAP-1 promoter in the TAP-deficient cells. This indicates that, in contrast to what was observed in TAP-expressing

cells, the -567 to -401 region of the TAP-1 promoter does not participate in the promoter's activity in TAP-deficient cells. Finally, it is important to note that the -401 construct yielded similar promoter activity in TAP-expressing and TAP-deficient cells. Taken together, these observations indicate that all the *cis*-acting elements responsible for the differential TAP-1 promoter activity in TAP-expressing versus TAP-deficient cells are located in the region encompassing base pairs -567 to -401.

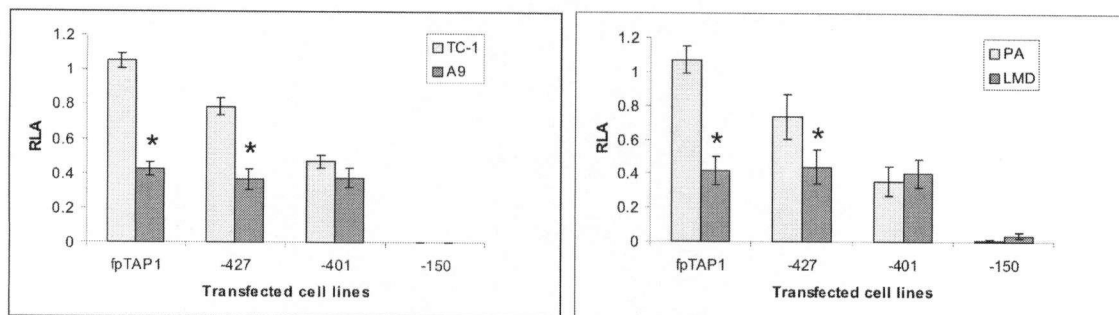


**Figure 3.3.3.2: A critical region that is responsible for differential activity of the TAP-1 promoter in TAP-expressing and TAP-deficient cells is found in-between -427 and -401 region of the promoter.** RLA was measured in stable transfectants. The largest value in each group of experiments was arbitrarily determined as 1. *Columns*, average of five experiments; *bars*, SEM. \*  $P < .05$  compared with TAP-expressing cells in the same group (Student's t-test).

A more detailed analysis revealed that the region encompassing base pairs -427 to -401 was sufficient to confer the differential TAP-1 promoter activity observed in TAP-expressing versus TAP-deficient cells. Analysis of putative transcription factor binding sites, using Tfsitescan software ([www.ifti.org](http://www.ifti.org)), suggested the presence of a CREB binding site within this region (Figure 3.3.3.1).

### 3.3.4 CBP binding to TAP-1 promoter is impaired in metastatic carcinomas

The existence of a putative CREB binding site in the region responsible for the differential activity of the TAP-1 promoter in TAP-expressing versus TAP-deficient cells is particularly interesting, since the CREB-binding protein (CBP) is one of the well-known transcriptional co-activators that possess intrinsic histone acetyltransferase (HAT) activity [27-29]. In addition, CBP is known to acetylate histone H3 [30], and the HAT activity and recruitment of CBP can be stimulated by various transcription factors [27] including SP-1 and AP-1 whose binding sites are also found in the TAP-1 promoter (Figure 3.3.3.1). These notions are consistent with the hypotheses that the differential TAP-1 promoter activity results from differences in chromatin structure at the *tap-1* locus, and that the *trans*-acting factors deficient or non-functional in TAP-deficient carcinomas can be those with the ability to control chromatin structures. Therefore, whether CBP plays a role in the differential TAP-1 promoter activity in TAP-expressing versus TAP-deficient cells was further analysed.

Western blot analysis showed that CBP is not lacking or truncated in TAP-deficient metastatic carcinomas (Figure 3.3.4.1).

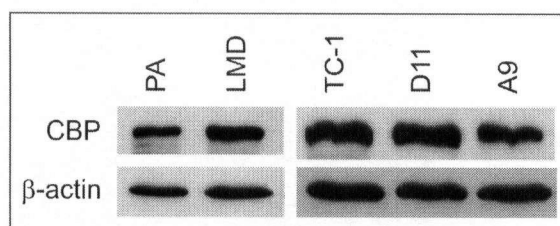


**Figure 3.3.4.1: Expression of CBP proteins is similar in TAP-expressing and in TAP-deficient carcinoma cells.**

However, chromatin immunoprecipitation analysis showed that CBP binding to the TAP-1 promoter was significantly lower in TAP-deficient, metastatic carcinomas compared to TAP-expressing, pre-metastatic cells (Figure 3.3.4.2). These results suggest that, in TAP-deficient cells, the lack of HAT activity normally exerted by CBP in TAP-1 promoter is likely to play a role in the inaccessibility of the promoter to the RNA pol II complex and in the subsequent impairment of TAP-1 transcription.

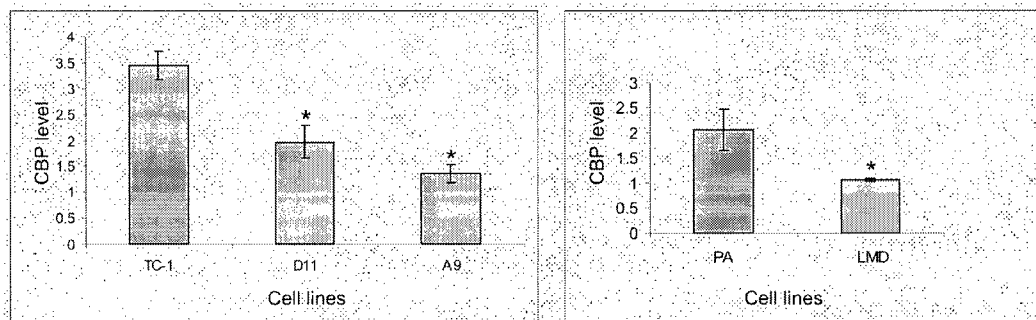


**Figure 3.3.4.2: CBP binding to TAP-1 promoter is impaired in TAP-deficient, metastatic carcinomas.** Chromatin immunoprecipitation using anti-CBP antibody was performed as described earlier. *Columns*, average of four experiments; *bars*, SEM. \*  $P < .05$  compared with cells that expressed the highest TAP-1 and MHC class I in the same group of cells (Student's t-test).

### 3.3.5 IFN- $\gamma$ treatment increases the level of CBP, acetyl-histone H3 and RNA polymerase II recruitment to the TAP-1 promoter in TAP-deficient metastatic carcinomas

Since the lack of CBP-mediated acetylation of histone H3 at the TAP-1 promoter appears to contribute to the TAP-1 deficiency in metastatic carcinomas, the hypothesis

that IFN- $\gamma$ , a well-known inducer of TAP-1 expression [9, 15, 31, 32], restored TAP-1 expression by increasing histone H3 acetylation at this locus was tested. The results showed that IFN- $\gamma$  increased the level of CBP, acetyl-histone H3 and RNA pol II recruitment to the TAP-1 promoter (Figure 3.3.5.1 A, B and C, respectively).

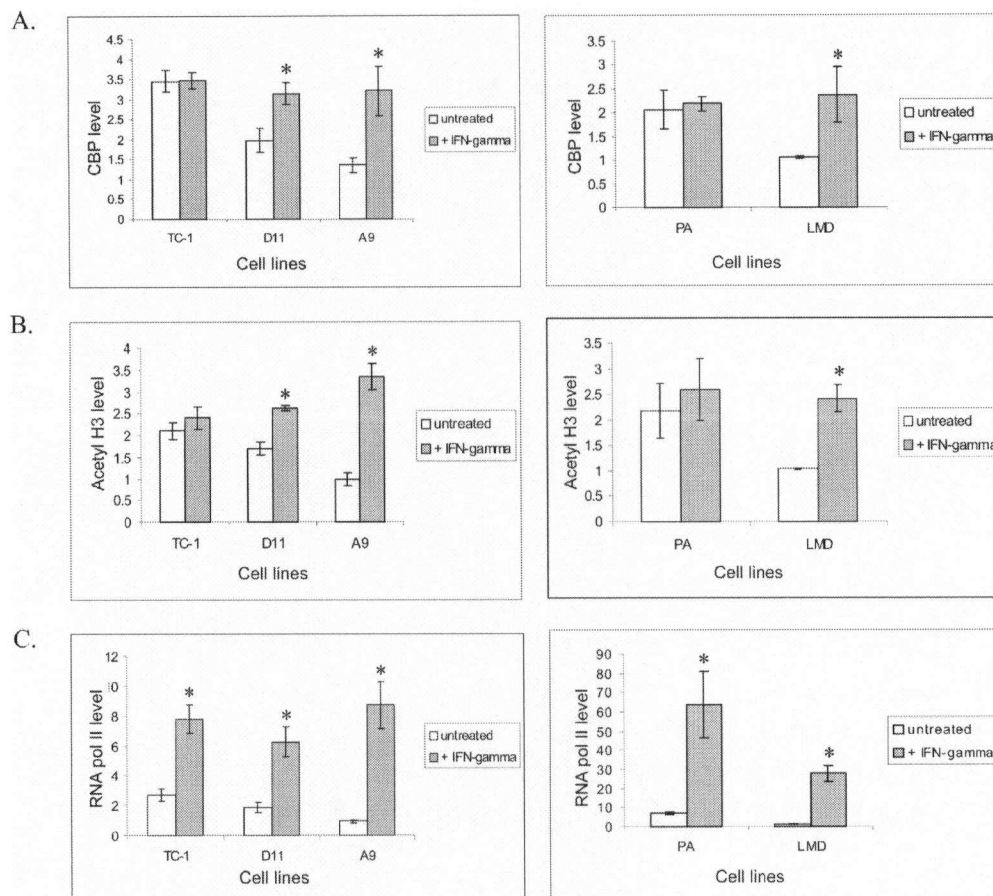


**Figure 3.3.5.1: IFN- $\gamma$  treatment improves the recruitment of CBP, acetyl-histone H3 and RNA pol II to TAP-1 promoter, most significantly in TAP-deficient cells.** Chromatin immunoprecipitation using *A*, anti-CBP, *B*, anti-acetyl-histone H3 or *C*, anti-RNA pol II antibody was performed as described earlier. *Columns*, average of three to four experiments; *bars*, SEM. \*  $P < .05$  compared with untreated cells (Student's t-test).

Based on these results, a possible mechanism of TAP-1 induction by IFN- $\gamma$  is proposed to be via the improvement of CBP binding to the TAP-1 promoter, thereby promoting histone H3 acetylation in the region and leading to relaxation of the surrounding chromatin. This would in turn increase the accessibility of RNA polymerase II complex to the TAP-1 promoter and promote transcription of this gene.

### **3.3.6 Trichostatin A (TSA), a histone deacetylase inhibitor, increases the expression of TAP-1 and other antigen-processing machinery (APM) components in metastatic (TAP-deficient) and pre-metastatic (TAP-expressing) carcinomas**

As the acetylation level of histones in the TAP-1 promoter seems to regulate TAP-1 expression in carcinomas, an investigation was performed to test whether inhibition of histone deacetylase (HDAC) activity in TAP-deficient carcinoma cells with TSA would restore TAP-1 expression. TSA is a highly specific, hydroxamic acid-based HDAC inhibitor (HDACi) [33-35]. By chromatin immunoprecipitation assays, it was found that TSA treatment, indeed, enhanced the recruitment of RNA pol II complex to the TAP-1 promoter in most cell lines (Figure 3.3.6.1A). This phenomenon was particularly prominent in the TAP-deficient cells, in which TSA treatment enhanced the recruitment of RNA pol II to levels similar to those in TAP-expressing cells. In addition, TAP-1 promoter activity also increased significantly in TAP-deficient cells upon treatment with TSA (Figure 3.3.6.1B). The fact that TSA treatment increases TAP-1 promoter activity confirms that chromatin remodeling plays a crucial role in the regulation of TAP-1 promoter activity.

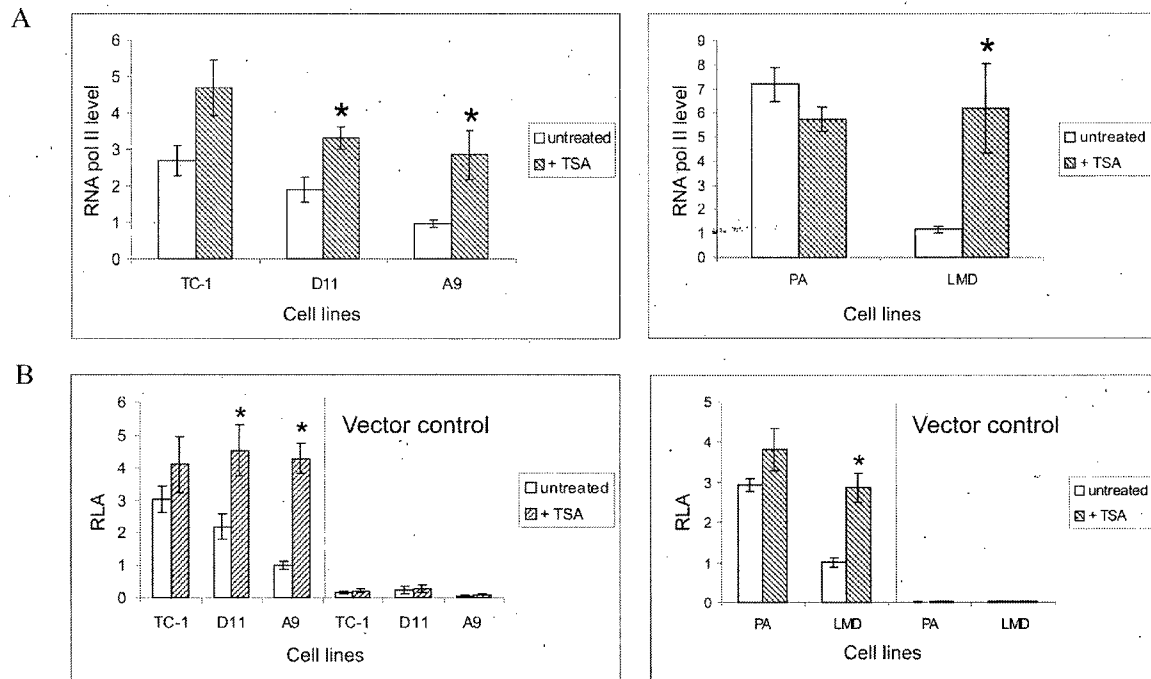


**Figure 3.3.6.1: TSA treatment enhances RNA pol II recruitment to TAP-1 promoter and TAP-1 promoter activity.** *A*, The levels of RNA Pol II in TAP-1 promoter of each cell line were assessed by chromatin immunoprecipitation using anti-RNA pol II. *B*, TAP-1 promoter activity in stable transfectants was determined by luciferase assay. *Columns*, average of three to six experiments; *bars*, SEM. \*  $P < .05$  compared with untreated cells (Student's t-test).

Based on the observations that levels of histone H3 acetylation correlate with TAP-1 expression and that TSA treatment enhances TAP-1-promoter activity, it was tempting to speculate that the effect of TSA on TAP-1 promoter activity could be occurring via an increase in histone H3 acetylation. However, chromatin immunoprecipitation results showed that TSA treatment did not significantly alter the levels of acetyl-histone H3 in TAP-1 promoter in any of cell lines tested (Figure 3.3.6.2). This suggests that the mechanism by which TSA increases the TAP-1 promoter activity does not involve a direct improvement of histone H3 acetylation within the TAP-1 promoter itself. Further investigation will be required to delineate the exact mechanism underlying the effect of TSA on TAP-1 promoter activity.

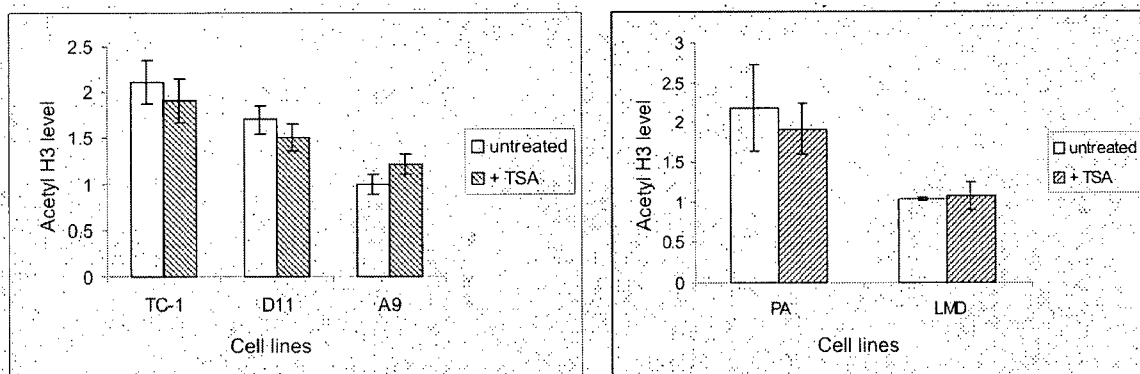


**Figure 3.3.6.2: TSA treatment does not significantly alter the levels of histone H3 acetylation in TAP-1 promoter.** The levels of acetyl-histone H3 in TAP-1 promoter of each cell line were assessed by chromatin immunoprecipitation using anti-acetyl-histone H3 antibody. *Columns*, average of three to six experiments; *bars*, SEM.

### 3.3.7 TSA treatment increases the expression of TAP-1 and surface MHC class I, resulting in an increased susceptibility of TAP-deficient metastatic carcinomas to CTL killing

Consistent with the increase in TAP-1 promoter activity, the expression of TAP-1 at the mRNA and protein levels (as assessed by RT-PCR and Western Blot) was enhanced in response to TSA or IFN- $\gamma$  treatment (Figure 3.3.7.1).

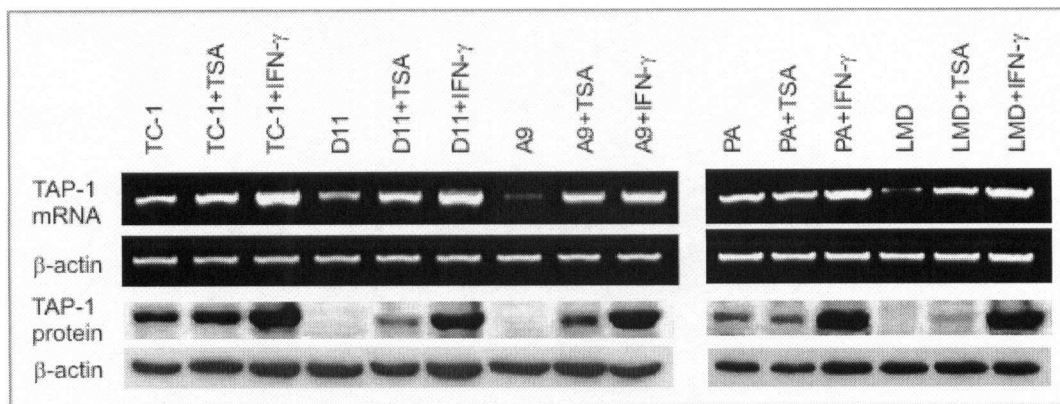


**Figure 3.3.7.1: TAP-1 expression in all cell lines, particularly in the TAP-deficient carcinomas, was up-regulated with TSA treatment. Up-regulated TAP-1 expression from IFN- $\gamma$ -treated cells was used as a positive control.  $\beta$ -actin expression served as a loading control. Data are representatives of three experiments.**

RT-PCR analyses were performed to test whether treatment with TSA or IFN- $\gamma$  also restored the expression of LMP-2 and possibly other APM components, since the TAP-1 promoter is a bi-directional promoter that also controls the expression of the *LMP-2* gene

[36]. The results showed that the *Lmp-2* and *Tap-2* genes have similar patterns of expression as the *Tap-1* gene in TC-1, D11 and A9 cells (high, moderate and low, respectively) (Figure 3.3.7.2). The expression of LMP-2, as well as TAP-2 and tapasin, was also increased by TSA or IFN- $\gamma$  treatment in the HPV-positive carcinoma cell lines.

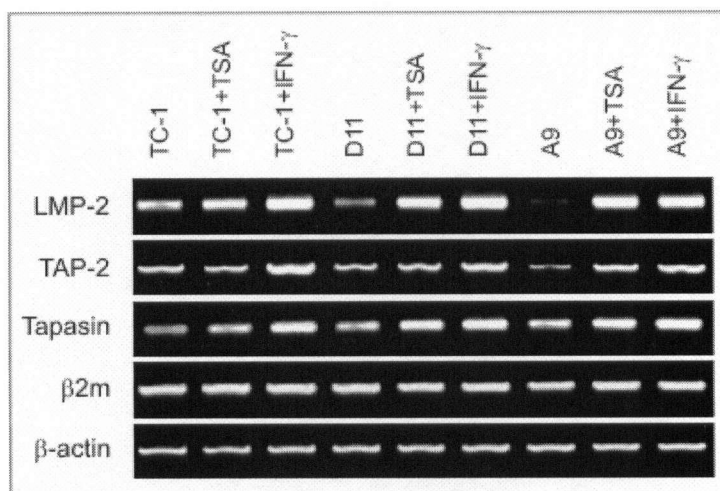


**Figure 3.3.7.2: Expression of LMP-2, TAP-2 and tapasin in all cell lines, particularly in the TAP-deficient carcinomas, was up-regulated with TSA treatment.** Amplification of APM cDNA from IFN- $\gamma$ -treated cells was used as a positive control.  $\beta$ -actin expression served as a loading control. Data are representatives of three experiments.

Flow cytometric analyses of surface H-2K<sup>b</sup> expression were performed to test whether TSA treatment would also result in an increase of MHC class I antigen presentation in the metastatic carcinoma cells, since the expression of several antigen processing components increases upon TSA treatment. The results demonstrated that TSA treatment increased the H-2K<sup>b</sup> surface expression by approximately 10 fold in TAP-

deficient cells, whereas the levels were unchanged in PA and TC-1 cells, which naturally express high levels of surface H-2K<sup>b</sup> (Figure 3.3.7.3). IFN- $\gamma$  treatment increased the surface H-2K<sup>b</sup> expression in all cell lines.

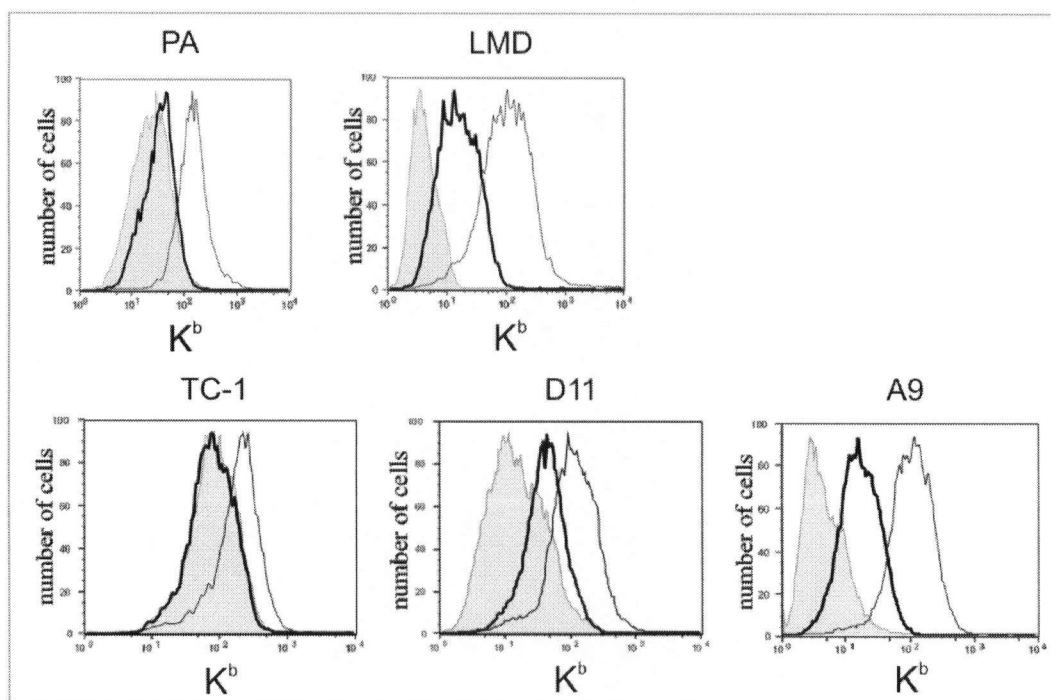


**Figure 3.3.7.3: Surface H-2K<sup>b</sup> expression, particularly on MHC class I-deficient cells, was enhanced by TSA treatment.** Cells untreated (shaded areas) or treated with 100 ng/ml TSA (thick lines) or 50 ng/ml IFN- $\gamma$  (thin lines) were stained with PE-conjugated anti-H-2K<sup>b</sup> mAb. Data are representatives of three experiments.

Furthermore, cytotoxicity (CTL) assays were performed to test whether the increased expression of H-2K<sup>b</sup> at the cell surface after TSA treatment would improve the recognition and the killing of virally-infected cancer cells by virus-specific cytotoxic T

lymphocytes. In this assay, VSV-derived peptides are presented by the infected target cells in the context of H-2K<sup>b</sup> only if the cells have functional antigen processing and presenting machinery [1, 8]. As expected, D11 and A9 cells, which express lower surface K<sup>b</sup> than the TC-1, are less susceptible to killing by the CTLs (Figure 3.3.7.4). TSA treatment of the virus-infected D11 and A9 cells enhanced CTL killing by approximately 6 and 7 fold, respectively. IFN- $\gamma$  treatment resulted in a drastic increase in the killing of all VSV-infected cell lines. However, LMD cells remained resistant to CTL killing despite a significant induction of APM and MHC class I expression by IFN- $\gamma$  due to unknown mechanisms independent of MHC class I expression [15].

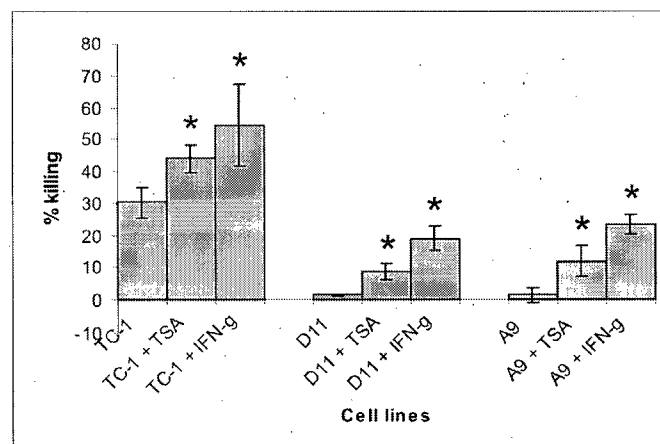


**Figure 3.3.7.4: TSA treatment improves HPV-positive tumor cell killing by CTLs.** Target cells were uninfected or VSV-infected, untreated or treated with TSA or IFN- $\gamma$  for 24 hours before infection with the VSV. CTL assays were performed using effector:target ratio of 0.8:1 to 200:1. Representative data using 22:1 effector:target ratio are shown in this figure. All cells were infected with VSV at a MOI of 7.5 for 16hr. *Columns*, average of three experiments; *bars*, SEM. \*  $P \leq .05$  compared with untreated cells (Student's t-test).

An additional experiment using VSV-infected, TAP-deficient B16F10 as target cells also showed a similar improvement in the ability of specific CTLs to kill the cancer cells upon TSA treatment (Figure 3.3.7.5). Taken together, these results indicate that TSA or IFN- $\gamma$  treatment increases TAP-1 expression, and ultimately results in an increase in immune recognition of metastatic carcinoma cells.

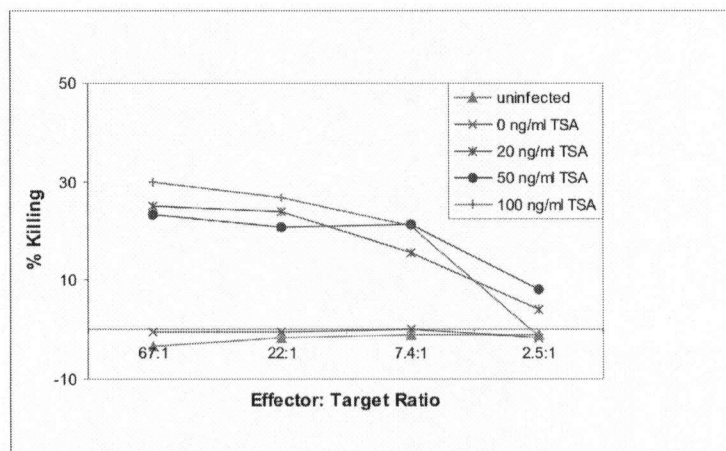


**Figure 3.3.7.5: TSA treatment improves B16F10 tumor cell killing by CTLs.**

Target cells were uninfected or VSV-infected, untreated or treated with various concentrations of TSA for 24 hours before infection with the VSV. CTL assay was performed using effector:target ratio of 2.5:1 to 67:1. All cells were infected with VSV at a MOI of 7.5 for 16hr.

### **3.3.8 TSA treatment suppresses the growth of TAP-deficient, metastatic tumors *in vivo***

As TSA treatment increased CTL killing of TAP-deficient cells *in vitro*, it was further investigated whether it would result in a decrease in tumor formation *in vivo*. The

results indicate that indeed, daily treatment of mice with TSA reduced the growth rate of A9 tumors (Figure 3.3.8.1). In addition, as expected, the TAP-expressing TC-1 cells were significantly less tumorigenic than the TAP-deficient A9 cells. Only four out of nine mice injected subcutaneously with TC-1 cells grew small tumors that only appeared at approximately 3-4 weeks after the injection, as compared to one week in all mice injected with the A9 cells.

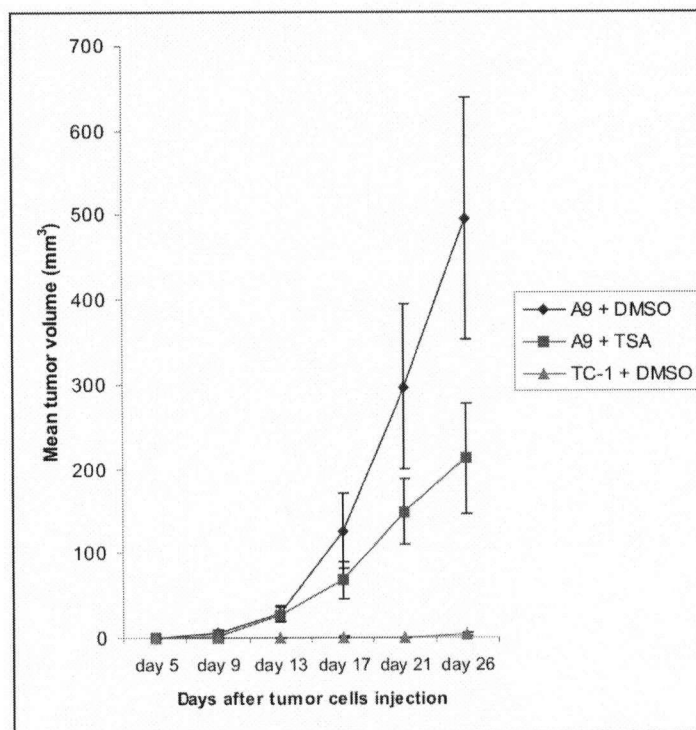


**Figure 3.3.8.1: TSA treatment suppresses tumor growth *in vivo*.** A9 (MHC class I-deficient cells) tumor growth was suppressed in mice treated with 500  $\mu\text{g}/\text{kg}$  of TSA daily compared to in those treated with DMSO vehicle control ( $n = 8$  per treatment group). TC-1 group represented tumor growth in mice injected with high MHC class I-expressing cells ( $n = 9$ ). Data represent the mean tumor volume  $\pm$  SEM.

TAP-1 promoter activity in A9 tumor cells isolated from the TSA-treated mice was found to be significantly higher than in those isolated from the control mice (Figure 3.3.8.2). These observations support the hypothesis that the improvement of TAP-1 expression and MHC class I antigen presentation leads to increased killing of the TAP-deficient metastatic cancer cells, thus suppresses tumor growth *in vivo*.

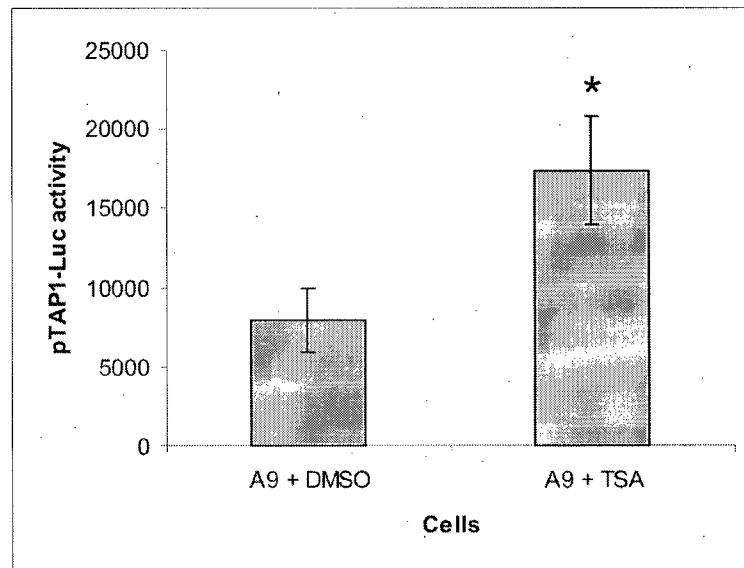


**Figure 3.3.8.2: TAP-1 promoter activity is enhanced in TAP-deficient tumor cells isolated from TSA-treated mice.** TAP-1 promoter-driven Luciferase (pTAP1-Luc) expression is higher in A9 cells isolated from TSA-treated mice than in those isolated from DMSO-treated mice (n=4 per treatment group). \* P < .05 compared with cells from DMSO-treated mice (Student's t-test).

### **3.4 Discussion**

The regulation of chromatin structure plays an important role in controlling gene expression. The observations that silencing of the TAP-1 promoter reporter construct occurs exclusively after the construct integrates into the genome, and that levels of RNA pol II bound to the TAP-1 promoter are relatively low in metastatic, TAP-deficient cells suggest that access of the RNA pol II complex to the TAP-1 promoter is limited in the TAP-deficient cells. A compact nucleosome structure around a promoter region can act as a physical barrier that prevents the binding of transcriptional activators to the promoter and consequently, halts the transcription process [37]. Therefore, it was tested if TAP deficiency in metastatic cancer cells results from a repressive state of chromatin structure.

A high level of acetylated core histones in a chromatin template, particularly in the proximal region of an acetylation-sensitive promoter [37, 38], has been associated with active transcription [23, 24, 26, 27, 38]. As the results in this study demonstrate a role for chromatin remodeling in the regulation of TAP-1 expression, the specific players involved were sought to be identified. Although histone H3 is not the only core histone whose modification has been shown to influence gene expression [23, 39], the correlation between the acetylation of histone H3 and activation of several genes has been widely studied and is now well established [23-25, 39]. Therefore, histone H3 acetylation status within TAP-1 promoter was investigated in this study. The results demonstrate that the levels of acetylated histone H3 within the TAP-1 promoter show a trend similar to the levels of RNA pol II binding to TAP-1 promoter, and to TAP-1 expression at both the RNA and the protein levels in all the cell lines tested. These observations suggest that the level of histone H3 acetylation within the TAP-1 promoter plays a role in the regulation

of TAP-1 transcription, although it is not likely to be the sole mechanism involved, since the activation of transcription generally involves synergistic actions of several factors [24].

Furthermore, it was found that the region in the TAP-1 promoter that is responsible for the differential activity in the TAP-expressing versus the TAP-deficient carcinoma cells is located between bases -427 and -401, and that this region encompasses a putative CREB binding motif. CBP, a mammalian histone acetyltransferase, is known to associate with CREB [28, 29]. Therefore, the recruitment of CBP to the TAP-1 promoter in TAP-deficient cells was investigated. It was found that, indeed, the levels of CBP binding to TAP-1 promoter in TAP-deficient cells were lower than in cells that express higher levels of TAP-1. CBP is known to acetylate histones around promoter regions, resulting in increased accessibility of the promoters to essential transcriptional regulators [29]. Current findings suggest that in the metastatic cancer cells, the lack of CBP binding to TAP-1 promoter potentially contributes to the TAP-1 deficiency, probably by impairing histone H3 acetylation. In the study described in the previous chapter, it was proposed that the lack of expression or activity of *trans*-acting factors is one of the mechanisms that contributes to TAP-1 deficiency in malignant cells [9]. CBP is likely to be one of these factors. The exact mechanisms responsible for the decreased recruitment of CBP to the TAP-1 promoter remain to be identified.

IFN- $\gamma$  is known to be a potent inducer of TAP-1 and surface MHC class I expression in cancer cells [9, 15, 31, 32]; however, little is known about molecular mechanisms that lead to TAP-1 induction by IFN- $\gamma$ . The findings that the improvement of CBP recruitment to the TAP-1 promoter correlated with higher levels of histone H3

acetylation, and therefore, active transcription of the *Tap-1* gene, provide one mechanism by which IFN- $\gamma$  increases TAP-1 expression.

Furthermore, it was demonstrated for the first time that treatment of TAP-deficient cells with TSA resulted in a significant increase in RNA pol II binding to the TAP-1 promoter and in the promoter's activity. TSA belongs to a group of hydroxamic acid-based histone deacetylase inhibitors (HDACi) that act on selective genes, altering the transcription of only approximately 2% of expressed genes in cultured tumor cells [35]. Consistent with this notion is the fact that histone acetylases and deacetylases act selectively on specific genes, and hence do not universally affect the transcription of all genes [38]. TSA has been shown to confer anti-tumor effects *in vitro* and *in vivo* [33-35]. However, the mechanism underlying the effect of TSA in tumor antigen presentation was not fully understood.

In addition to the improvement in TAP-1 expression, it was found that treatment with TSA also resulted in the upregulation of several other APM components, such as TAP-2, LMP-2 and tapasin. Given the proximity of *Tap-1*, *Tap-2* and *Lmp-2* genes within the MHC class II locus, and the location of gene encoding tapasin in the same chromosomal region [40], it is likely that these genes are co-regulated at the chromatin level. It has been reported previously that a small region (approximately 300 bp) could control the transcription of a cluster of genes by serving as a binding site for factors involved in chromatin remodeling [41, 42]. Since transcription of a TAP-1 promoter-driven reporter gene in TAP-deficient cells was silenced as the construct integrated into random sites of the genome, and since both the endogenous and the transfected TAP-1 promoter activity improved upon TSA treatment, it is possible that

an autonomous chromatin condensation regulatory element (ACCRE) at the MHC class II locus exists within the LMP-2/TAP-1 intergenic region.

Despite the efficacy of TSA in improving MHC class I antigen presentation in metastatic cancer cells, it was observed that the levels of induction resulting from TSA treatments were never as strong as the effects generated by IFN- $\gamma$ . The results showed that one of the key differences is their distinct ability to enhance the levels of histone H3 acetylation in the TAP-1 promoter. IFN- $\gamma$  treatment of TAP-deficient cells enhanced histone H3 acetylation within the TAP-1 promoter to much higher levels than TSA did, up to similar or even higher levels than in the TAP-expressing cells. It is conceivable that IFN- $\gamma$  treatment results in a maximal state of relaxation of chromatin structures around the TAP-1 locus, thus enabling optimal levels of binding of general transcription factors and RNA pol II to the TAP-1 promoter, sufficient to support high levels of transcription of this gene.

Finally, results from *in vivo* experiments showed that daily treatment with TSA suppressed tumor growth in mice inoculated with A9 cancer cells. The increase in TAP-1 promoter activity, hence enhanced transcription of the *Tap-1* gene and possibly the expression of other APM components in TAP-deficient A9 tumor cells of TSA-treated mice, may significantly contribute to the reduction of tumor growth in these mice. These findings are encouraging for the development of therapeutic approaches that aim to increase tumor antigen presentation as a way to improve the recognition and the killing of neoplastic cells by specific CTLs. Nevertheless, further studies are required to improve the *in vivo* efficiency of natural HDACi, such as TSA, depudecin, trapoxins, apicidins, sodium butyrate, phenylbutyrate and suberoyl anilide hydroxamic acid (SAHA) as anti-

cancer agents, as their effectiveness is greatly impaired by their instability and low retention *in vivo* [43].

This study presents a great support for the notion that TAP-deficient carcinomas lack *trans*-acting factors that would normally enable relaxation of the chromatin structure to allow access of general transcription factors and RNA pol II to the *Tap-1* gene promoter. This provides new insights into the epigenetic mechanisms responsible for the immune escape of cancer cells. Further research that aims to identify more chromatin remodeling factors that play roles in tumor antigen processing deficiencies will be essential for the development of novel therapeutic approaches against MHC class I-deficient cancers. In contrast to genetic etiology of cancer, the possibility of reversing epigenetic codes may provide new targets for therapeutic intervention in cancer.

### 3.5 References

1. Gabathuler, R., G. Reid, G. Kolaitis, J. Driscoll, and W.A. Jefferies. Comparison of cell lines deficient in antigen presentation reveals a functional role for TAP-1 alone in antigen processing. *J Exp Med*, 1994. 180:1415-25.
2. Seliger, B., M.J. Maeurer, and S. Ferrone. Antigen-processing machinery breakdown and tumor growth. *Immunol Today*, 2000. 21:455-64.
3. Seliger, B., M.J. Maeurer, and S. Ferrone. TAP off--tumors on. *Immunol Today*, 1997. 18:292-9.
4. Seliger, B., U. Wollscheid, F. Momburg, T. Blankenstein, and C. Huber. Coordinate downregulation of multiple MHC class I antigen processing genes in chemical-induced murine tumor cell lines of distinct origin. *Tissue Antigens*, 2000. 56:327-36.
5. Lankat-Buttgereit, B. and R. Tampe. The transporter associated with antigen processing: function and implications in human diseases. *Physiol Rev*, 2002. 82:187-204.
6. Ritz, U. and B. Seliger. The transporter associated with antigen processing (TAP): structural integrity, expression, function, and its clinical relevance. *Mol Med*, 2001. 7:149-58.
7. Johnsen, A.K., D.J. Templeton, M. Sy, and C.V. Harding. Deficiency of transporter for antigen presentation (TAP) in tumor cells allows evasion of immune surveillance and increases tumorigenesis. *J Immunol*, 1999. 163:4224-31.

8. Alimonti, J., Q.J. Zhang, R. Gabathuler, G. Reid, S.S. Chen, and W.A. Jefferies. TAP expression provides a general method for improving the recognition of malignant cells in vivo. *Nat Biotechnol*, 2000. 18:515-20.
9. Setiadi, A.F., M.D. David, S.S. Chen, J. Hiscott, and W.A. Jefferies. Identification of mechanisms underlying transporter associated with antigen processing deficiency in metastatic murine carcinomas. *Cancer Res*, 2005. 65:7485-92.
10. Klenova, E.M., H.C. Morse, 3rd, R. Ohlsson, and V.V. Lobanenkova. The novel BORIS + CTCF gene family is uniquely involved in the epigenetics of normal biology and cancer. *Semin Cancer Biol*, 2002. 12:399-414.
11. Maio, M., S. Coral, E. Fratta, M. Altomonte, and L. Sigalotti. Epigenetic targets for immune intervention in human malignancies. *Oncogene*, 2003. 22:6484-8.
12. Lund, A.H. and M. van Lohuizen. Epigenetics and cancer. *Genes Dev*, 2004. 18:2315-35.
13. Lin, K.Y., F.G. Guarnieri, K.F. Staveley-O'Carroll, H.I. Levitsky, J.T. August, D.M. Pardoll, and T.C. Wu. Treatment of established tumors with a novel vaccine that enhances major histocompatibility class II presentation of tumor antigen. *Cancer Res*, 1996. 56:21-6.
14. Smahel, M., P. Sima, V. Ludvikova, I. Marinov, D. Pokorna, and V. Vonka. Immunisation with modified HPV16 E7 genes against mouse oncogenic TC-1 cell sublines with downregulated expression of MHC class I molecules. *Vaccine*, 2003. 21:1125-36.

15. Lee, H.M., T.L. Timme, and T.C. Thompson. Resistance to lysis by cytotoxic T cells: a dominant effect in metastatic mouse prostate cancer cells. *Cancer Res*, 2000. 60:1927-33.
16. Franks, L.M., A.W. Carbonell, V.J. Hemmings, and P.N. Riddle. Metastasizing tumors from serum-supplemented and serum-free cell lines from a C57BL mouse lung tumor. *Cancer Res*, 1976. 36:1049-55.
17. Poste, G., J. Doll, I.R. Hart, and I.J. Fidler. In vitro selection of murine B16 melanoma variants with enhanced tissue-invasive properties. *Cancer Res*, 1980. 40:1636-44.
18. Giraud, S., F. Bienvenu, S. Avril, H. Gascan, D.M. Heery, and O. Coqueret. Functional interaction of STAT3 transcription factor with the coactivator NcoA/SRC1a. *J Biol Chem*, 2002. 277:8004-11.
19. Zhang, Q.J., R.P. Seipp, S.S. Chen, T.Z. Vitalis, X.L. Li, K.B. Choi, A. Jeffries, and W.A. Jefferies. TAP expression reduces IL-10 expressing tumor infiltrating lymphocytes and restores immunosurveillance against melanoma. *Int J Cancer*, 2007.
20. Canes, D., G.J. Chiang, B.R. Billmeyer, C.A. Austin, M. Kosakowski, K.M. Rieger-Christ, J.A. Libertino, and I.C. Summerhayes. Histone deacetylase inhibitors upregulate plakoglobin expression in bladder carcinoma cells and display antineoplastic activity in vitro and in vivo. *Int J Cancer*, 2005. 113:841-8.
21. Mishra, N., C.M. Reilly, D.R. Brown, P. Ruiz, and G.S. Gilkeson. Histone deacetylase inhibitors modulate renal disease in the MRL-lpr/lpr mouse. *J Clin Invest*, 2003. 111:539-52.

22. Vigushin, D.M., S. Ali, P.E. Pace, N. Mirsaidi, K. Ito, I. Adcock, and R.C. Coombes. Trichostatin A is a histone deacetylase inhibitor with potent antitumor activity against breast cancer in vivo. *Clin Cancer Res*, 2001. 7:971-6.
23. Berger, S.L. Histone modifications in transcriptional regulation. *Curr Opin Genet Dev*, 2002. 12:142-8.
24. Eberharter, A. and P.B. Becker. Histone acetylation: a switch between repressive and permissive chromatin. Second in review series on chromatin dynamics. *EMBO Rep*, 2002. 3:224-9.
25. Mahadevan, L.C., A.L. Clayton, C.A. Hazzalin, and S. Thomson. Phosphorylation and acetylation of histone H3 at inducible genes: two controversies revisited. *Novartis Found Symp*, 2004. 259:102-11; discussion 111-4, 163-9.
26. Eberharter, A., R. Ferreira, and P. Becker. Dynamic chromatin: concerted nucleosome remodelling and acetylation. *Biol Chem*, 2005. 386:745-51.
27. Legube, G. and D. Trouche. Regulating histone acetyltransferases and deacetylases. *EMBO Rep*, 2003. 4:944-7.
28. Giordano, A. and M.L. Avantaggiati. p300 and CBP: partners for life and death. *J Cell Physiol*, 1999. 181:218-30.
29. Kalkhoven, E. CBP and p300: HATs for different occasions. *Biochem Pharmacol*, 2004. 68:1145-55.
30. Davie, J.R. and V.A. Spencer. Control of histone modifications. *J Cell Biochem*, 1999. Suppl 32-33:141-8.
31. Mikyskova, R., J. Bubenik, V. Vonka, M. Smahel, M. Indrova, J. Bieblova, J. Simova, and T. Jandlova. Immune escape phenotype of HPV16-associated

- tumours: MHC class I expression changes during progression and therapy. *Int J Oncol*, 2005. 26:521-7.
32. Matsui, M., S. Machida, T. Itani-Yohda, and T. Akatsuka. Downregulation of the proteasome subunits, transporter, and antigen presentation in hepatocellular carcinoma, and their restoration by interferon-gamma. *J Gastroenterol Hepatol*, 2002. 17:897-907.
  33. Mukhopadhyay, N.K., E. Weisberg, D. Gilchrist, R. Bueno, D.J. Sugarbaker, and M.T. Jaklitsch. Effectiveness of trichostatin A as a potential candidate for anticancer therapy in non-small-cell lung cancer. *Ann Thorac Surg*, 2006. 81:1034-42.
  34. Zhu, W.G. and G.A. Otterson. The interaction of histone deacetylase inhibitors and DNA methyltransferase inhibitors in the treatment of human cancer cells. *Curr Med Chem Anticancer Agents*, 2003. 3:187-99.
  35. Marks, P.A., V.M. Richon, R. Breslow, and R.A. Rifkind. Histone deacetylase inhibitors as new cancer drugs. *Curr Opin Oncol*, 2001. 13:477-83.
  36. Wright, K.L., L.C. White, A. Kelly, S. Beck, J. Trowsdale, and J.P. Ting. Coordinate regulation of the human TAP1 and LMP2 genes from a shared bidirectional promoter. *J Exp Med*, 1995. 181:1459-71.
  37. Gregory, P.D., K. Wagner, and W. Horz. Histone acetylation and chromatin remodeling. *Exp Cell Res*, 2001. 265:195-202.
  38. Struhl, K. Histone acetylation and transcriptional regulatory mechanisms. *Genes Dev*, 1998. 12:599-606.

39. Keen, J.C., E. Garrett-Mayer, C. Pettit, K.M. Mack, J. Manning, J.G. Herman, and N.E. Davidson. Epigenetic regulation of protein phosphatase 2A (PP2A), lymphotactin (XCL1) and estrogen receptor alpha (ER) expression in human breast cancer cells. *Cancer Biol Ther*, 2004. 3:1304-12.
40. Janeway, C., P. Travers, M. Walport, and M. Shlomchik. *Immunobiology: the immune system in health and disease*. 5th ed. 2001, New York, NY Garland Publishing.
41. Kaneko, T., H. Hosokawa, M. Yamashita, C.R. Wang, A. Hasegawa, M.Y. Kimura, M. Kitajima, F. Kimura, M. Miyazaki, and T. Nakayama. Chromatin remodeling at the Th2 cytokine gene loci in human type 2 helper T cells. *Mol Immunol*, 2007. 44:2249-56.
42. Takemoto, N., Y. Kamogawa, H. Jun Lee, H. Kurata, K.I. Arai, A. O'Garra, N. Arai, and S. Miyatake. Cutting edge: chromatin remodeling at the IL-4/IL-13 intergenic regulatory region for Th2-specific cytokine gene cluster. *J Immunol*, 2000. 165:6687-91.
43. Monneret, C. Histone deacetylase inhibitors. *Eur J Med Chem*, 2005. 40:1-13.

## Chapter 4 : Characterization of Novel TAP-1 Regulator Genes

### 4.1 Introduction

Previous studies have demonstrated that one of the underlying mechanisms contributing to TAP deficiency in metastatic carcinomas is the lack of activation or expression of TAP-1 transcriptional activators [1]. Therefore, expression of the functional activator(s) in TAP-deficient carcinoma cells should lead to increased TAP-1 expression and restoration of tumor antigen presentation. Results from a parallel study provided deeper insight into the characteristics of the unknown transcriptional activators, in that they might play a role in chromatin remodeling within the *Tap-1* gene locus (Chapter 3). The present chapter describes the development of a new method and preliminary results obtained in the attempt to characterize novel TAP regulator genes.

In this classical complementation study, a stable clone of pTAP1-EGFP-transfected CMT.64 cells [1] was transduced with high complexity, human cDNA library retroviral supernatants derived from normal human lung or spleen specimens (ViraPort; Stratagene). The cDNA-packaging virus possesses vesicular stomatitis virus G (VSV-G) envelope protein, which recognizes common membrane phospholipids, such as phosphatidylserine [2]. Therefore, the VSV-G-coated retrovirus is capable of infecting a wide variety of living cells with enhanced transduction efficiency, unlike viruses with other commonly-used envelope proteins that recognize only specific cell surface receptors [2]. cDNA libraries from human sources were used since at the time of this work, the only VSV-G-packaged mouse cDNA library available was derived from testes,

which was certainly not a good source of TAP and MHC class I activators, since a testis was an immune privilege site that displayed downregulated expression of MHC class I [3]. Normal lung-derived cDNA library was initially chosen since the CMT.64 target cells were originated from murine lung tumor cells. Expression of TAP-1 activators from normal lungs could potentially restore TAP and MHC class I expression in the metastatic cancer cells. A similar experiment using normal spleen-derived cDNA was performed to observe any similarities in the identity of TAP-activator candidates obtained from the lung cDNA library screening.

## **4.2 Materials and Methods**

### **4.2.1 Cell lines**

The CMT.64 cell line established from a spontaneous lung carcinoma of a C57BL/6 mouse [4], the Ltk and NIH/3T3 mouse fibroblasts (ATCC, Manassas, VA), and A549 human lung carcinoma cell line (ATCC) were grown in DMEM media. CMT.64 cells used for infection targets in this study were derived from a clone of pTAP1-EGFP stable transfectants [1], named 1E10. The LMD cell line was derived from a metastatic prostate carcinoma of a 129/Sv mouse (a kind gift of Dr. T. C. Thompson) [5] and maintained in RPMI 1640 media. Both the RPMI 1640 and the DMEM media were supplemented with 10% heat-inactivated FBS or calf serum for the NIH/3T3, 2 mM L-glutamine, 100 U/ml penicillin, 100 µg/ml streptomycin, and 10 mM HEPES.

### **4.2.2 Human cDNA library**

ViraPort cDNA library retroviral supernatants from different sources, the normal human lung and human spleen specimens, were purchased from Stratagene (La Jolla, CA). Individual cDNA library was harbored in pFB retroviral vector (Stratagene).

### **4.2.3 Cell Fusion and FACS analysis**

A fusion between human (A549) and mouse (1E10) cells was performed as a preliminary experiment to test whether proteins originated from human cells would be able to modulate mouse TAP-1 promoter activity. The two groups of cell lines were fused in a 1:1 ratio, following a polyethylene glycol cell fusion protocol [6]. Cells were then incubated with PE-conjugated anti-HLA-A, B, C mouse monoclonal antibody (BD

Pharmingen, San Diego, CA) at 4°C for 30 minutes. The fused cells, which displayed both red (PE-anti-HLA) and green (EGFP) fluorescence, were selected by FACS (FACSVantage DiVa, Becton Dickinson, Mountain View, CA). TAP-1 promoter-driven EGFP expression in the fused cells were then analysed by FACScan (Becton Dickinson).

#### **4.2.4 Determination of target cell transduction efficiency using the pFB-Luc control viral supernatant**

Prior to the actual library screenings, both the 1E10 and the NIH/3T3 cell lines were infected with the pFB-Luc control retroviral supernatant, in order to assess both the quality of the retroviral supernatants and the transduction efficiency of 1E10 as compared to that of the NIH/3T3 cells. This experiment was done according to the manufacturer's protocol.

#### **4.2.5 Transduction of 1E10 cells with ViraPort cDNA library retroviral supernatants**

The multiplicity of infection (MOI) was adjusted so approximately 20% of the 1E10 cells were transduced, since positive transductants obtained with low MOI screens have higher probability of containing a single cDNA of interest [7].

#### **4.2.6 Selection of positive transductants**

Forty eight hours after transduction with the cDNA library retroviral supernatants, human lung cDNA-infected 1E10 cells that displayed up-regulated expression of TAP-1 promoter-driven EGFP were selected by FACS (FACSVantage DiVa). Alternatively, human spleen cDNA-infected 1E10 cells were incubated with PE-conjugated anti-K<sup>b</sup> mouse monoclonal antibody (BD Pharmingen) at 4°C for 30 minutes. Then, cells that

displayed up-regulated expression of both the H-2K<sup>b</sup> and the EGFP were selected by FACS. Selection and expansion in culture was repeated twice before the cells were finally sorted into single-cell clones.

#### 4.2.7 Recovery of cDNA clones from positive transductants

Genomic DNA from the positive transductants, as well as from the pFB-Luc-infected 1E10 cells (control) was extracted and used as a template for PCR recovery of the cDNA inserts. The primers used are specific for regions flanking the multiple cloning site (MCS) of the pFB vector (Stratagene): GGCTGCCGACCCCGGGGTGG (forward) and CGAACCCAGAGTCCCGCTCA (reverse). Two microliters aliquots of genomic DNA were used as a template in a total of 50 µl reaction mixture containing 1x PCR buffer, 250 µM deoxynucleotide triphosphate, 1.5 mM MgCl<sub>2</sub>, 200 nM of each primer and 2.5 units Platinum Taq DNA Polymerase. cDNA amplifications were carried out in a thermocycler (Uno II, Biometra, Goettingen, Germany) with 35 cycles of denaturation (1 min, 95°C), annealing (4 min, 65°C), and elongation (2 min, 72°C). The cycling was concluded with a final extension at 72°C for 10 min. Twenty microliters of amplified products were analysed on agarose gels and then purified. All PCR reagents were obtained from Invitrogen (Burlington, ON) and Fermentas (Burlington, ON).

The PCR products were sequenced and identified through a bioinformatics database search (<http://www.ncbi.nlm.nih.gov/BLAST/>). BLASTn was used to compare nucleotide sequences obtained from the screenings with known nucleotide sequences in the database; BLASTx was used to compare translated nucleotide sequences with known amino acid sequences in the database.

#### 4.2.8 Sub-cloning of TAP-regulator gene candidates

Several gene candidates obtained from the screening were PCR-amplified from either genomic DNA from positive transductants or cDNA from wild type cells, using gene-specific primers (Sigma-Genosys, Oakville, ON) (Table 4.2.8.1). Gene expression constructs (pIRES2-gene) were created by ligating the PCR products into the XhoI and EcoRI sites of pIRES2-EGFP vector (Clontech, Palo Alto, CA) (Appendix B).

**Table 4.2.8.1: Primers used for PCR amplification.**

Oligonucleotide	Primer sequence (5'-3') <sup>a</sup>	bp <sup>b</sup>	Template <sup>c</sup>
ENO-1	F: <u>ctcgag</u> AGTGGCTAGAAGTTCACCATGTCTA R: <u>gaattc</u> TGCCTGCCACAGCTTACTT	1337	Lungs (2 <sup>nd</sup> sort) genomic DNA
SFTPC	F: <u>ctcgag</u> TAGCACCTGCAGCAAGATG R: <u>gaattc</u> TCCTAGATGTAGTAGAGCGGCA	612	Clone 2B5 genomic DNA
HLA-Cw*04 null allele	F: <u>ctcgag</u> ATGCGGGTCATGGCG R: <u>gaattc</u> TCAGATGCCTTTGCAGAAAG	1197	Lungs (2 <sup>nd</sup> sort) genomic DNA
Human chr. 3 ORF (HC3)	F: G <u>Actcgag</u> GAAATGGGATTTGGCCTCCT R: <u>gaattc</u> AATGGGTCAAACAGCAGCC	723	Clone 1C6 genomic DNA
Mouse PNKP (MPNKP)	F: <u>ctcgag</u> GAGGATGTCACAGCTTGGATC R: <u>gaattc</u> GCTCAGCCCTCGGAGAACT	1569	Ltk cDNA
Human PNKP (HPNKP)	F: <u>ctcgag</u> ACACAAGGATGCAAATCCTGAC R: <u>gaattc</u> GCTCAGCCCTCGGAGAACT	1459	Clone P4-B9 genomic DNA
27376 (unknown protein)	F: <u>ctcgag</u> GAACCATGGAAACCCAGC R: <u>gaattc</u> GGCACTTCTCCCTCTAACACTCT	726	Clone P5-E10 genomic DNA

<sup>a</sup> F: forward primer; R: reverse primer. Restriction enzyme sites are underlined.

<sup>b</sup> Length of the PCR amplification product.

<sup>c</sup> Genomic DNA from 1E10 positive transductants or cDNA from wild type cells.

#### 4.2.9 Transfection and selection

CMT.64 and LMD cells were transfected with the pIRES2-gene constructs or the pIRES2-EGFP vector using ExGen 500 *in vitro* Transfection Reagent (Fermentas). Because the IRES sequence enables EGFP to be translated from the same mRNA transcript as the cloned gene, EGFP-positive cells were selected by FACS. The selected cells were then cultured in 1 mg/ml G418-containing media prior to further analyses, in order to obtain a rich population of cells that overexpress the gene of interest.

#### 4.2.10 Reverse transcription-PCR analysis

Total cellular RNA was extracted from pIRES2-gene and pIRES2-EGFP (control) stable transfectants using Trizol Reagent (Invitrogen); contaminating DNA was removed by treatment with DNase 1 (Ambion Inc., Austin, TX). Reverse transcription of 1 µg of total cellular RNA was performed using the reverse transcription kit (SSII RT) from Invitrogen, in a total volume of 20 µl. TAP-1 expression was assessed by RT-PCR analysis using TAP-1-specific primers (Sigma): TGGCTCGTTGGCACCCCTCAAA (forward) and TCAGTCTGCAGGAGCCGCAAGA (reverse). Mouse β-actin was amplified as an internal control using the following primers (Sigma): ATGGATGACGATATCGCTGC (forward) and TTCTCCAGGGAGGAAGAGGAT (reverse). Two microliters aliquots of cDNA were used as a template for PCR in a total of 50 µl reaction mixture containing 1x PCR buffer, 250 µM deoxynucleotide triphosphate, 1.5 mM MgCl<sub>2</sub>, 200 nM of each primer and 2.5 units Taq or Platinum Taq DNA Polymerase. cDNA amplifications were carried out in a *T-gradient* thermocycler (Biometra) with 25-35 cycles of denaturation (1 min, 95°C), annealing (1 min, 54-64°C), and elongation (2 min, 72°C). The cycling was concluded with a final extension at 72°C

for 10 min. Twenty microliters of amplified products were analysed on agarose gels, stained with ethidium bromide and photographed under UV light.

#### **4.2.11 Flow cytometry**

Flow cytometric analysis of H-2K<sup>b</sup> expression was performed using PE-conjugated anti-K<sup>b</sup> mouse monoclonal antibody (BD Pharmingen) and a FACScan cytometer (Becton Dickinson).

## 4.3 Results

### 4.3.1 Mouse TAP-1 promoter activity is up-regulated in the fused 1E10-A549 cells

Since the cDNA libraries available were derived from human specimens, a preliminary experiment was performed to test whether proteins from TAP-expressing human cells could up-regulate mouse TAP-1 promoter activity in the TAP-deficient CMT.64 cells. Flow cytometric analysis results showed that mouse TAP-1 promoter-driven EGFP expression was indeed up-regulated in the fused 1E10-A549 cells (Figure 4.3.1.1). The extent of this up-regulation was similar to that obtained from the fusion between murine carcinomas and fibroblasts (Figure 2.3.5.1). This indicates that transducing 1E10 cells with normal human cDNA library retroviral supernatants would be a valid method to screen for genes (cDNAs) that can enhance TAP-1 promoter activity in mouse cells.

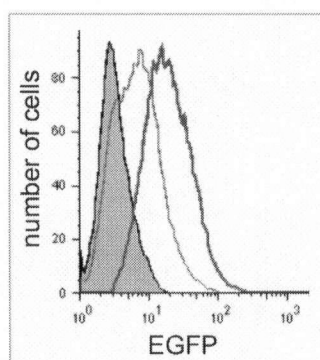


**Figure 4.3.1.1: TAP-1 promoter-driven EGFP expression is enhanced in the fused 1E10-A549 cells.** The levels of EGFP expression in untransfected CMT.64 cells, 1E10 (pTAP1-EGFP-transfected CMT.64) cells and fused 1E10-A549 cells are represented by a shaded area, a thin line and a thick line, respectively.

### **4.3.2 The transduction efficiency of 1E10 cells is three times lower than that of the NIH/3T3 cells**

The luciferase activity displayed by NIH/3T3 cells, 48 hours after transduction with 10-10,000x dilutions of pFB-Luc retroviral supernatant, was on average  $3.2 \pm 1.2x$  higher as compared to 1E10 cells. This indicates that the NIH/3T3 cells are transduced approximately three times more effectively than the 1E10 cells. Therefore, three times less 1E10 cells than NIH/3T3 cells were plated one day prior to transduction with the cDNA library retroviral supernatant.

### **4.3.3 Identification of gene candidates from human lung cDNA library transductants**

Forty eight hours after infection of the 1E10 cells with the human lung cDNA library retroviral supernatant, 0.12% of the infected cells were found to display a high expression of TAP-1 promoter-driven EGFP. These cells were selected by FACS and expanded in culture. Two weeks later, cells that still expressed high EGFP (8.3%) were re-selected by FACS. Six integrants were recovered from the 1E10 bulk transductants. The results obtained from BLASTx or BLASTn hit are summarized in Table 4.3.3.1 below.

A sequence obtained from the 1.3 kb band showed a homology to a region in human chromosome 3; however, no known protein is translated from this region. Interestingly, an open reading frame (ORF) consisting of 218 amino acids was detected, opening a possibility that a novel protein may be translated from this region (Figure 4.3.3.1). BLAT analysis (UCSC Genome Browser, [www.genome.ucsc.edu](http://www.genome.ucsc.edu)) indicated that this ORF is located in the p25.1 locus of human chromosome 3.

**Table 4.3.3.1: Identity of cDNAs recovered from bulk-sorted cells of human lung cDNA library transductants.**

BLASTn (nucleotide sequence) or BLASTx (protein sequence) hit	Amino acid identity (human)	Insert size (kb)	NCBI accession #
Enolase-1 (ENO-1)	182/185 (98%) Total protein: 434 aa	2.0	NP_001419
HLA-Cw*04 null allele	255/291 (87%) Total protein: 367 aa	1.7	CAC05372
Prostaglandin-D2 synthase (PTGDS)	189/190 (99%) Total protein: 190 aa	1.6	CAI12758
Human chr.3 clone RP11-27016 map 3p (HC3)	218 aa ORF	1.3	AC090885
Pulmonary surfactant protein C isoform CRA_a (SFTPC)	174/191 (91%) Total protein: 240 aa	0.9	EAW63705
Tropomyosin-2 beta	121/160 (75%) Total protein: 284 aa	0.7	AAH11776

```

                                atgggat ttggcctcct
20581 gggtgacatt ccctcaagca ccagtcctctg gagctgggtc agagccatcc tctggttgga
20641 gttcctgggt coaggtcacc acagtcctccg gggtcctctg gccagggccc tgtcctctgcc
20701 tctccatgcc tgccccctgc aggtctctga gtttgttgc ctcaactcaa gcctgtggag
20761 tgtcacatct gtcacctggg aatgaggac acgtcaggct agcctgcttt ggctcccaag
20821 tggattaaag gggctgagaa tgcagcctc gagcaggggc tggcgagacc cctgaaggg
20881 taacctctcc cgcctcctt ccaggggagc caaggctaca ggaagggag aggtggccga
20941 ggctcggacc ctggcaagag ctgggaagaa ccgctgctgg gcagcgtcct ctggaaggca
21001 gcctccctctg tcatcctcca atgtgcccc tcaccaccag cccctcgcct ccccttcttg
21061 ctactctgt ctgggcagtc cccacaccog ccatgctggg ggttgattc cagggttagc
21121 actgacagct gcagcctctc acagtgatga gtgcaggccc cccacatccc aaagcgcagc
21181 tcatccagca cagcagggct gtgaggtagc tctgtttga

```

**Figure 4.3.3.1: The ORF found in the homologous region of human chromosome 3 clone RP11-27016 map 3p (NCBI accession no. AC090885) and the 1.3 kb sequence obtained from human lung cDNA library screening.**

Furthermore, the 1E10 bulk transductants were sorted into single-cell clones and expanded in culture. From the 20 clones that were analysed, 10 clones contained single integrants (Table 4.3.3.2). No integrants were detected in the remaining 10 clones. cDNAs that correspond to the SFTPC and the HC3 that were detected in previous screening of bulk transductants were recovered individually from the single-cell clones. A new sequence corresponding to the 3'-untranslated region of the *N-deacetylase/N-sulfotransferase (NDST-1)* gene, was obtained from two of the clones. No cDNAs that encode for human ENO-1, HLA-Cw\*04 null allele, PTGDS and Tropomyosin 2 were recovered from the single-cell clones.

**Table 4.3.3.2: Identity of cDNAs recovered from single-cell clones of human lung cDNA library transductants.**

Clone	BLASTn (nucleotide sequence) or BLASTx (protein sequence) hit	Base pairs or amino acid identity (human)	Insert size (kb)	NCBI accession #
2B5	Pulmonary surfactant protein C isoform CRA_a (SFTPC)	188/194 (96%) Total protein: 240 aa	0.9	EAW63705
1A2	Pulmonary surfactant protein C isoform CRA_a (SFTPC)	194/194 (100%) Total protein: 240 aa	0.9	EAW63705
1F3	Pulmonary surfactant protein C isoform CRA_a (SFTPC)	193/194 (99%) Total protein: 240 aa	0.9	EAW63705
1E3	Pulmonary surfactant protein C ?	n/a (bad sequence)	0.9	
1C6	Human chr.3 clone RP11-27016 map 3p (HC3)	218 aa ORF	1.3	AC090885
2H1	Human chr.3 clone RP11-27016 map 3p ?	n/a (bad sequence)	1.3	
2A10	Human chr.3 clone RP11-27016 map 3p ?	n/a (bad sequence)	1.3	
1H7	?	n/a (bad sequence)	1.6	
1C9	N-deacetylase/N-sulfotransferase (heparan glucosaminyl) 1 (NDST1)	583/585 (99%) (outside of CDS) Total gene: 7913 bp	2.0	NM_001543
1E11	N-deacetylase/N-sulfotransferase (heparan glucosaminyl) 1 (NDST1)	534/535 (99%) (outside of CDS) Total gene: 7913 bp	2.0	NM_001543

Levels of surface K<sup>b</sup> expression in the single-cell clones were then analysed by flow cytometry, since the upregulation of TAP-1 promoter activity may lead to enhanced transcription of the gene and reconstitution of MHC class I expression on the surface of 1E10 cells. However, no increase in the surface K<sup>b</sup> expression on any of the clones was detected. This may be caused by low levels or total loss of protein expression encoded by the cDNA inserts, inability of the foreign proteins to induce MHC class I expression in CMT.64 cells, or false positive signals during the selection process. Indeed, loss of induction of TAP-1 promoter-driven EGFP expression was observed in most cells over the period in culture, indicating the instability of its enhanced state.

#### **4.3.4 Identification of gene candidates from human spleen cDNA library transductants**

After several TAP-1-activator gene candidates were obtained from the screening of human lung cDNA library, a similar experiment using human cDNA library derived from human spleen specimens was performed. However, in this experiment, the positive transductants were selected based on up-regulated expression of both the TAP-1 promoter-driven EGFP and the H-2K<sup>b</sup> molecule.

Forty eight hours after the infection with human spleen cDNA library retroviral supernatant, 0.1% of the infected 1E10 cells were found to display an up-regulated expression of both the EGFP and H-2K<sup>b</sup>. After a month of expansion in culture, a population of cells that remained double-positive (0.5%) was re-selected by FACS and sorted into single-cell clones. Unfortunately, similar to the problem encountered during the lung cDNA library screening, most cells were no longer EGFP- and K<sup>b</sup>-positive after being expanded in culture. From the 20 clones that were analysed, 5 clones contained

single integrants, 5 clones contained two integrants, and 10 clones contained no integrants (Table 4.3.4.1). No identical hits to those obtained from the lung cDNA library screening were discovered in this screening.

**Table 4.3.4.1: Identity of cDNAs recovered from single-cell clones of human spleen cDNA library transductants.**

Clone	BLASTn (nucleotide sequence) or BLASTx (protein sequence) hit	Base pairs or amino acid identity (human)	Insert size (kb)	NCBI accession #
P4-A3	Polynucleotide kinase 3'-phosphatase (PNKP) and	81/95 (85%) Total protein: 482 aa (bad sequence)	1.3	AAH02519.2
	RNA binding protein, autoantigenic (hnRNP-associated with lethal yellow homolog (mouse)) (RALY), transcript variant 2, mRNA	87/98 (88%) Total CDS: 1541 bp (bad sequence)	.6	NM_007367
P4-B9	Polynucleotide kinase 3'-phosphatase (PNKP)	469/482 (97%) Total protein: 482 aa	1.3	AAH02519.2
P5-A6	Polynucleotide kinase 3'-phosphatase (PNKP) ? and	n/a (bad sequence)	1.3	CAI40836
	Prosaposin (variant Gaucher disease and variant metachromatic leukodystrophy) or sphingolipid activator proteins 1 and 2 processed mutant	38/38 (100%) Total protein: 559 aa	.75	
P4-E3	Human chromosome 5 genomic contig and	92/100 (92%) Total: 48999907 bp	.8	NW_922784
	Glucocorticoid receptor-interacting protein GRIP1 associated protein 1 (GRIPAP1)	115/120 (95%) Total CDS: 3032 bp	.4	NM_020137
P5-F9	Human chromosome 5 genomic contig and	91/100 (91%) Total: 48999907 bp	.75	NW_922784
	Glucocorticoid receptor-interacting protein (GRIP)1 associated protein 1 (GRIPAP1)	106/111(95%) Total CDS: 3032 bp	.4	NM_020137
P4-F1	Actin, gamma 1 (ACTG1)	812/931 (87%) Total CDS: 1919 bp	1.2	NM_001614
P5-B3	Unnamed protein product (from MHC II alpha domain)	253/254 (99%) Total protein: 254 aa	1.1	CAA24917
P5-E4	Unknown (protein for MGC:27376) ?	n/a (bad sequence)	1.2	
P5-E10	Unknown (protein for MGC:27376)	210/235 (89%) Total protein: 235 aa	1.2	AAH16380
P5-F10	Immunoglobulin light chain variable region and	112/179 (62%) Total protein: 209 aa	1.5	AAF86917
	Unknown (protein for MGC:27376)	104/165 (63%) Total protein: 235 aa	1.4	AAH16380

#### **4.3.5 Cancer-related information about the screened genes**

Aberrant expression of many of the genes obtained from both screenings has been reported to contribute to development of various cancers (Table 4.3.5.1). Interestingly, some of these gene products, such as the ENO-1 homolog, PTGDS, PNKP and RALY, have been reported to confer tumor-suppressing functions [8-12]. However, no cancer-related information related to SFTPC, NDST1, GRIPAP1 and ACTG1 has been reported to date.

**Table 4.3.5.1: Cancer-related information about the proteins that match the hits obtained from the screenings of human lung and spleen cDNA libraries.**

Isolated from	Protein name	Cancer-related information
<b>Lung cDNA library</b>		
	Enolase-1	<ul style="list-style-type: none"> <li>• Glycolytic enzyme, often overexpressed in metastatic cancers [13-15]</li> <li>• Shares a great structural similarity with c-myc promoter binding protein (MBP)-1, a transcriptional repressor of <i>c-myc</i> oncogene [12]</li> </ul>
	HLA-Cw	<ul style="list-style-type: none"> <li>• A ligand for an inhibitory NK cell receptor [16]</li> <li>• Allotypes are used as prognostic markers for autologous transplantation in lymphoma patients [16]</li> <li>• Null alleles are not expressed on cell surface [17, 18]</li> </ul>
	PTGDS	<ul style="list-style-type: none"> <li>• Down-regulated in brain tumors and pre-malignant oral lesions [8, 19]</li> <li>• Inhibit oral cancer cell proliferation <i>in vitro</i> [8]</li> <li>• PTGDS metabolites inhibit prostate cancer cell growth via a peroxisome proliferator-activated receptor gamma (PPARgamma)-dependent mechanism [10]</li> </ul>
	Tropomyosin 2	<ul style="list-style-type: none"> <li>• Loss of expression was reported in esophageal and lung cancer tissues [20, 21]</li> </ul>
	SFTPC	No record
	NDST1	No record
<b>Spleen cDNA library</b>		
	PNKP	<ul style="list-style-type: none"> <li>• Involved in base excision repair as a mechanism to prevent cancer development due to oxidative damage of DNA [9]</li> </ul>
	RALY	<ul style="list-style-type: none"> <li>• RNA binding protein; mutation is associated with lethal yellow homolog in mice that phenotypes include a predisposition to tumor growth [11]</li> </ul>
	GRIPAP1	<ul style="list-style-type: none"> <li>• p160 nuclear receptor co-activator</li> <li>• One of the two autonomous activation domains of GRIP1 is mediated by CBP/p300 [22, 23]</li> <li>• Increased binding of GRIP1 to ERalpha promoter mediated growth and survival of breast cancer cells [24]</li> <li>• no record about GRIPAP1 deregulation and development of cancers</li> </ul>
	ACTG1	No record

#### 4.3.6 Overexpression of several TAP-regulator gene candidates in CMT.64 and LMD cells up-regulates TAP-1 expression, but not H-2K<sup>b</sup> expression

To overexpress the TAP-regulator gene candidates, individual cDNA was sub-cloned into pIRES2-EGFP vector. This vector contains a *neomycin* gene for selection of positive transfectants in G418-containing media. Seven pIRES2-gene constructs: the ENO-1, SFTPC, HLA-Cw\*04 null allele, unknown protein (27376), mouse PNKP (MPNKP), human PNKP (HPNKP) and human chromosome 3 ORF (HC3) were completed.

CMT.64 and LMD cells were independently transfected with pIRES2-gene constructs or pIRES2-EGFP vector. Overexpression of the transfected genes was confirmed by RT-PCR analysis using gene-specific primers (Figure 4.3.6.1).

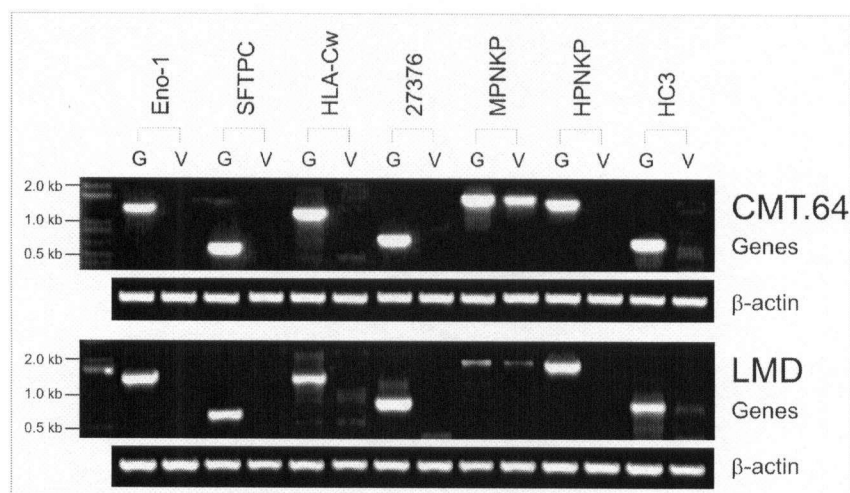


**Figure 4.3.6.1: RT-PCR analysis of the overexpression of the TAP-1 activator candidate genes in CMT.64 and LMD cells.** G: cDNA template was derived from pIRES2-gene transfectants; V: cDNA template was derived from pIRES2-EGFP transfectants. Amplification of β-actin cDNA served as a loading control.

Overexpression of the TAP-regulator gene candidates appeared to induce TAP-1 expression in TAP-deficient CMT.64 and LMD cells, although the levels of induction were very low compared to those from IFN- $\gamma$  treatment (Figure 4.3.6.2). Most inductions observed in three independent transfection experiments (two groups of CMT.64 cells and one group of LMD cells) were inconsistent, with the exception of HLA-Cw\*04 null allele and the unknown protein from human chromosome 3 (HC3). In all the three experiments done, TAP-1 expression was consistently up-regulated in both the CMT.64 and LMD cells that overexpressed the HLA-Cw\*04 null allele and the HC3 (Figure 4.3.6.2).

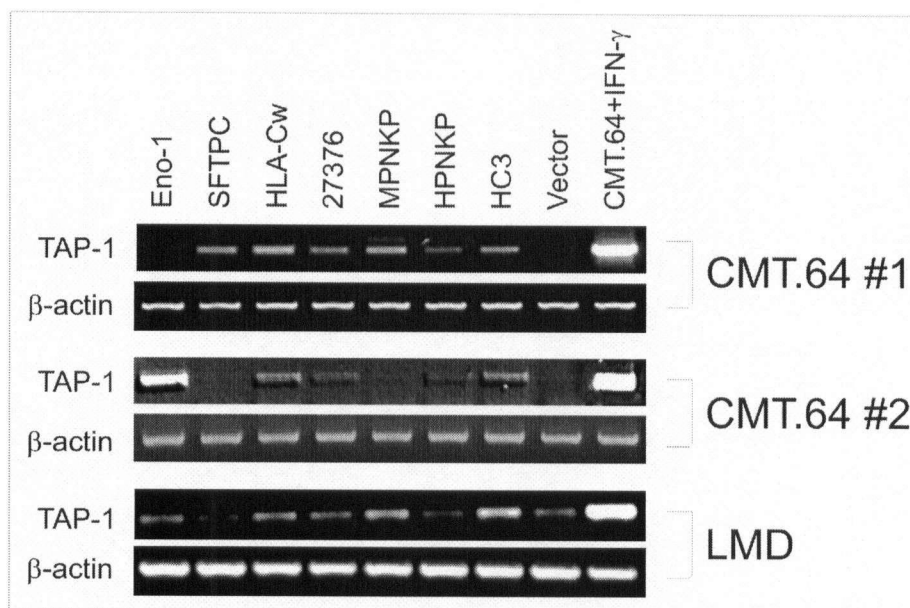


**Figure 4.3.6.2: TAP-1 expression was up-regulated in some of the CMT.64 and LMD cells transfected with individual pIRES2-gene constructs.** Amplification of cDNA from IFN- $\gamma$ -treated cells was used as a positive control.  $\beta$ -actin expression served as a loading control. Data are representatives of one set of RT-PCR analysis per group of CMT.64 and LMD transfectants.

Finally, flow cytometric analyses were performed in order to assess induction of surface H-2K<sup>b</sup> expression in the positive transfectants of CMT.64 and LMD cells. Unfortunately, no improvement in surface H-2K<sup>b</sup> expression could be detected in any of the cell lines tested. This may be due to fairly low levels of induction of TAP-1 expression in the transfectants. Representative data from HLA-Cw\*04 null allele- and HC3-overexpressing LMD cells are shown in Figure 4.3.6.3.

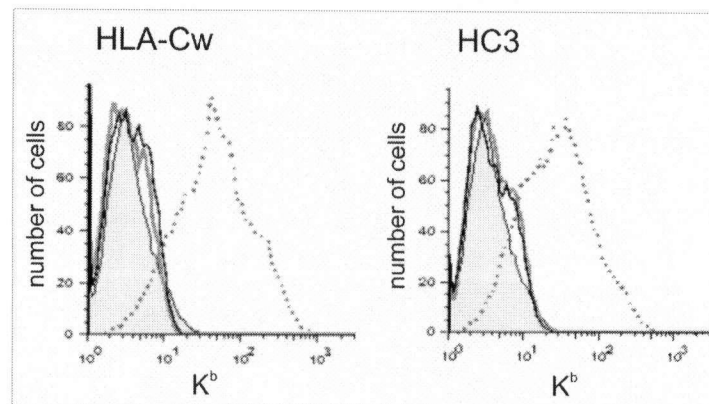


**Figure 4.3.6.3: No upregulation of H-2K<sup>b</sup> expression was detected on the surface of LMD cells overexpressing HLA-Cw\*04 null allele and HC3 (thick lines). H-2K<sup>b</sup> expression in pIRES-2-EGFP-transfected LMD cells (shaded areas) was similar to the negative control, the unstained pIRES-2-gene-transfected cells (thin lines). As a positive control, H-2K<sup>b</sup> expression was assessed in IFN- $\gamma$ -treated LMD cells (broken lines).**

Further research is needed to confirm the ability of the TAP-1 regulator gene candidates, particularly the HLA-Cw\*04 null allele and HC3, to up-regulate TAP-1 at the protein level, and possibly surface MHC class I expression in other TAP-deficient cell lines. In addition, ten further candidates obtained from the screenings remain to be sub-cloned and analysed.

#### 4.4 Discussion

In order to identify novel TAP-1 activators, cDNA libraries from human lung and spleen specimens were screened for gene products that could up-regulate either TAP-1 promoter activity, or both the promoter's activity and surface MHC class I expression in pTAP1-EGFP stable transfectants of CMT.64 cells. A total of seven and nine candidates were obtained from the lung and the spleen cDNA library screening, respectively. Interestingly, deregulation of many of the genes identified, such as *ENO-1*, *PTGDS*, *Tropomyosin-2*, *PNKP*, and *RALY*, had been shown to associate with the development of various types of cancers (Table 4.3.5.1).

To-date, only PTGDS and HLA-C have been shown to be involved in antigen processing. PTGDS, an enzyme responsible for the bio-synthesis of prostaglandin D2, is produced by resident macrophages and dendritic cells in spleen, thymus, and Peyer's patch of intestine [25]. Prostaglandin D2 was shown to affect the differentiation and functions of human dendritic cells [26]. In the presence of prostaglandin D2, dendritic cells demonstrated upregulated endocytic and antigen processing activities; however, their ability to stimulate naive T cells was impaired [26]. It has been reported that a variety of alleles in HLA-C locus increases the risk of bone marrow graft rejection in transplantations [27]. This might be caused by presentation of allogeneic, possibly null-derived peptides, by HLA class I molecules on cell surface, thus triggering allospecific T cell responses [18]. The precise role of HLA class I molecules with no cell surface expression, such as the HLA-Cw\*04.null allele, in antigen presentation remains to be elucidated [18].

Interestingly, several candidates showed significant similarities to regions of human chromosomes with no known genes or to unnamed protein products. One

sequence, with a similarity to an open reading frame encoding 218 amino acids in human chromosome 3, named HC3, was particularly intriguing. Overexpression of HC3 in three independent groups of transfectants of TAP-deficient CMT.64 and LMD cells consistently showed up-regulated expression of TAP-1, as assessed by RT-PCR using cDNA templates from the transfectants (Figure 4.3.6.2). This result indicates that a novel protein with the ability to modulate TAP-1 expression could be translated from the newly-found ORF (Figure 4.3.3.1). However, TAP-1 upregulation was not consistently observed in CMT.64 and LMD cells that overexpressed most of the other gene candidates. More independent transfections of CMT.64, LMD and possibly other TAP-deficient cells, RT-PCR and Western Blot analyses are required to confirm the consistency of TAP-1 induction in cells that overexpressed a specific gene of interest.

Several problems encountered during the screening process include the acquisition of EGFP and K<sup>b</sup>-positive clones with no integrants ("empty clones"), the loss of EGFP and K<sup>b</sup> expression as the cells were expanded in culture, and the difficulty in obtaining sequencing results from PCR products. The first problem may result from the loss of cDNA inserts from the infected cells during the period in culture, prior to genomic DNA extraction, although this is unlikely as plasmids introduced by retroviral infection generally integrate into the genome of the infected cells. Also, false positive signals during FACS selection could result in unwanted selection of non-infected cells. Nevertheless, one or two inserts were successfully detected in many of the single-cell clones analysed, indicating that the multiplicity of infection (MOI) was correctly adjusted [7]. If the MOI used was too low, very few cells would be transduced. In contrast, transduction at high MOI would yield a higher number of cells transduced; however, the majority of the cells would bear multiple integrants, making it difficult to determine

which of those was actually responsible for the phenotype. A similar problem was encountered during PCR recovery of cDNA inserts from selected bulk transfectants. Therefore, in future experiments, it is best to first sort positive transductants into single-cell clones. An independent transduction of CMT.64 cells by human cDNA library retroviral supernatant from the same source is necessary to test the reproducibility of the primary screen hits.

The absence of EGFP and K<sup>b</sup> expression in selected cells after a period in culture may result from either false positive signal during the selection or diminishing expression of the inserted gene products. An independent method, such as sub-cloning the cDNA into a different vector and over-expressing the gene product in TAP-deficient cancer cells (Figure 4.3.6.1), must be performed to confirm the validity of the acquired phenotypes.

Difficulty in obtaining good quality results from the sequencing of PCR products accounts for errors in the percentage of sequence identity recorded in the data tables (Table 4.3.3.1, Table 4.3.3.2 and Table 4.3.4.1). It may also be one of the reasons many of the recovered cDNAs showed sequence similarities only to a part of specific genes, instead of to full-length cDNAs or protein products. However, some sequences were recovered from bands that were clearly smaller than the known, full-length sequences, for example the RALY, prosaposin and GRIPAP1 (Table 4.3.4.1), indicating that sequencing errors were not the only reason for the finding of several incomplete sequences. The sequencing results could generally be improved by sub-cloning all PCR products individually into a TOPO vector (Invitrogen); however, this method is ineffective for screening large numbers of clones due to cost and time demands.

Future research should include refinement of the screening method and verification of the results, followed by application of independent methods to confirm the

validity of the primary screen hits, as discussed in the previous paragraph. Furthermore, a TAP-expressing, human primary cell line and its TAP-deficient, metastatic derivative may be used to assess differential endogenous expression levels and functionality of several strong candidates obtained from the initial screenings. Finally, it is intriguing to investigate whether disruption of a specific gene in TAP-expressing cells would cause detrimental effects on MHC class I antigen presentation. For example, it would be interesting to observe whether deletion of a region within the newly identified "HC3" ORF would transform human cells that displayed a functional antigen presentation pathway into antigen presentation-defective, metastatic cells. This would confirm whether the particular gene product has fundamental roles in tumor antigen processing and human malignancies.

#### 4.5 References

1. Setiadi, A.F., M.D. David, S.S. Chen, J. Hiscott, and W.A. Jefferies. Identification of mechanisms underlying transporter associated with antigen processing deficiency in metastatic murine carcinomas. *Cancer Res*, 2005. 65:7485-92.
2. Lee, H., J.J. Song, E. Kim, C.O. Yun, J. Choi, B. Lee, J. Kim, J.W. Chang, and J.H. Kim. Efficient gene transfer of VSV-G pseudotyped retroviral vector to human brain tumor. *Gene Ther*, 2001. 8:268-73.
3. Ito, T., N. Ito, A. Bettermann, Y. Tokura, M. Takigawa, and R. Paus. Collapse and restoration of MHC class-I-dependent immune privilege: exploiting the human hair follicle as a model. *Am J Pathol*, 2004. 164:623-34.
4. Franks, L.M., A.W. Carbonell, V.J. Hemmings, and P.N. Riddle. Metastasizing tumors from serum-supplemented and serum-free cell lines from a C57BL mouse lung tumor. *Cancer Res*, 1976. 36:1049-55.
5. Lee, H.M., T.L. Timme, and T.C. Thompson. Resistance to lysis by cytotoxic T cells: a dominant effect in metastatic mouse prostate cancer cells. *Cancer Res*, 2000. 60:1927-33.
6. Fuller, S.A., M. Takahashi, and J.G.R. Hurrell, *Production of antibodies*, in *Current protocols in molecular biology*, F.M. Ausubel, et al., Editors. 2001, John Wiley & Sons, p. 11.7.1-11.7.4.
7. Onishi, M., S. Kinoshita, Y. Morikawa, A. Shibuya, J. Phillips, L.L. Lanier, D.M. Gorman, G.P. Nolan, A. Miyajima, and T. Kitamura. Applications of retrovirus-mediated expression cloning. *Exp Hematol*, 1996. 24:324-9.

8. Banerjee, A.G., I. Bhattacharyya, and J.K. Vishwanatha. Identification of genes and molecular pathways involved in the progression of premalignant oral epithelia. *Mol Cancer Ther*, 2005. 4:865-75.
9. Hazra, T.K., A. Das, S. Das, S. Choudhury, Y.W. Kow, and R. Roy. Oxidative DNA damage repair in mammalian cells: A new perspective. *DNA Repair (Amst)*, 2006.
10. Kim, J., P. Yang, M. Suraokar, A.L. Sabichi, N.D. Llansa, G. Mendoza, V. Subbarayan, C.J. Logothetis, R.A. Newman, S.M. Lippman, and D.G. Menter. Suppression of prostate tumor cell growth by stromal cell prostaglandin D synthase-derived products. *Cancer Res*, 2005. 65:6189-98.
11. Michaud, E.J., S.J. Bultman, M.L. Klebig, M.J. van Vugt, L.J. Stubbs, L.B. Russell, and R.P. Woychik. A molecular model for the genetic and phenotypic characteristics of the mouse lethal yellow (Ay) mutation. *Proc Natl Acad Sci U S A*, 1994. 91:2562-6.
12. Onyango, P., B. Lubyova, P. Gardellin, R. Kurzbauer, and A. Weith. Molecular cloning and expression analysis of five novel genes in chromosome 1p36. *Genomics*, 1998. 50:187-98.
13. Dowling, P., P. Meleady, A. Dowd, M. Henry, S. Glynn, and M. Clynes. Proteomic analysis of isolated membrane fractions from superinvasive cancer cells. *Biochim Biophys Acta*, 2007. 1774:93-101.
14. Zhang, D., L.K. Tai, L.L. Wong, L.L. Chiu, S.K. Sethi, and E.S. Koay. Proteomic study reveals that proteins involved in metabolic and detoxification pathways are highly expressed in HER-2/neu-positive breast cancer. *Mol Cell Proteomics*, 2005. 4:1686-96.

15. Altenberg, B. and K.O. Greulich. Genes of glycolysis are ubiquitously overexpressed in 24 cancer classes. *Genomics*, 2004. 84:1014-20.
16. Skerrett, D., O. Rosina, C. Bodian, L. Isola, O. Gudzowaty, E. Scigliano, and S. Fruchtman. Human leukocyte antigens (HLA)-Cw as prognostic indicators in autologous transplantation for lymphoma. *Cancer Invest*, 2001. 19:487-94.
17. Wang, Z.C., A.G. Smith, E.J. Yunis, A. Selvakumar, S. Ferrone, S. McKinney, J.H. Lee, M. Fernandez-Vina, and J.A. Hansen. Molecular characterization of the HLA-Cw\*0409N allele. *Hum Immunol*, 2002. 63:295-300.
18. Balas, A., S. Santos, M.J. Aviles, F. Garcia-Sanchez, R. Lillo, A. Alvarez, L.M. Villar-Guimerans, and J.L. Vicario. Elongation of the cytoplasmic domain, due to a point deletion at exon 7, results in an HLA-C null allele, Cw\*0409 N. *Tissue Antigens*, 2002. 59:95-100.
19. Saso, L., M.G. Leone, C. Sorrentino, S. Giacomelli, B. Silvestrini, J. Grima, J.C. Li, E. Samy, D. Mruk, and C.Y. Cheng. Quantification of prostaglandin D synthetase in cerebrospinal fluid: a potential marker for brain tumor. *Biochem Mol Biol Int*, 1998. 46:643-56.
20. Jazii, F.R., Z. Najafi, R. Malekzadeh, T.P. Conrads, A.A. Ziaee, C. Abnet, M. Yazdznbod, A.A. Karkhane, and G.H. Salekdeh. Identification of squamous cell carcinoma associated proteins by proteomics and loss of beta tropomyosin expression in esophageal cancer. *World J Gastroenterol*, 2006. 12:7104-12.
21. Pitterle, D.M., E.M. Jolicoeur, and G. Bepler. Hot spots for molecular genetic alterations in lung cancer. *In Vivo*, 1998. 12:643-58.
22. Huang, S.M. and Y.S. Cheng. Analysis of two CBP (cAMP-response-element-binding protein-binding protein) interacting sites in GRIP1 (glucocorticoid-

- receptor-interacting protein), and their importance for the function of GRIP1. *Biochem J*, 2004. 382:111-9.
23. Liu, P.Y., T.Y. Hsieh, W.Y. Chou, and S.M. Huang. Modulation of glucocorticoid receptor-interacting protein 1 (GRIP1) transactivation and co-activation activities through its C-terminal repression and self-association domains. *Febs J*, 2006. 273:2172-83.
  24. Wei, X., H. Xu, and D. Kufe. MUC1 oncoprotein stabilizes and activates estrogen receptor alpha. *Mol Cell*, 2006. 21:295-305.
  25. Urade, Y., M. Ujihara, Y. Horiguchi, K. Ikai, and O. Hayaishi. The major source of endogenous prostaglandin D2 production is likely antigen-presenting cells. Localization of glutathione-requiring prostaglandin D synthetase in histiocytes, dendritic, and Kupffer cells in various rat tissues. *J Immunol*, 1989. 143:2982-9.
  26. Gosset, P., M. Pichavant, C. Faveeuw, F. Bureau, A.B. Tonnel, and F. Trottein. Prostaglandin D2 affects the differentiation and functions of human dendritic cells: impact on the T cell response. *Eur J Immunol*, 2005. 35:1491-500.
  27. Petersdorf, E.W., G.M. Longton, C. Anasetti, E.M. Mickelson, S.K. McKinney, A.G. Smith, P.J. Martin, and J.A. Hansen. Association of HLA-C disparity with graft failure after marrow transplantation from unrelated donors. *Blood*, 1997. 89:1818-23.

## Chapter 5 : General Discussion

### 5.1 Summary and Conclusions

To-date, low immunogenic response to tumor immunotherapy due to escape mechanisms utilized by tumor cells remains the main challenge in clinical trials [1-4]. This is at least partially caused by the high incidence of MHC class I downregulation in cancer cells [1-3], which has been attributed to the decreased expression of several APM components, including the heterodimer of TAP-1 and TAP-2 molecules [5-10]. Interestingly, restoration of the TAP-1 alone in cells with multiple deficiencies of other APM components has been shown to reconstitute MHC class I antigen presentation and killing of the tumor cells by specific CTLs [5, 11-13]. These effects can also be attained by treatment of TAP-deficient cancer cells with IFN- $\gamma$  *in vitro* [5, 6, 11, 14]. However, the mechanism through which this occurs is unknown. In order to develop effective immunotherapy approaches that aim to restore TAP-1 expression in cancer cells, a better understanding of the mechanisms by which cancer cells down-regulate TAP-1 expression is essential. This thesis contributes to the elucidation of molecular mechanisms by which metastatic carcinomas down-regulate TAP-1 expression and escape immune surveillance. It appears that TAP-1 deficiency in carcinomas is caused by two main mechanisms: lack of transcriptional activators and rapid TAP-1 mRNA degradation [14].

Studies aimed at identifying the transcriptional activator(s) indicated that these factors play important roles in chromatin remodeling within the TAP-1 locus. By performing a chromatin immunoprecipitation assay, it was found that histone H3 acetylation was deficient in TAP-1 promoter of TAP-deficient cells. This lack of histone

H3 acetylation likely leads to a condensed nucleosomal structure around the TAP-1 promoter, which prevents the binding of RNA pol II complex and of other general transcription factors to the promoter region. As a result, further transcriptional activity is halted.

Comparison of full TAP-1 promoter activity and that of its truncations revealed a region that is responsible for differential activity of the promoter in TAP-expressing and TAP-deficient cells. Intriguingly, this region was found to contain a CREB binding site, prompting the speculation that CREB-binding protein (CBP), a well-known histone acetyltransferase (HAT) [15-18], was one of the possible factors responsible for the differential activity of the promoter. It was found that indeed, CBP binding to TAP-1 promoter was impaired in TAP-deficient, metastatic carcinomas, strengthening the hypothesis that the lack of histone acetyltransferase activities around the TAP-1 promoter leads to a repressive structure of the chromatin that is inaccessible by transcriptional machinery complexes.

Furthermore, an interesting link was found between TAP-1 induction and improvement of CBP binding to TAP-1 promoter upon treatment of TAP-deficient cells with IFN- $\gamma$ . This effect may result from IFN- $\gamma$ -induced association of STAT-1 $\alpha$  and CBP [19]. This in turn modulates the TAP-1 promoter activity upon association of the factors with the promoter and improvement of histone acetylation around the region, thus promoting a permissive state of the chromatin structure. This provides a novel epigenetic mechanism by which IFN- $\gamma$  enhances TAP-1 transcription. Alternatively, IFN- $\gamma$  may also act through STAT-1 independent pathways, such as through a novel IFN- $\gamma$ -activated transcriptional element or through immediate early proteins and transcription factors [20].

---

By interacting simultaneously with the basal transcription machinery and with one or more upstream transcription factors, CBP may function as a physical bridge that stabilizes the transcription complex [17]. All the described mechanisms are summarized in Figure 5.1.1.

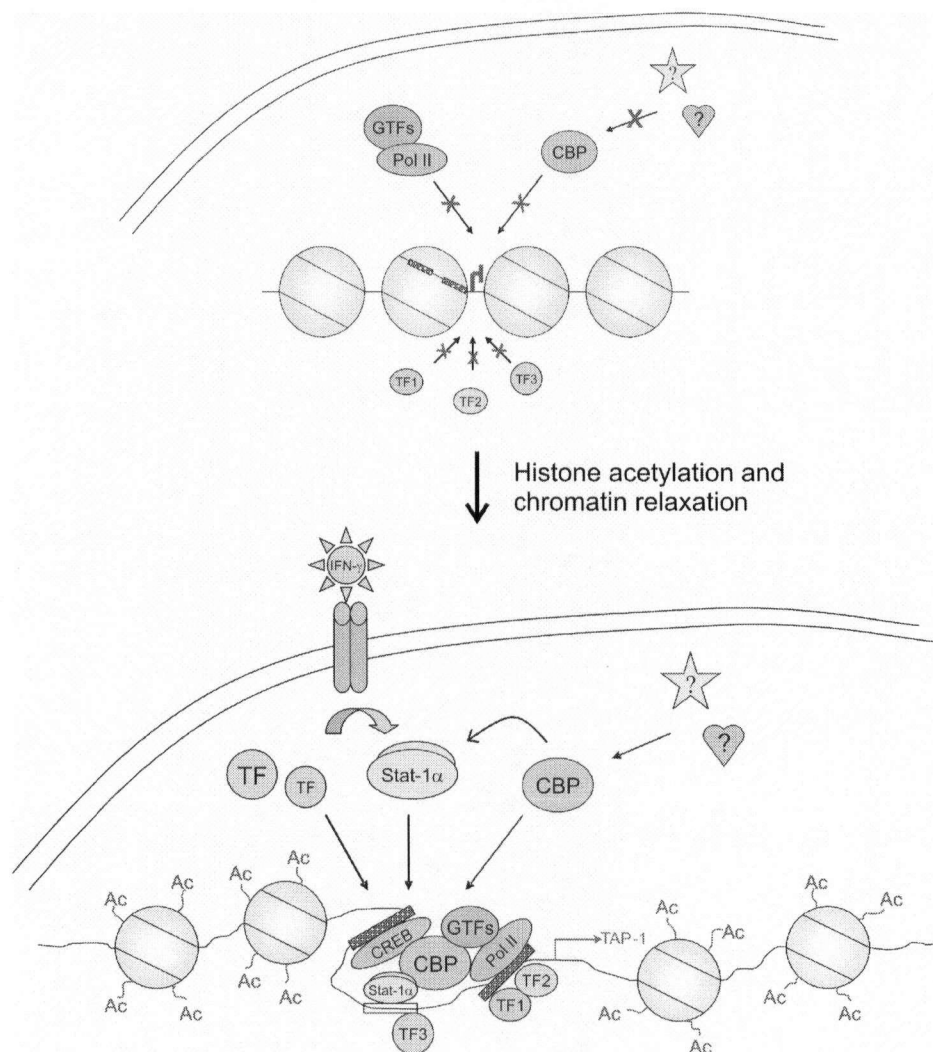


**Figure 5.1.1: A proposed model of the mechanisms underlying TAP-1 deficiency in carcinomas and release of the transcriptional repression upon relaxation of chromatin structure around the *Tap-1* gene locus.** The boxes on the DNA strand represent critical binding sites for various transcription factors that regulate TAP-1 transcription. CBP is a transcriptional co-activator that possesses intrinsic HAT activity. In this model, the recruitment of CBP to TAP-1 promoter facilitates histone acetylation that leads to relaxation of the chromatin structure around the region, increasing the accessibility of the DNA template by transcription factors (TFs) and RNA pol II complex.

In addition to the mechanisms described above, this thesis also contributes to the finding that trichostatin A (TSA), a histone deacetylase inhibitor (HDACi) that has been used in clinical trials for anti-cancer agents [21-23], has the ability to improve TAP-1 expression, MHC class I antigen presentation and killing of malignant cells by MHC class I antigen-restricted, tumor antigen-specific cytotoxic T lymphocytes (CTLs). The effects seen were not as strong as those generated by IFN- $\gamma$  treatment; however, this finding is encouraging for the development of non-toxic, small molecular compounds with the ability to improve patients' immunogenic responses in cancer therapy.

Finally, a new method based on cDNA library screening was developed as an approach to identify other proteins which may improve TAP-1 expression and MHC class I antigen presentation in metastatic cancer cells. By screening of cDNA libraries originating from human lung and spleen specimens, several gene candidates that showed the ability to activate the *Tap-1* gene were discovered. Further research is required to refine the screening methods and to confirm the validity of the primary screen hits.

In this thesis, the second mechanism that was found to cause TAP-1 deficiency in metastatic carcinomas, the low stability of TAP-1 mRNA [14], has not been further investigated. Accelerated degradation of TAP-1 mRNA due to a mutation within the TAP-1 coding sequence in a melanoma cell line has been reported [24]. However, the mechanisms remain unknown in the absence of mutations within the TAP-1 coding sequence itself, which is the case in most TAP-deficient carcinoma lesions [7, 9].

The presence of a destabilizing AU-rich element (ARE) in the 3'-untranslated region (3'UTR) found in a large variety of cellular transcripts is generally responsible for mRNA degradation in a normal turnover process of coordinated gene expression [25, 26].

ARE was originally identified as a component of the granulocyte-macrophage colony-stimulating factor (GM-CSF) mRNA 3'-UTR [27]. Identification of binding proteins with the ability to either promote or inhibit ARE-mediated mRNA instability is of great interest in the field of post-transcriptional regulation of gene expression [28]. A widely-studied group of proteins that was found to accelerate mRNA degradation is the tristetraprolin (TTP) family of CCCH tandem zinc finger proteins that binds UUAUUUAUU consensus sequence in AREs of mRNA [26, 28]. TTP recruits mRNA decay complexes to ARE sequences, promoting removal of the poly(A) tail (deadenylation) and degradation of the mRNA [26].

Interestingly, the core heptamer of the ideal TTP binding site, UAUUUAU, that is conserved in mice and humans [28], is also present in the 3'-untranslated region (3'-UTR) of human and rat TAP-1 mRNA (NCBI accession no. NM\_000593 and NM\_032055, respectively). However, no polyA site was specified in a mouse TAP-1 mRNA sequence provided in the NCBI website (NM\_013683). Nevertheless, the presence of TTP binding site in human and rat TAP-1 mRNA opens the possibility that the TAP-1 mRNA is regulated in TTP-dependent manner. Therefore, it is intriguing to study whether deregulation of TTP function in TAP-deficient cells is responsible for the accelerated degradation of TAP-1 mRNA.

## 5.2 Future Work

Based on the findings of pre- and post-transcriptional, as well as epigenetic mechanisms underlying TAP-1 deficiencies in carcinomas, the research presented in this thesis could go forward in a number of interesting ways:

1. Characterization of TAP-activating factors.

This would require a thorough dissection of specific mechanisms outlined in this thesis. Differential states of core histone modifications in TAP-1 promoter of TAP-expressing and TAP-deficient cells need to be explored in greater details. The strongest correlations of histone modifications and gene transcription observed so far are: methylation of lysine 4, 36 and 79 in histone H3 (H3K4me, H3K36me and H3K79me, respectively), as well as acetylation of lysine 9 and 14 (H3K9ac and H3K14ac) and lysine 16 in histone H4 (H4K16ac) with activation, while methylation of lysine 9 and 27 in histone H3 (H3K9me and H3K27me) and lysine 20 in histone H4 (H4K20me) with repression [4, 29]. The finding of more specific differences will aid the identification of specific factors involved.

Exact mechanisms responsible for the impaired recruitment of CBP to TAP-1 promoter in TAP-deficient cancer cells are yet to be determined. It is important to determine whether the CBP itself is dysfunctional in TAP-deficient cancer cells, or whether the impairment is caused by deregulation of one or more upstream factors/co-activators. This study could be initiated by observing the effect of overexpressing normal CBP in TAP-deficient cells. If the results indicated that the defect does not lie in the CBP itself, it would be worth exploring the functionality of several CBP-associated factors,

such as p/CIP and PCAF [17, 30, 31]. It is also interesting to test whether the HAT activity of CBP is a critical factor responsible for histone acetylation and activation of TAP-1 promoter. This may be tested by overexpression of dominant-negative mutants of CBP that lack the HAT domain.

The cDNA library screening method could be refined by developing a ViraPort-like (Stratagene) cDNA library from a TAP-expressing, primary cancer cell line. The cDNA library retroviral supernatant could then be used to transduce its TAP-deficient, metastatic derivatives. Screening of positive transductants and recovery of candidate genes (cDNAs) could be performed as described in Chapter 4. This way, the candidates obtained would likely to be more specific to the type of tissues from which the cancers arose.

Microarray analysis could be performed to observe differential expression of genes in a TAP-expressing, primary cancer cell line and its TAP-deficient, metastatic derivative. Aberrant expression of genes in the metastatic cells might be responsible for the downregulated expression of TAP and immune evasion mechanisms.

2. Investigation of the mechanisms by which TSA improved TAP-1 expression and tumor antigen presentation.

The studies in Chapter 3 indicated that unlike the IFN- $\gamma$ , TSA effects did not occur through the improvement of histone H3 acetylation in TAP-1 promoter. One approach would be to isolate TSA-responsive element(s) in TAP-1 promoter by testing the response of full TAP-1 promoter and its truncations to TSA treatment. Identifying the mechanism by which TSA up-regulates TAP-1 expression is of fundamental importance,

since any non-toxic compounds with the ability to enhance TAP and MHC class I expression in cancer cells are of great interest for the development of cancer immunotherapy approaches. In the future, the efficacy of the treatment may be improved by the invention of synthetic TSA-like molecules with a greater ability to induce TAP and MHC class I expression in cells with down-regulated expression of APM components.

3. Broader applications of the use of pTAP1-EGFP construct for screening novel TAP-1-regulator genes.

In contrast to the use of this system to search for TAP-activating cDNAs in TAP-deficient cells, it may also be used to hunt for novel genes with the ability to repress TAP-1 promoter activity in TAP-expressing cells. TAP-suppressing compounds may be incorporated in immunotherapeutic approaches that aim to inhibit immune responses in transplant rejection and autoimmune diseases.

4. Investigation of the mechanisms responsible for rapid TAP-1 mRNA degradation in TAP-deficient carcinomas.

This investigation may be initiated by mutating the TTP-binding sequence in the 3'-UTR region of TAP-1 and testing whether this would increase TAP-1 mRNA stability in TAP-deficient cells. Whether TTP plays a role in regulating TAP-1 mRNA stability could also be determined by comparing TAP-1 mRNA stability in cells originated from normal versus TTP-deficient mice [32]. This may be followed by studies that aim to

characterize proteins with the ability to prevent de-adenylation [33], thus protecting TAP-1 mRNA transcripts from rapid degradation in a poly(A)-dependent fashion.

### **5.3 The Big Picture**

According to Burnet's immune surveillance theory, thousands of tumor cells emerged *de novo* everyday and the hosts' immune surveillance system was able to kill these antigenic tumor cells [34]. Unfortunately, this perfect scenario does not always happen, since MHC class I antigen presentation is often disrupted in cancer cells, due to downregulation of APM components, followed by immune selective pressure that works in favor of the outgrowth of cells that are unable to present tumor-specific antigens [3]. These cells can proliferate uncontrollably as they remain invisible by the circulating killer T cells (CTLs). This phenomenon remains a challenge for the development of anti-cancer vaccines and T-cell-based tumor immunotherapy methods that largely rely on the ability of CTLs to recognize abnormal cells expressing tumor-specific antigens. Effective approaches that lead to the induction of immune responses against neoplastic cells are of interest for the advancement of cancer immunotherapy. TAP-1-based therapy is a particularly attractive approach to be developed, since the entire MHC class I antigen presentation pathway in cells with multiple deficiencies of APM components may be reconstituted by restoring the expression of this particular component. A successful clinical approach would require a combination of fundamental knowledge and application of TAP-1-activating factors and effective delivery methods.

## 5.4 References

1. Bubenik, J. MHC class I down-regulation: tumour escape from immune surveillance? *Int J Oncol*, 2004. 25:487-91.
2. Campoli, M., C.C. Chang, and S. Ferrone. HLA class I antigen loss, tumor immune escape and immune selection. *Vaccine*, 2002. 20 Suppl 4:A40-5.
3. Chang, C.C. and S. Ferrone. Immune selective pressure and HLA class I antigen defects in malignant lesions. *Cancer Immunol Immunother*, 2007. 56:227-36.
4. Tomasi, T.B., W.J. Magner, and A.N. Khan. Epigenetic regulation of immune escape genes in cancer. *Cancer Immunol Immunother*, 2006. 55:1159-84.
5. Abele, R. and R. Tampe. Modulation of the antigen transport machinery TAP by friends and enemies. *FEBS Lett*, 2006. 580:1156-63.
6. Lankat-Buttgereit, B. and R. Tampe. The transporter associated with antigen processing: function and implications in human diseases. *Physiol Rev*, 2002. 82:187-204.
7. Seliger, B., T. Cabrera, F. Garrido, and S. Ferrone. HLA class I antigen abnormalities and immune escape by malignant cells. *Semin Cancer Biol*, 2002. 12:3-13.
8. Seliger, B., M.J. Maeurer, and S. Ferrone. TAP off--tumors on. *Immunol Today*, 1997. 18:292-9.
9. Seliger, B., M.J. Maeurer, and S. Ferrone. Antigen-processing machinery breakdown and tumor growth. *Immunol Today*, 2000. 21:455-64.

10. Restifo, N.P., F. Esquivel, Y. Kawakami, J.W. Yewdell, J.J. Mule, S.A. Rosenberg, and J.R. Bennink. Identification of human cancers deficient in antigen processing. *J Exp Med*, 1993. 177:265-72.
11. Alimonti, J., Q.J. Zhang, R. Gabathuler, G. Reid, S.S. Chen, and W.A. Jefferies. TAP expression provides a general method for improving the recognition of malignant cells in vivo. *Nat Biotechnol*, 2000. 18:515-20.
12. Gabathuler, R., G. Reid, G. Kolaitis, J. Driscoll, and W.A. Jefferies. Comparison of cell lines deficient in antigen presentation reveals a functional role for TAP-1 alone in antigen processing. *J Exp Med*, 1994. 180:1415-25.
13. Seliger, B., U. Ritz, R. Abele, M. Bock, R. Tampe, G. Sutter, I. Drexler, C. Huber, and S. Ferrone. Immune escape of melanoma: first evidence of structural alterations in two distinct components of the MHC class I antigen processing pathway. *Cancer Res*, 2001. 61:8647-50.
14. Setiadi, A.F., M.D. David, S.S. Chen, J. Hiscott, and W.A. Jefferies. Identification of mechanisms underlying transporter associated with antigen processing deficiency in metastatic murine carcinomas. *Cancer Res*, 2005. 65:7485-92.
15. Davie, J.R. and V.A. Spencer. Control of histone modifications. *J Cell Biochem*, 1999. Suppl 32-33:141-8.
16. Giordano, A. and M.L. Avantaggiati. p300 and CBP: partners for life and death. *J Cell Physiol*, 1999. 181:218-30.
17. Kalkhoven, E. CBP and p300: HATs for different occasions. *Biochem Pharmacol*, 2004. 68:1145-55.

18. Legube, G. and D. Trouche. Regulating histone acetyltransferases and deacetylases. *EMBO Rep*, 2003. 4:944-7.
19. Ma, Z., M.J. Chang, R.C. Shah, and E.N. Benveniste. Interferon-gamma-activated STAT-1alpha suppresses MMP-9 gene transcription by sequestration of the coactivators CBP/p300. *J Leukoc Biol*, 2005. 78:515-23.
20. Ramana, C.V., M.P. Gil, R.D. Schreiber, and G.R. Stark. Stat1-dependent and -independent pathways in IFN-gamma-dependent signaling. *Trends Immunol*, 2002. 23:96-101.
21. Jung, M. Inhibitors of histone deacetylase as new anticancer agents. *Curr Med Chem*, 2001. 8:1505-11.
22. Taddei, A., D. Roche, W.A. Bickmore, and G. Almouzni. The effects of histone deacetylase inhibitors on heterochromatin: implications for anticancer therapy? *EMBO Rep*, 2005. 6:520-4.
23. Yoshida, M., R. Furumai, M. Nishiyama, Y. Komatsu, N. Nishino, and S. Horinouchi. Histone deacetylase as a new target for cancer chemotherapy. *Cancer Chemother Pharmacol*, 2001. 48 Suppl 1:S20-6.
24. Yang, T., B.A. McNally, S. Ferrone, Y. Liu, and P. Zheng. A single-nucleotide deletion leads to rapid degradation of TAP-1 mRNA in a melanoma cell line. *J Biol Chem*, 2003. 278:15291-6.
25. Benjamin, D., M. Colombi, G. Stoecklin, and C. Moroni. A GFP-based assay for monitoring post-transcriptional regulation of ARE-mRNA turnover. *Mol Biosyst*, 2006. 2:561-7.

26. Hau, H.H., R.J. Walsh, R.L. Ogilvie, D.A. Williams, C.S. Reilly, and P.R. Bohjanen. Tristetraprolin recruits functional mRNA decay complexes to ARE sequences. *J Cell Biochem*, 2006.
27. Shaw, G. and R. Kamen. A conserved AU sequence from the 3' untranslated region of GM-CSF mRNA mediates selective mRNA degradation. *Cell*, 1986. 46:659-67.
28. Lai, W.S., J.S. Parker, S.F. Grissom, D.J. Stumpo, and P.J. Blackshear. Novel mRNA targets for tristetraprolin (TTP) identified by global analysis of stabilized transcripts in TTP-deficient fibroblasts. *Mol Cell Biol*, 2006. 26:9196-208.
29. Loyola, A., T. Bonaldi, D. Roche, A. Imhof, and G. Almouzni. PTMs on H3 variants before chromatin assembly potentiate their final epigenetic state. *Mol Cell*, 2006. 24:309-16.
30. Torchia, J., D.W. Rose, J. Inostroza, Y. Kamei, S. Westin, C.K. Glass, and M.G. Rosenfeld. The transcriptional co-activator p/CIP binds CBP and mediates nuclear-receptor function. *Nature*, 1997. 387:677-84.
31. Herrera, J.E., R.L. Schiltz, and M. Bustin. The accessibility of histone H3 tails in chromatin modulates their acetylation by P300/CBP-associated factor. *J Biol Chem*, 2000. 275:12994-9.
32. Lai, W.S., E. Carballo, J.M. Thorn, E.A. Kennington, and P.J. Blackshear. Interactions of CCCH zinc finger proteins with mRNA. Binding of tristetraprolin-related zinc finger proteins to Au-rich elements and destabilization of mRNA. *J Biol Chem*, 2000. 275:17827-37.

- 
33. Conrad, N.K., S. Mili, E.L. Marshall, M.D. Shu, and J.A. Steitz. Identification of a rapid mammalian deadenylation-dependent decay pathway and its inhibition by a viral RNA element. *Mol Cell*, 2006. 24:943-53.
  34. Burnet, M. *Cancer; a biological approach*. I. The processes of control. *Br Med J*, 1957. 1:779-86.

## **Appendix A: Details of Methods**

### ***A.1 Chromatin Immunoprecipitation Assay***

Twenty million cells were trypsinized, washed twice with PBS, pelleted, and incubated for 10 minutes at room temperature in PBS supplemented with a cross-linker reagent, 1% formaldehyde (Sigma). Cross-linking was stopped by addition of glycine to a final concentration of 125 mM for 5 min. Cells were washed twice with ice-cold PBS and centrifuged for 5 min at 4°C. Cells were then lysed in 1 ml cytoplasmic lysis buffer (5 mM Pipes, pH 8.0, 85 mM KCl, 0.5% NP-40, and protease inhibitor (Complete Mini, Roche)), and the pelleted fraction was then lysed in and 500 µl of nuclear lysis buffer (1% SDS, 10 mM EDTA, 50 mM Tris-HCl, pH 8.0 and protease inhibitor). Both steps of lysis were conducted for 10 minutes. Then, chromatin was sheared by sonication (Microson XL sonicator, Misonix Inc., Farmingdale, NY) (power setting 13 Watts; 3 x 15 seconds burst) to obtain 0.5-1 kb fragments. Samples were centrifuged to pellet debris and diluted 4 times in dilution buffer (1% Triton X-100, 2 mM EDTA, 20 mM Tris-HCl, pH 8.0, 150 mM NaCl and protease inhibitor). Two micrograms salmon sperm DNA (Sigma) was added, and samples were pre-cleared with 100 µl slurry of protein A agarose beads (Protein A Sepharose CL-4B, Amersham Biosciences, Uppsala, Sweden) for 2 hours at 4°C. Immunoprecipitations were carried out overnight at 4°C with 5 µg of anti-RNA polymerase II antibody (N-20, sc-899, Santa Cruz). Immunoprecipitations without antibody were also included as controls to assess levels of background signals. Immune complexes were collected with protein A agarose beads for 1 hour and washed successively in low salt buffer, high salt buffer and LiCl buffer for 10 minutes, then twice

in TE for 2 minutes. The complexes were then eluted in 1% SDS, 0.1 M NaHCO<sub>3</sub> and cross-links were reversed by heating at 65°C for 6 hours to overnight. Following 1 hour of proteinase K (Invitrogen) digestion at 45°C, DNA was phenol-chloroform extracted and ethanol precipitated. Pellets were resuspended in 50 µl milliQ water, and 2 µl of the immunoprecipitated DNA was used in each PCR sample.

## ***A.2 Calculation of copy numbers of pTAP-1-EGFP construct integrated in stable transfectants***

$$(6 \times 10^{23} \text{ [copies/mol]} \times \text{concentration [g/}\mu\text{l]}) / \text{MW [g/mol]} = \text{amount [copies/}\mu\text{l]}$$

1 mol = molecular weight (MW) [g]

1 mol =  $6 \times 10^{23}$  molecules (= copies)

Standard size of mouse DNA:  $2.7 \times 10^9$  bp. Assume this is per cell.

Standard conversion of µg to pmol:

$$1 \mu\text{g of a } 100 \text{ bp dsDNA fragment} = (1 \mu\text{g} \times 1515) / 100 = 15.2 \text{ pmol}$$

$$\text{Therefore, } 100 \text{ ng of } 2.7 \times 10^9 \text{ bp dsDNA fragment} = (0.1 \mu\text{g} \times 1515) / (2.7 \times 10^9)$$

$$= 5.61 \times 10^{-8} \text{ pmol} = 5.61 \times 10^{-20} \text{ mol} = 33,660 \text{ copies}$$

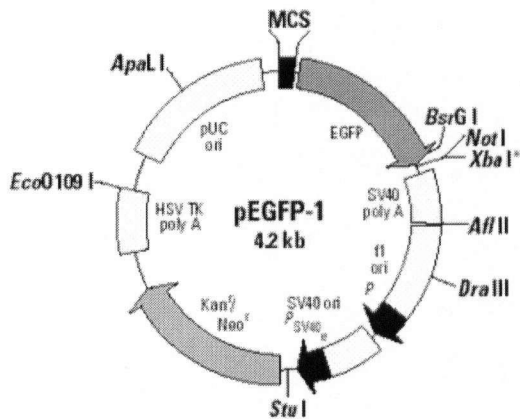
Thus, in 100 ng mouse DNA, there are 33,660 copies of genomic DNA.

### Sample calculation:

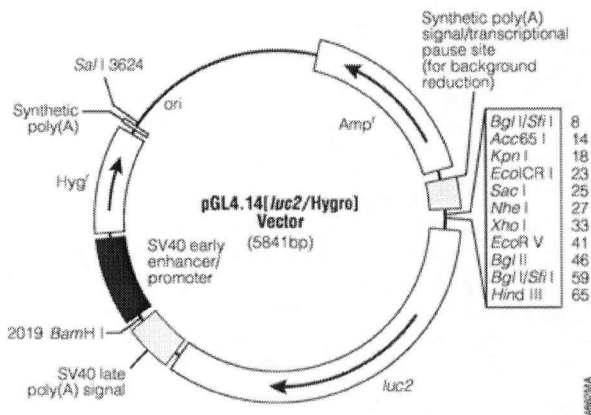
Using 100 ng of CMT.64 (pTAP1-EGFP stable transfectants) genomic DNA as a real-time PCR template, the average number of pTAP1-EGFP constructs integrated into the CMT.64 cells was determined to be 53,535 copies.

$$\text{Therefore, average number of plasmid per cell} = 53,535 / 33,660 = 1.59$$

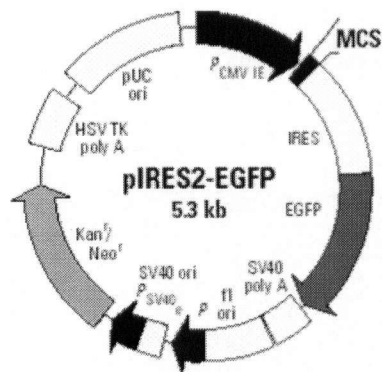
## Appendix B: List of Cloning Vectors



© Clontech Laboratories, Inc. Reprinted by permission.



© Promega Corporation. Reprinted by permission.



© Clontech Laboratories, Inc. Reprinted by permission.

## Appendix C: Comparison of TAP-1 Coding Sequence of CMT.64 and Ltk cells

Black: Ltk sequence; Italics: CMT.64 sequence; Bold: polymorphic regions.

1	ATGGCTGCGC	ACGTCTGGCT	GGCGGCCGCC	CTGC <b>T</b> CCTTC	TGGTGGACTG	GCTGCTGCTG
1	<i>ATGGCTGCGC</i>	<i>ACGTCTGGCT</i>	<i>GGCGGCCGCC</i>	CTGC <b>C</b> CCTTC	<i>TGGTGGACTG</i>	<i>GCTGCTGCTG</i>
61	CGGCCCATGC	TCCCGGGAAT	CTTCTCCCTG	TTGGTTCCCG	AGGTGCCGCT	GCTCCGGGTC
61	<i>CGGCCCATGC</i>	<i>TCCCGGGAAT</i>	<i>CTTCTCCCTG</i>	<i>TTGGTTCCCG</i>	<i>AGGTGCCGCT</i>	<i>GCTCCGGGTC</i>
121	TGGGTGGTGG	GCCTGAGTCG	CTGGGCCATC	CTAGGACTAG	GGGTCCGCGG	GGTCCCTCGGG
121	<i>TGGGTGGTGG</i>	<i>GCCTGAGTCG</i>	<i>CTGGGCCATC</i>	<i>CTAGGACTAG</i>	<i>GGGTCCGCGG</i>	<i>GGTCCCTCGGG</i>
181	GTCACCGCAG	GAGCCCATGG	CTGGCTGGCT	GCTTTGCAGC	CGCTGGTGGC	CGCACTGAGT
181	<i>GTCACCGCAG</i>	<i>GAGCCCATGG</i>	<i>CTGGCTGGCT</i>	<i>GCTTTGCAGC</i>	<i>CGCTGGTGGC</i>	<i>CGCACTGAGT</i>
241	TTGGCCCTGC	CTGGACTTGC	CTTGTCCGA	GAGCTGGCCG	CCTGGGGAAC	ACTCCGGGAG
241	<i>TTGGCCCTGC</i>	<i>CTGGACTTGC</i>	<i>CTTGTCCGA</i>	<i>GAGCTGGCCG</i>	<i>CCTGGGGAAC</i>	<i>ACTCCGGGAG</i>
301	GGTGACAGCG	CTGGATTACT	GTA CTGGAAC	AGTCGTCCAG	ATGCCTTCGC	TATCAGTTAT
301	<i>GGTGACAGCG</i>	<i>CTGGATTACT</i>	<i>GTA CTGGAAC</i>	<i>AGTCGTCCAG</i>	<i>ATGCCTTCGC</i>	<i>TATCAGTTAT</i>
361	GTGGCAGCAT	TGCCCGCAGC	CGCCCTGTGG	CACAAGTTGG	GGAGCCTCTG	GGCGCCAGC
361	<i>GTGGCAGCAT</i>	<i>TGCCCGCAGC</i>	<i>CGCCCTGTGG</i>	<i>CACAAGTTGG</i>	<i>GGAGCCTCTG</i>	<i>GGCGCCAGC</i>
421	GGCAACAGGG	ACGCTGGAGA	CATGCTGTGT	CGGATGCTGG	GCTTCCTGGG	CCCTAAGAAG
421	<i>GGCAACAGGG</i>	<i>ACGCTGGAGA</i>	<i>CATGCTGTGT</i>	<i>CGGATGCTGG</i>	<i>GCTTCCTGGG</i>	<i>CCCTAAGAAG</i>
481	AGACGTCTCT	ACCTGGTTCT	GTTTCTCTTG	ATTCTCTCTT	GCCTTGGGGA	AATGGCCATT
481	<i>AGACGTCTCT</i>	<i>ACCTGGTTCT</i>	<i>GTTTCTCTTG</i>	<i>ATTCTCTCTT</i>	<i>GCCTTGGGGA</i>	<i>AATGGCCATT</i>
541	CCCTTCTTCA	CGGGCCGCAT	CACTGACTGG	ATTCTTCAGG	ATAAGACAGT	TCCTAGCTTC
541	<i>CCCTTCTTCA</i>	<i>CGGGCCGCAT</i>	<i>CACTGACTGG</i>	<i>ATTCTTCAGG</i>	<i>ATAAGACAGT</i>	<i>TCCTAGCTTC</i>
601	ACCCGCAACA	TATGGCTCAT	GTCCATTCTC	ACCATAGCCA	GCACAGCGCT	GGAGTTTGCA
601	<i>ACCCGCAACA</i>	<i>TATGGCTCAT</i>	<i>GTCCATTCTC</i>	<i>ACCATAGCCA</i>	<i>GCACAGCGCT</i>	<i>GGAGTTTGCA</i>
661	AGTGATGGAA	TCTACAACAT	CACCATGGGA	CACATGCACG	GCC <b>A</b> TGTGCA	CAGAGAGGTG
661	<i>AGTGATGGAA</i>	<i>TCTACAACAT</i>	<i>CACCATGGGA</i>	<i>CACATGCACG</i>	GCC <b>G</b> TGTGCA	<i>CAGAGAGGTG</i>
721	TTTCGGGCCG	TCCTTCGCCA	GGAGACAGGG	TTTTTCCTGA	AGAACCCAGC	AGGTTCCATC
721	<i>TTTCGGGCCG</i>	<i>TCCTTCGCCA</i>	<i>GGAGACAGGG</i>	<i>TTTTTCCTGA</i>	<i>AGAACCCAGC</i>	<i>AGGTTCCATC</i>
781	ACATCTCGGG	TGACTGAGGA	CACAGCCAAC	GTGTGCGAGT	CCATTAGTGG	CACGCTGAGC
781	<i>ACATCTCGGG</i>	<i>TGACTGAGGA</i>	<i>CACAGCCAAC</i>	<i>GTGTGCGAGT</i>	<i>CCATTAGTGG</i>	<i>CACGCTGAGC</i>
841	CTGCTGCTGT	GGTACCTGGG	GCGAGCCCTG	TGTCTCTTGG	TGTTTCATGTT	TTGGGGGTCA
841	<i>CTGCTGCTGT</i>	<i>GGTACCTGGG</i>	<i>GCGAGCCCTG</i>	<i>TGTCTCTTGG</i>	<i>TGTTTCATGTT</i>	<i>TTGGGGGTCA</i>

901 CCGTACCTCA CTCTGGTCAC CCTGATCAA**T** CTGCCCCTGC TTTTCTTTT GCCTAAGAAG  
901 CCGTACCTCA CTCTGGTCAC CCTGATCAA**C** CTGCCCCTGC TTTTCTTTT GCCTAAGAAG

961 CTGGGAAAAG TGCA**C**CAGTC ACTGGCAGTG AAGGTGCAGG AGTCTCTAGC AAAGTCCACG  
961 CTGGGAAAAG TGCA**T**CAGTC ACTGGCAGTG AAGGTGCAGG AGTCTCTAGC AAAGTCCACG

1021 CAGGTGGCCC TTGAGGCCTT ATCGGC**A**ATG CCTACTGTGC GGAGCTTTGC CAACGAGGAG  
1021 CAGGTGGCCC TTGAGGCCTT ATCGGC**G**ATG CCTACTGTGC GGAGCTTTGC CAACGAGGAG

1081 GGTGAGGCC AGAAGTTCAG GCAGAAGTTG GAAGAAATGA AGAC**G**CTAAA CAAGAAGGAG  
1081 GGTGAGGCC AGAAGTTCAG GCAGAAGTTG GAAGAAATGA AGAC**T**CTAAA CAAGAAGGAG

1141 GCCTTGGCTT A**T**G**T**C**G**CTGA AGTCTGGACC ACGAGTGTCT CGGGAATGCT GCTGAAGGTG  
1141 GCCTTGGCTT A**C**G**T****G**GCTGA AGTCTGGACC ACGAGTGTCT CGGGAATGCT GCTGAAGGTG

1201 GGAATTCTGT ACCTGGGCGG GCAGCTGGTG ATCAGAGGG**A** CTGTCAGCAG CGGCAACCTT  
1201 GGAATTCTGT ACCTGGGCGG GCAGCTGGTG ATCAGAGGG**G** CTGTCAGCAG CGGCAACCTT

1261 GTCTCATTCG TTCTCTACCA GCTTCAGTTC ACCCA**C**GCTG TTCAGGTCCT GCTCTCCCTC  
1261 GTCTCATTCG TTCTCTACCA GCTTCAGTTC ACCCA**G**GCTG TTCAGGTCCT GCTCTCCCTC

1321 TACCCCTCCA TGCAGAAGGC TGTGGGCTCC TCAGAGAAAA TATTCGAATA CTGGACCGG  
1321 TACCCCTCCA TGCAGAAGGC TGTGGGCTCC TCAGAGAAAA TATTCGAATA CTGGACCGG

1381 ACTCCTTGCT CTCCACTCAG TGGCTCGTTG GCACCCCTCAA ACATGAAAGG CCTTGTGGAG  
1381 ACTCCTTGCT CTCCACTCAG TGGCTCGTTG GCACCCCTCAA ACATGAAAGG CCTTGTGGAG

1441 TTCCAAGATG TCTCTTTTGC CTACCCAAAC CAGCCCAAAG TCCAGGTGCT TCAGGGGCTG  
1441 TTCCAAGATG TCTCTTTTGC CTACCCAAAC CAGCCCAAAG TCCAGGTGCT TCAGGGGCTG

1501 ACGTTCACCC TGCATCCTGG AACGGTGACA GCGTTGGTGG GACCCAATGG ATCAGGGAAG  
1501 ACGTTCACCC TGCATCCTGG AACGGTGACA GCGTTGGTGG GACCCAATGG ATCAGGGAAG

1561 AGCACCGTGG CTGCCCTGCT GCAGAACCTG TACCAGCCCA CCGGGGGCCA GCTGCTGCTG  
1561 AGCACCGTGG CTGCCCTGCT GCAGAACCTG TACCAGCCCA CCGGGGGCCA GCTGCTGCTG

1621 GATGGCCAG**C** GCCTGGTCCA GTATGATCAC CATTACCTGC AACTCAGGT **A**GCCGCAGTG  
1621 GATGGCCAG**T** GCCTGGTCCA GTATGATCAC CATTACCTGC AACTCAGGT **G**GCCGCAGTG

1681 GGACAAGAGC CGCTGCTATT TGGAAGAAGC TTTCGAGAAA ATATTGCGTA TGGCCTGAAC  
1681 GGACAAGAGC CGCTGCTATT TGGAAGAAGC TTTCGAGAAA ATATTGCGTA TGGCCTGAAC

1741 CGGACTCCAA CCATGGAGGA AATCACAGCT GTGGCCGTGG AGTCTGGAGC CCACGATTC  
1741 CGGACTCCAA CCATGGAGGA AATCACAGCT GTGGCCGTGG AGTCTGGAGC CCACGATTC

1801 ATCTCTGGGT TCCCTCAGGG CTATGACACA GAGGTAGGTG AGACTGGGAA CCAGCTGTCA  
1801 ATCTCTGGGT TCCCTCAGGG CTATGACACA GAGGTAGGTG AGACTGGGAA CCAGCTGTCA

1861 GGAGGTCAGC GACAGGCAGT GGCCTTGGCC CGAGCCTTGA TCCGGAAGCC ACTCCTGCTT  
1861 GGAGGTCAGC GACAGGCAGT GGCCTTGGCC CGAGCCTTGA TCCGGAAGCC ACTCCTGCTT

1921 ATCTTGGATG ATGCCACCAG TGCCCTGGAT GCTGGCAACC AGCTACGGGT CCAGCGGCTC  
1921 ATCTTGGATG ATGCCACCAG TGCCCTGGAT GCTGGCAACC AGCTACGGGT CCAGCGGCTC

1981 CTGTATGAGA GCCCCAAGCG GGCTTCTCGG ACGGTTCTTC TTATCACCCA GCAGCTCAGC  
1981 CTGTATGAGA GCCCCAAGCG GGCTTCTCGG ACGGTTCTTC TTATCACCCA GCAGCTCAGC

2041 CTGGCAGAGC AGGCCACCA CATCCTCTTT CTCAGAGAAG GCTCTGTCGG CGAGCAGGGC  
2041 CTGGCAGAGC AGGCCACCA CATCCTCTTT CTCAGAGAAG GCTCTGTCGG CGAGCAGGGC

2101 ACCCACCTGC AGCTCATGAA GAGAGGAGGG TGCTACCGGG CCATGGTAGA GGCTCTTGCG  
2101 ACCCACCTGC AGCTCATGAA GAGAGGAGGG TGCTACCGGG CCATGGTAGA GGCTCTTGCG

2161 GTCCTGCAG ACTGA  
2161 GTCCTGCAG ACTGA